University College of Southeast Norway
Faculty of Technology
Master's Thesis
System and Control Engineering
Spring 2016

Jeremiah Chigozie Ejimofor

Open Venturi-Channel Flow Metering Of Non-Newtonian Fluids

A Case Study with Emulated Drilling Fluids.

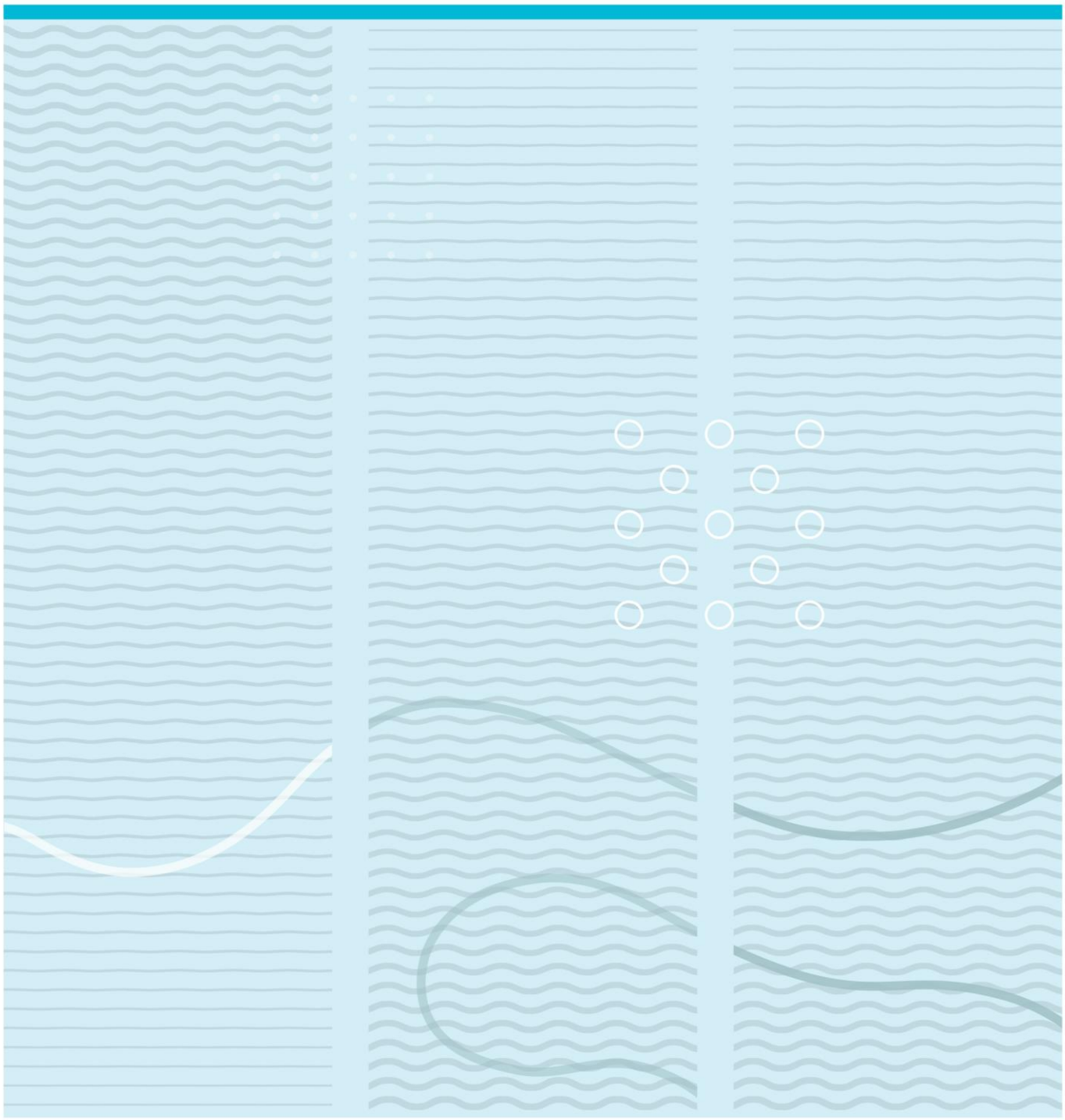

University College of Southeast Norway

MASTER'S THESIS, COURSE CODE FMH606

Student: Jeremiah Chigozie Ejimofor

Thesis title: Open Venturi-Channel Flow Metering of Non-Newtonian Fluids

Signature: . . . . . .

Number of pages: 149

Keywords: Newtonian fluid, non-Newtonian fluid, Coriolis flow meter and Venturi

Supervisor: Geir Elseth Sign.: .. . .

2nd supervisor: Kanagasabapath Mylvaganam Sign.: . . . . . .

External partner: Statoil Dept. Intelligent drilling, Porsgrunn Sign.: . . . . . .

Availability: Open

Archive approval (supervisor signature)**:** Sign:…… Date: . . ..

Abstract:

In the oil and gas industry, controlling the well pressure is a very important aspect of drilling, thus drilling fluids has been the forefront aspect in drilling operation, thereby acting as a barrier against hydrocarbon blowout. In controlling the well pressure, recent study have revealed that measuring the flow rate of the drilling fluid flowing out from the well is the best method for early kick detection or well breathing. However, since most drilling fluids are non-Newtonian in nature, this study is focused on using open channel venturi as a stand-alone flow meter for non -Newtonian fluids, commissioning test of newly installed Coriolis flow meter and comparing with previous installed Coriolis flow meter based on experimental data for Newtonian and non-Newtonian fluids.

In this study, two empirical models were developed; the first model used the partial least square method in multivariate data analysis to find the linear relationship between mass flow rate and other inputs variables such as density, pressure, temperature, differential pressure and the level measurement at the open venturi channel. The result from this model revealed that density, differential pressure and the three level measurement at the open venturi channel were the most important variables to estimate mass flow rate. Based on the information from the first model, the second model was developed using an artificial neural network which estimated mass flow rate with an estimated error of 4.14kg/min.

The result from the commissioning test of the newly installed Coriolis flow meter in USN, based on experimental data for Newtonian and non-Newtonian fluids shows that the position of the sensor which is very close to a bend is creating a turbulent flow. Fluids which has the characteristics of generating bubbles are affected by this problem, thus producing more errors for the flow meter. The study also reveals that the flow meter cannot measure the viscosity of non-Newtonian fluids.

Contents

,

List of Figures

List of Tables

Acknowledgement

This master thesis is the final work in System and Control Engineering master program at the University of Southeast Norway. This thesis was conducted during the spring of 2016, in collaboration with Statoil regarding intelligent drilling.

This study has been very interesting , challenging and a great learning experience. I have exploit lots of knowledge acquired throughout my studies and working experience in practical instrumentation and implementation of measuring instruments to an existing system.

This work is completed independently with the guidance of my supervisor Geir Elseth, his great support and enthusiasm in this work is infectious, and has inspired me throughout the completion of this study. He gave good guidance in the general experimentation and implementation of this study. He set a good example, for his professional dedications to this study. I would like avail this opportunity to say a big thank you to Geir Elseth for being my supervisor.

Also, I sincerely thank my Co-supervisors Prof. Saba Mylvaganam for his advice, support and guidance for the successful completion of this thesis. His profound knowledge deeply inspired me. I would also like to thank Håkon Viudal and Khim Chhantyal who gave me a lot of help in the experimental work and for being a kind friend. I won't have gotten those results without their help. I also like to say thank you to Statoil dept. Intelligent drilling, Porsgrunn for originating this thesis.

A special thanks go to my friends and family for their support and encouragement throughout my studies and all my affairs in life. A big thank goes to Manfred Abongwa who stood by me all this time to see this success, I won't have completed this Master degree without you.

USN, Norway, 2nd June 2016

Jeremiah Chigozie Ejimofor

Nomenclature

p	Pressure	N/m^2
ρ	Density	Kg/m^3
h	Height	m
μ	Viscosity	Kg/ms
τ	Stress	N/m^2
γ	Strain	s^{-1}
BHP	Bottomhole pressure	N/m^2
SPP	Stand pipe pressure	N/m^2
H_p	Hydrostatic pressure	N/m^2
F_p	Frictional Pressure	N/m^2
B_p	Back pressure	N/m^2
MPD	Manage pressure Drilling	
USN	University College of Southeast Norway	
CFD	Computational fluids dynamics	
g	Acceleration due to gravity	m/s^2
K	Flow consistency index	Pas^n
n	Flow behavior index	
τ_o	Yield stress	N/m^2
Q	Volume flow	m^3/s

A_1	Initial cross sectional area	m^2
A_2	Throat cross sectional area	m^2
z	Pipe elevation	mm
c	Discharge coefficient factor	
c_f	Speed of sound	m/s
T	Time	sec
L	Level	mm
$P_{\bar{x}}$	Random uncertainty of the mean	
α	Level of significance	
P_x	Random uncertainty of each measurement	
S_x	Population standard deviation	
v	Degree of freedom	
σ	Sample standard deviation	
B_x	Systematic uncertainty	

1 Introduction

In the oil and gas industry drilling fluids also called drilling mud has been the forefront aspect of drilling operations. Equipment and technologies have been developed and still been optimized for the purpose of safe and adequate drilling operation. Most drilling fluids used during drilling are non-Newtonian in nature with an objective of controlling the pressure, remove cuttings from the wellbore among others. During drilling operation, drilling fluids are used to prevent situations such as kick[1] or wellbore breathing[2] which are dangerous in nature and may lead to losing of life, property, environmental and economic damage [1].

Timing is very crucial for detecting and managing kick or wellbore breathing. However in the standard conventional drilling, the downhole pressure is monitored by monitoring the active pit volume and the fluid level in the tank. When the mud level is higher or lower than expected, then a kick or wellbore breathing is suspected and procedures such as adding more addictive to the mud (increasing hydrostatic pressure) or shutting the well may be carried out. This procedure is very time consuming and inefficient as compared to the timing of the kick occurrence. Currently due to the inefficient procedures of the conventional procedures, a technique called Manage pressure drilling (MPD) is been practiced, this system monitors the flow line instead of the mud pit by the introduction of back pressure system, thereby ensuring faster detection and higher efficiency [1].

An early investigation from [2, 3] has shown that flow measurement out from the well is the best procedure to control downhole pressure, thus, kick and wellbore breathing can be quickly detected before it escalates. As of today, the sensors used for outflow measurement from the well are paddle meter, Coriolis flow meter, electromagnetic flow meter (usually for conducting fluids like water) and rolling float meter [1]. These meters has its drawbacks and are still been optimized due to the complexity of non-Newtonian fluids rheology[3]. However, in an oil platform, since the out streams from the wellbore flows out through an open channel, an open venturi channel flow meter with minimal energy loss can be used as a stand-alone flow meter to measure the flow accurately.

[1] A dangerous situation which causes blowout, it is a situation where the hydrostatic pressure is below formation pressure, thus causing an influx of fluids.
[2] A situation which occurs when fluids are loss into the formation.
[3] The study of deformation and flow of matter

Open venturi channel flowmeter has no moving parts, less sensible to wear and used in many industrial processes, like in the agriculture industry. It is used in measuring wastewater contaminated fluids with solids, thus also making it ideal for measuring the mixture of drilling muds and cuttings out from the well in the oil and gas industry. Open venturi channel estimates flow rate by utilizing the change in velocity and level which is caused by the restricted region in the flow meter called the throat.

This thesis will be focusing on flow metering of non-Newtonian drilling fluid using open channel venturi flow metering. The University college of Southeast Norway has a trapezoidal open venturi channel flow meter which was commissioned in May 2014, therefore this thesis will be based on trapezoidal open channel venturi flow meter.

1.1 Previous work

Many works have been done generally on open channel venturi flow metering, the previous work presented here are those done at the University College of Southeast Norway.

In [4], a group of master students presented a CFD simulation model using FLUENT and CFX for estimating the flow rate of a Newtonian fluid in open channel venturi using velocity and depth as a parameter was presented. The results of their findings were compared with manufacturer data which shows that both FLUENT and CFX was able to predict flow rate with a maximum error of 2%.

Also in [5] a numerical method of one-dimensional saint venant equation was used to estimate the flow rate of a Newtonian and non-Newtonian fluid using a rectangular open channel venturi. In this study, both the steady state and dynamic state of the fluids were analyzed and the results show that the flow rate of the fluid can only be estimated at steady state. The work also presented a real-time estimate of flow rate with an accuracy of 0.5% using ensemble Kalman filter, merged level measurement with saint venant equation.

In [6], spring 2015 a group a bachelor's students made a model drilling fluid and tested the fluid with the trapezoidal open channel venturi to determine flow rate. Potassium carbonate was used to increase the density of the fluid while xanthan gum was used to increase the viscosity in a water-based fluid of the modelled fluid produced by the students. The result of the produced drilling mud tested in the open venturi channel shows a good correlation of flow rate when compared with the Coriolis flow meter. Also in [7] spring 2015, an improvement and expansion of the control and communication system for the venturi rig was implemented.

The system was tested with Newtonian fluid and the emulated drilling fluid made by [6]. The result shows that the venturi channel is accurate within 1% of the volumetric flow at a flow rate of 400kg/min and above.

In [8], a group of master student presented two empirical model for estimating the mass flow rate of drilling fluid at steady state using Multivariate data analysis approach and Neural Network approach to estimate both dynamic and steady state. The result of their findings shows that multivariate data analysis approach gave an estimated error of 19.3kg/min for mass flow rate estimation while the Neural Network approach gave an estimated error of 8.19kg/min for mass flow rate. Neural Network approach was also used to compare the model designed by [5] using Newtonian fluid and the result shows that the Neural Network had an estimated error of 6.38kg/min as compared to the numerical model of error 11.77kg/min for mass flow rate. The group also added an extra functionality for the control system for automatic set point change.

In [9] a design of three drilling fluids and density adjustment system was developed. The result showed the effect of the agitator on Coriolis flow measurement in the drilling fluids. The work also showed that as the flow rate of the drilling fluids increases the density increases slightly.

1.2 Scope of work

The main objective of this thesis includes:

1. A general survey on drilling mud flow.
2. A brief survey of measurement techniques used in monitoring flow with focus on venturi flow meters (both open channel and closed conduit) for both Newtonian and non-Newtonian fluids
3. An overview of the measurands monitored using a P&ID as used in the oil and gas industries.
4. The main features and challenges of flow metering of non-Newtonian fluids.
5. An overview of CFD work a dedicated to non-Newtonian fluids with clear description of parameters used and the output from the model. Status qua reaching 2015
6. A detailed overview of the UCSEN rig with open Venturi-channel with all the instruments installed with a list of their measurement capabilities.

7. Compare viscosity, density data with a laboratory based measurement from the Coriolis Meter with serial number K6071D02000.
8. Compare and discuss result from the two installed Coriolis flow meter focusing on any discrepancies.
9. Analyze the experimental data and extract parameter of interest including improved flow velocity estimate.

2 Drilling technology literature review

In this chapter, the concept of drilling will be presented, a brief understanding, purpose and properties of drilling fluids. drilling mud flow as used during drilling operation will be presented. The features and challenges of non-Newtonian fluids will also be discussed,venturi metering , flow regimes, and finally a brief survey of computational fluid dynamics will be discussed.

2.1 Concept of drilling

Drilling process is changing rapidly in areas of technology, safety and management. Thus, for effective drilling procedures, proper planning must be conducted in order to improve drilling efficiency and avoid unwanted problems. Drilling can be done vertically and also in various angles, usually called directional drilling. Directional drilling provides access to reservoirs that are too thin or compacted with the vertical well. In drilling the bottom hole pressure (BHP) must be controlled at all time to avoid kick, well breathing or well bore instability [1, 10, 11]. The major drilling techniques in operation depending on the reservoir site to be drilled and past experience of the drillers are overbalance, underbalanced and managed pressure drilling.

2.1.1 Overbalance drilling

This is the conventional drilling method where the hydrostatic pressure of the drilling fluids is designed to exceed the formation pressure. In this method of drilling the main objective is to minimise any influx into the wellbore, therefore the mud act as a barrier against the formation pressure. This conventional method of drilling is very difficult in a narrow drilling window[4] and its associated to problems such as formation damage, fluid loss, differential sticking and many others [1, 10, 11].

In the conventional overbalance drilling the well is open to the atmosphere and the bottom hole pressure (BHP) is equal to the hydrostatic pressure and frictional pressure loss. The bottom hole pressure (BHP) is controlled by manipulating the density of the drilling mud (hydrostatic pressure).

[4] This is the space between the pore pressure and the fracture pressure of the formation

2.1.2 Underbalance drilling

This is an alternative drilling technique to the conventional overbalanced drilling. In this method of drilling the main objective is to prevent drilling fluid loss into the formation. In underbalanced drilling the hydrostatic pressure of the drilling fluids is designed to be less than the formation pressure, thus, the drilling mud does not act as a barrier against formation pressure, but rather the formation fluids flows into the wellbore and out through the annulus. This method of drilling if properly designed and executed takes care of the problem of formation damage, fluid loss, differential sticking and also increases penetration rate [1, 10, 11].

2.1.3 Manage pressure drilling (MPD)

This is an optimized drilling technique adapted to precisely control the annular pressure profile throughout the wellbore with the introduction of back pressure pump which controls the pressure downhole. This method of drilling reduces drilling cost and it's very efficient in drilling difficult reservoirs where the conventional drilling techniques cannot perform adequately. In this closed system drilling technique, the bottom hole pressure (BHP) is equal to the hydrostatic pressure, frictional pressure loss and the back pressure. The bottom hole pressure (BHP) is controlled by manipulating the back pressure which can be controlled with the use of choke valve instead of the fluid density (hydrostatic pressure), thus saving more time as compared with the conventional techniques [1, 10, 11]. Figure 2- 1 shows MPD drilling operation.

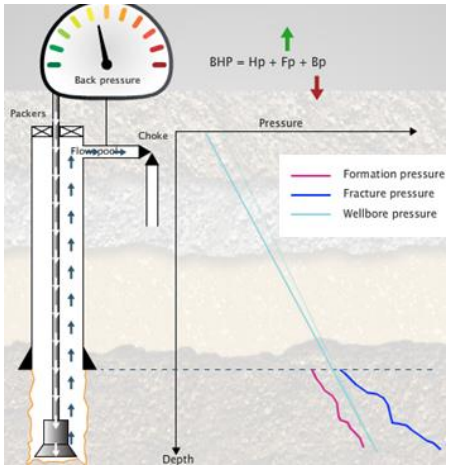

Figure 2- 1. Manage Pressure drilling operation [1]

2.2 Drilling bits

This is the tool designed to cut and crush rocks in order to produce the hole (wellbore) from which the oil and gas will be flowing out from. Drilling bits are located at the bottom end of the drill string. During drilling operations, the kind of drill bits to be used to drill depends on the formation to be drilled, the cost of the drill bits and the wellbore size. Drill bits can be changed in the process of drilling due to wear and tear of the drill bit or due to change in the formation rock in the drilling area. Factors such as drilling fluids, the hydraulic weight applied on bits and rate of rotation of the bits can affect the efficiency of drilling bits. An efficient and perfect drilling bit is characterised by long life span, high durability and moderate cost. To achieve best drilling performance and reduced cost, it is very important to use the right bits, some of the various types of bits are discussed here.

2.2.1 Drag bit

These type of bits are also called fixed cutter bits and do not have any moving parts. They are categorised into two, diamond bit and polycrystalline diamond compact (PDC) bit.

2.2.1.1 PDC bit

This type of bit is constructed with cutters made of man-made diamond materials. This bits are mostly used in soft and medium hard rock formation and cut rock by shearing. It is also

used in drilling deep expensive well to increase penetration and reduce drilling time and cost [12].

Figure 2- 2. PDC bit

shows a PDC drilling bit.

Figure 2- 2. PDC bit *[13]*

2.2.1.2 Diamond bit

This type of bit is constructed with a natural diamond which is set into the bit head. This bit are usually not mass produced but are designed for a particular job base on request. The size of the diamond determines the type of rocks to be drilled. The widely spaced diamonds are used to drill soft formation while closely spaced diamond are used to drill hard and abrasive formation [12]. Diamond bits cuts rocks by grinding and also used to drill deep and offshore wells where rig cost is very expensive. *Figure 2- 3* shows a diamond drilling bit.

Figure 2- 3. Diamond bits *[13]*

2.2.1.3 Rotatory bit

This is also called roller cone bits, it is mostly used in the oil and gas, mining industry and water well drilling. This bit is constructed with metal cones (cuttings) that rotate independently, with each cones tooth designed with hard steel, tungsten carbide, PDC, diamond or combination of these materials with grinding and chipping action. Commonly used types of rotatory drilling bits are the two cone, three cone and four cone bits, Figure 2-4 shows the rotatory drilling bits

- Two cone bits: Mostly used in directional drilling.
- Three-cone bits: This is also called tricone bits, it is the most common type of drilling bit used in a drilling operation.
- Four cone bits: This is mostly used in drilling large big holes.

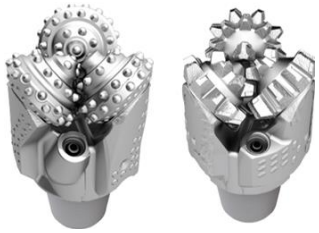

Figure 2- 4. Rotatory drilling bits [13]

2.3 Drilling rig/ platforms

This is the equipment that is used in the extraction of oil and gas from the well to the surface. The construction of various drilling platforms depends on locations, climatic conditions, size,

the cost of the facility and environmental safety. Drilling platforms can be constructed both on land and also on water. The two main types of drilling platforms are rotary drilling and cable tool drilling platforms. Figure 2- 5 shows the classification of drilling platforms.

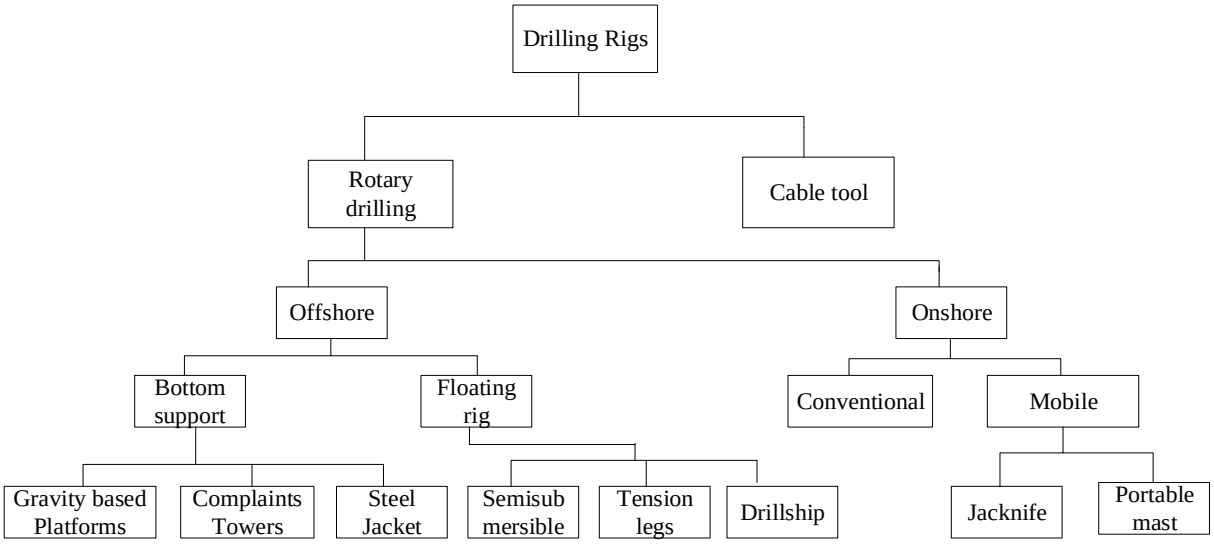

Figure 2- 5. Classification of drilling Rigs

2.3.1 Cable tool drilling

This is the oldest type of drilling platforms, it was first introduced in china for water drilling. It is very slow and characterized with low penetration rate. In this type of drilling, a drill bit is attached to the drill stem which provides the weight that is needed to force the bit into the ground by repeated pounding to achieve a hole.

2.3.2 Rotary drilling

This is the most common drilling platforms used today, it is used to drill deeper formations using a sharp rotating drill bit. Rotary drilling rig can be characterized as onshore and offshore drilling.

2.3.2.1 Onshore drilling rig

This is a type drilling platform is situated on land. It consists of various type which depends on the size and portability. These rigs are usually categorized from small to largely constructed rigs and mobile rigs (portable mast and jackknife). The majority of the onshore

rigs are usually disassembled after the well has been completed to be used again in other locations.

2.3.2.2 Offshore drilling rig

This is the type of drilling platform is situated on water. In the offshore rig, the structures have the capability of housing workers, drilling equipment and the production of oil and gas. Offshore drilling rigs are designed to withstand arctic conditions and are sub-divided into floating rig and bottom support rig. *Figure 2- 6* shows both bottom support rigs and floating rigs.

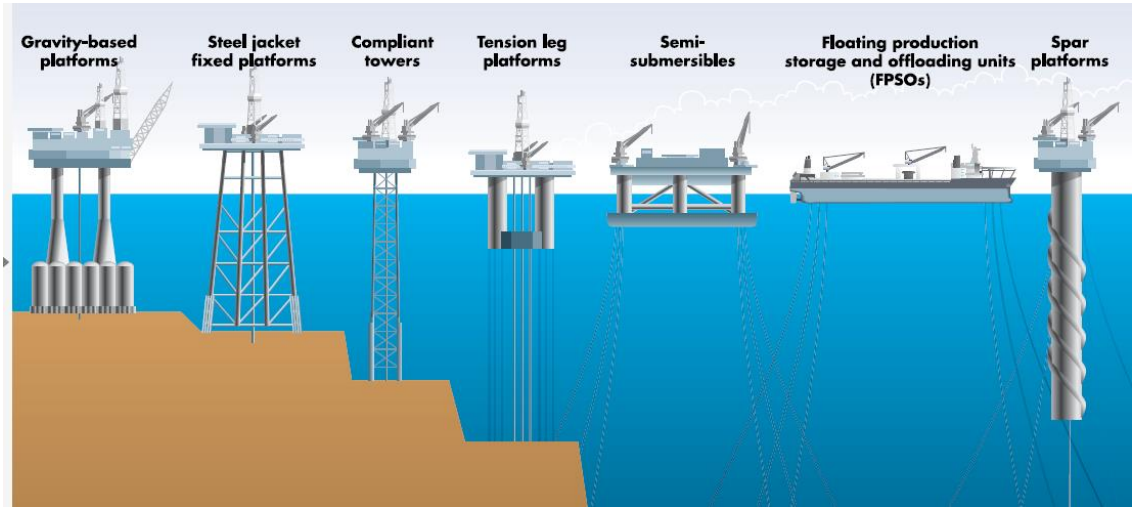

Figure 2- 6. Offshore rigs [14]

2.3.2.2.1 Bottom support rigs

These rigs can be totally submerged in water or sometimes firmly rooted at the bottom of the sea floor. An example of bottom support rigs is the steel jacket fixed platforms, gravity-based platforms, tension leg platform and compliant towers [14].

- Gravity based platform: This is a fixed platform which is held in place by gravity, made of steel or concrete to provide support for heavy drilling and production equipment. This platform is characterized by large size to support large facilities and designed for long time use in deeper water depth.
- Steel Jacket fixed platform: This is the most common oil platform, it stands on legs on the sea bottom and constructed with steel. This platform is more economical as compared to gravity based platform.

- Compliant towers: This is a narrow and flexible platform designed to sustain and absorb forces exerted by wind and sea waves. These platforms are typically used in depth of 1000 to 3000 feet [14].

2.3.2.2.2 Floating rigs

These are rigs that have the capability to move on water. There are semi-submersible rig, floating production and offloading units, tension leg platform and spars [14].

- Tension-leg Platform: This is a floating platform similar to fixed platform which is held in place by vertical tendons connected to the sea floor, it uses floating hull (barge hull and steel post) to support the drilling equipment and deck.
- Semi-submersible rig: This uses pontoons submerge only a few feet in the water but not in contact with the sea floor. This floating platform can be moved to a different location when required.
- Spars: This is a drilling rig supported by a floating hollow cylinder having extra weight at the bottom for more support. This platform is similar to tension leg platform and it is more stable, more economical to construct for small and medium size rigs.
- Floating production storage and offloading units: This is a ship-like vessel rig suitable in a remote location where climatic conditions are not too harsh and limited pipeline system of transporting the produced oil.

2.4 Well completion

This is the process of preparing a well for production, it involves the post-drilling procedures involved for an efficient and successful hydrocarbon production. Before any well is completed adequate testing, planning, evaluation, technical and economic optimization must be done before any action of completion can be taken on the well. Some of the elements of well completions include; casing, cementing, production equipment (tubing and packers) and surface flow control (Christmas tree). Figure 2- 7 shows the activities stages of well completions.

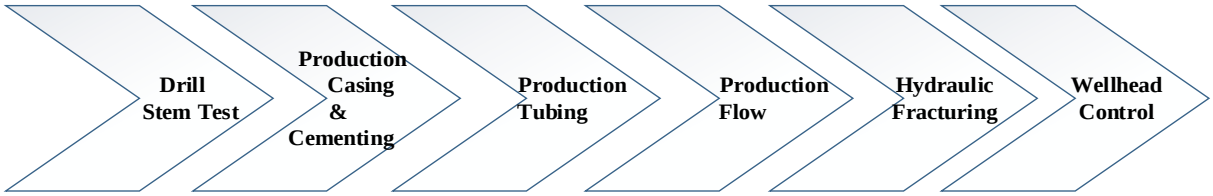

Figure 2- 7. Stages of well completion

- Drill stem test: This is an activity conducted to determine the formation potentials to produce oil and gas. In performing a drill stem test, the formation pressure is tested and if these testing procedures fail the well may be abandoned.
- Production Casing and Cementing: This activity is performed only if the formation has the capability of producing oil. If the production of the formation has been ascertained, the production casing is set into the wellbore and cemented to support the well, prevent water into the wellbore and allows pressure controls.
- Production tubing: This is the process of inserting a smaller diameter tube through the large diameter production casing.
- Production flow: These are the activities that are performed on the well for easy flow of the oil to the surface. The activities include washing and cleaning the drilling fluids out from the well, swapping (using wire line), installation of parkers[5], landing nipples[6] and simulations[7].
- Hydraulic Fracturing: This is the process of piecing production tubing, casing and the cemented wellbore to allow a pathway for oil and gas to flow into the wellbore. The process involves the use of water or sand pumped at high pressure into the wellbore to fracture the formation.
- Wellhead control: This is the installation of valves, chokes and pressure gauges to control fluid flow from the well into the environment. This device includes Christmas tree (wellhead control) which contains components that allow equipment to be inserted into the wellbore and blow out preventer which prevents loss of well control during drilling and completion operations [15]. Figure 2- 8 shows well head control device, blowout preventer at the left and Christmas tree at the right.

[5] The Sealing device that provides hydraulic separation between the production tubing and casing.
[6] Where plugs or chokes may be landed for flow control and monitoring
[7] Artificial process of lifting oil to the surface by using pumping equipment, injecting water, sand or chemicals

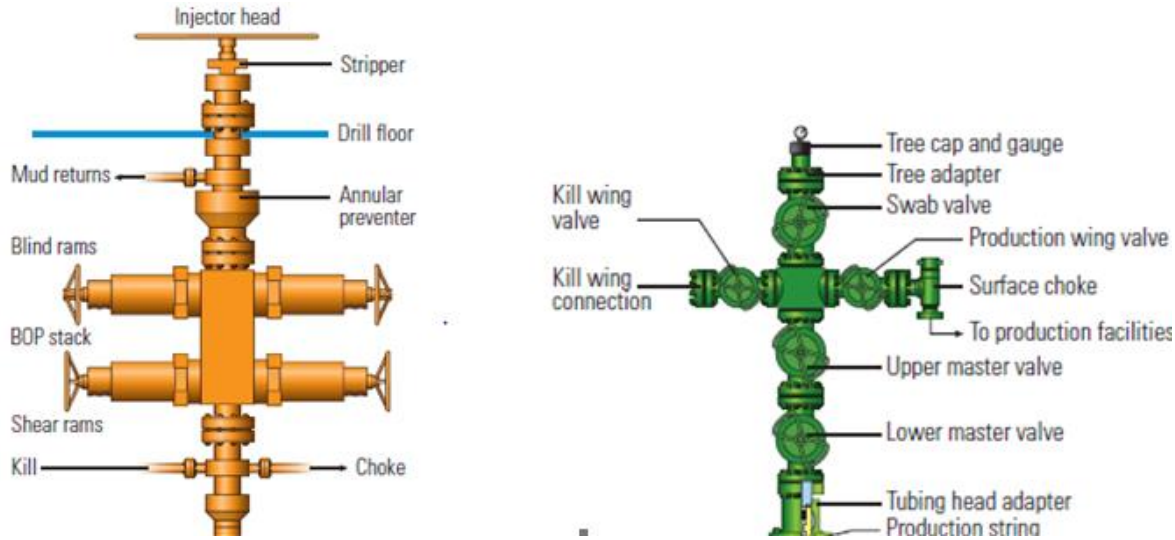

Figure 2- 8. Well head control device. (blowout preventer(left) and Christmass tree(right) [15]

2.5 Drilling fluids

The technology of drilling fluids for effective drilling was known as early as the 1880s, where the mining industry used the traditional air- gas drilling technique to drill pneumatic percussion boreholes [16]. In 256 BC the Chinese used water as a drilling fluid to drill deep water well for brines which aid for softening the formation and removing cutting from the well [17]. The practice of drilling fluid in a closed loop for drilling was introduced in England in 1845 by Robert Beart [18].The introduction of mixing water and plastic material to form an impermeable wall along the wellbore for formation pressure control was introduced in 1880. This technique forms the beginning of science mud engineering [17]. In the 1920s, major changes in the drilling fluid with the addition of additives such as iron oxide, barite, mercury and the usage of bentonite clay was developed to improve fluid rheology, fluid loss control, shale inhibition and resistance to contamination. In 1930 many Engineering companies were formed to produce and research on a more sophisticated drilling mud for drilling more compact, deeper and difficult drilling conditions [19]. In 1960 the invert emulsion oil based fluids were introduced, this provided a significant improvement in drilling performance to the usage of water base drilling fluid. In 1990 synthetic based fluid was developed due to the environmental impact of oil-based fluid which was a major concern to environmental expert, leading to the formation of regulations on the use of oil-based drilling. The synthetic-based fluid also has the high-performance characteristics of the oil based fluid with an advantage of no significant impact to the environment [18]. The usage of

drilling fluids for drilling depends on factors like the technical performance, cost and environmental impact of the fluids. Drilling fluids are the first line of defense during drilling, it is therefore important to properly monitor and control the fluid properties for a safe and efficient drilling operation [20].

2.5.1 Type of drilling fluids

Drilling fluid system is composed of the continuous phase, the discontiuous phase and sometimes gaseous phase which exist either by design or as a result of formation gas entrainment. The continuous phase comprises of liquid while the discontinuous phase comprises of solids[21]. The type of fluid to be used during drilling depends on the well condition and environmental impact. Drilling fluids are sometimes customized to suit the drilling process and the well conditions in order to withstand the pressure in the well. Figure 2- 9 shows the different drilling fluid as classified according to their base.

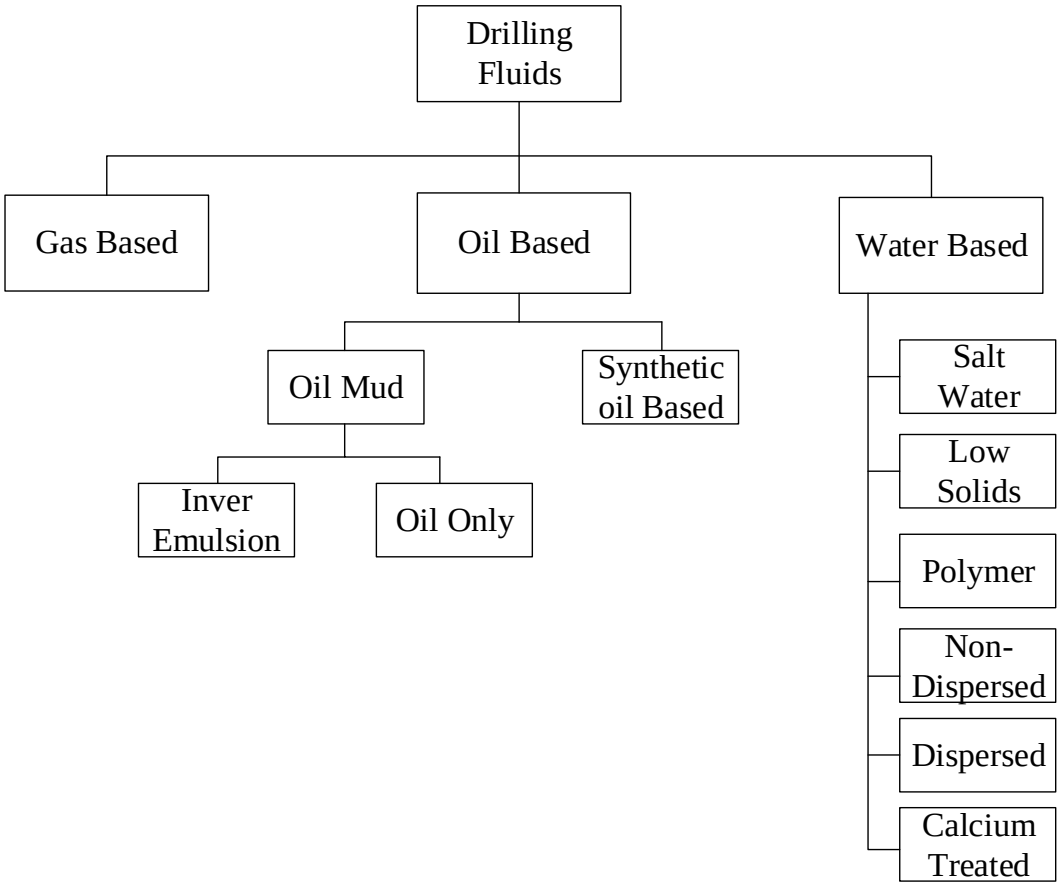

Figure 2- 9. Types of drilling fluids

2.5.1.1 Gaseous / foam based drilling fluid

This is a very effective drilling fluid for drilling dry formation or frozen ground [16]. It requires specialized equipment for safe management of cuttings and drilling fluids. This drilling fluid comprises of the following categories.

- Air: This involves using compressed air or gas into the wellbore at the rate capable of achieving annulus velocity for effective cutting removal. Gaseous based fluid are usually used in underbalanced drilling and characterized with an advantage of high penetration, no solid contamination and no circulation lost [17].
- Foam: This involves the mixture of air and detergent or drilling soap (forming agent) to drill large holes. This process is adequate in a dusty environment in order to suppress dust, remove sticky clay, wet sand and resist small water inflow to the well.
- Aerated fluid: This involves the use of compressed air (sometimes with foam) and drilling fluid (water or mud) to reduce the density of the fluid in the wellbore, such that the hydrostatic pressure within the wellbore is slightly less or balances the formation pressure [16].

2.5.1.2 Water-based drilling fluid

This is is the most common type of drilling fluids, also referred to as aqueous drilling fluid. In order to increase the viscosity of the fluids, thus increasing the carrying capacity of cuttings and improved drilling penetration rate, additive such as clay (bentonite) and polymers are added to produce a colloidal suspension. Other categories of water-based fluids are dispersed, non-dispersed, calcium treated, low solids and saturated salt [16]. This drilling fluid is environmentally friendly, thus, cuttings can be easily disposed.

2.5.1.3 Oil-base drilling fluid

This fluid is mostly used in high temperature wells, drilling deep holes and used in situations where wellbore stability pose a great problem. This fluid reduces friction between the drilling pipe and formation [18]. Drilling with oil fluid is sometimes very expensive mostly because of its environmental impact when disposing of the cuttings. Oil base fluid consists of three categories

- Oil only: This oil based fluid consist only of oil as the liquid phase in its design. Additive of oil based mud may include high molecular weight soaps, surfactants, clay, emulsifiers and wetting agents such as fatty acid and amine derivatives [18].

- Invert Emulsion: This is water-in-oil fluid. The water act as the dispersed phase while oil is the continuous phase.
- Synthetic oil based fluid: This is an improved oil based fluid with no environmental hazard. It is environmentally friendly and therefore mostly used in drilling operation [18].

2.5.2 Purpose of drilling fluid

Drilling fluids as the first line of defense during drilling operation are designed to perform numerous functions. The key functions of drilling fluid are summarized as follows;

- Controlling formation pressure: Drilling fluids are used to control the formation pressure, in doing this it is very important that the hydrostatic pressure of drilling fluid must not exceed the fracture pressure of the rock being drilled else they will be a loss of fluid to the formation. Also, the hydrostatic pressure must exceed the pore (formation) pressure to prevent blowout (inflow of formation fluid into the wellbore).
- Cooling and lubricating drilling bit: Drilling fluid helps in cooling and lubricating drilling bit. The thermal energy of the drill bits is transferred to the drilling fluid which transports the heat to the surface [21].
- Removing cuttings from the wellbore: The efficient removal of cutting from the wellbore to the surface minimizes the possibility of stuck pipe. To accomplish this, mud rheology and flow rate are adjusted for efficient carrying capacity while avoiding high equivalent circulating density [21].
- Maintaining wellbore stability: Drilling fluids must be able to stabilize the wellbore and the integrity of the cuttings by effectively controlling the fluid effect on the formation [21].
- Collection of geological Information: The drilled cuttings transported to the surface by the drilling mud can be analysed to derive information about the formation.
- Transmit Hydraulic Energy to the bit: Since the drilling fluids are discharged through the nozzle of the bit, hydraulic energy is released to the downhole tools which steer the bit [21].

2.5.3 Drilling fluid properties

The property of a drilling fluid determines safe and efficient drilling procedure. The two main principal properties of drilling fluid for adequate functioning are density (mud weight) and viscosity.

2.5.3.1 Density

The hydrostatic pressure of a drilling mud depends solely on the depth of the formation, the density of the fluid and the geological condition [19]. The density of drilling fluids can be estimated from basic principle using equation (2.1).

$$p = \rho g h \tag{2.1}$$

Where p is the pressure, ρ is the density, g is the acceleration due to gravity and h is the depth.

The density of a drilling fluid determines the hydrostatic pressure into the wellbore, thereby forming the basis for formation pressure control. In controlling the formation fluid it is sometimes a natural possibility to increase mud density above the actually needed density, but this poses great disadvantages such as increased pore (formation) pressure causing the well to collapse, loss of drilling fluid and increased drilling cost [19].

2.5.3.2 Viscosity

This is the ratio of shear stress to shear rate, it is the internal resistance of a fluid in motion. The higher the viscosity of a fluid the slower the flow rate of the fluid. The viscosity of a fluid varies depending on the type of fluids. The viscosity of some fluids is expressed via coefficient while in most fluids it depends on some properties not limited to temperature, pressure and share rate. Viscosity is expressed mathematically as;

$$\mu = \frac{\tau}{\gamma} \tag{1.2}$$

Where μ is the viscosity, τ is the stress and γ is the shear rates.

Fluids with constant viscosity are commonly referred to as Newtonian fluids, where their shear rate is independent of the viscosity of the fluids. An example of Newtonian fluids are water, mineral oil, alcohol etc. Some fluids such as pseudoplastic (shear thinning) and dilatant (shear thickening) are described as non-Newtonian fluids. This fluid viscosity

changes with shear rate and also with time. If a shear stress is applied to Non-Newtonian fluids, the fluid thickens and gets thicker as stress increases, therefore acting like a solid, but as stress is reduced it return back to its normal liquid form [20]. Examples of non-Newtonian fluids are drilling fluids, paint, yoghurt, starch etc. The instrument mostly used to measure the viscosity of drilling fluid are marsh funnel, viscometer (piston, rotational U-tube) and rheometer. Figure 2- 10 show the change in shear rate with the viscosity of Newtonian and non -Newtonian fluids.

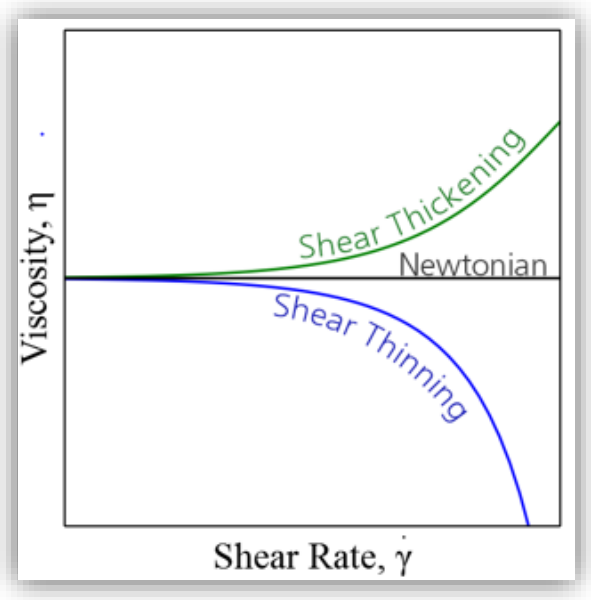

Figure 2- 10. Newtonian and Non-Newtonian Fluids [20]

2.5.4 Drilling mud flow

Drilling fluid flows in a closed circulation loop, lifting cutting, cooling the bits and then release waste materials to the surface. The fluids are subjected to numerous processes which may alter its physical characteristics during the circulation system in the loop. Figure 2- 11 show the drilling fluid circulation system.

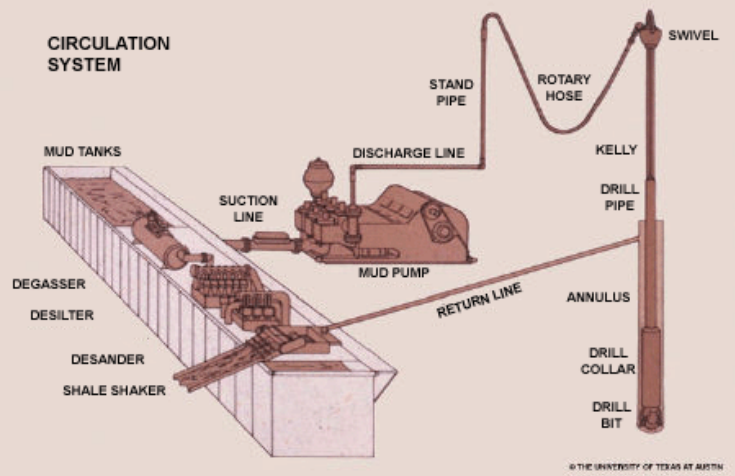

Figure 2- 11. Drilling fluid flow circulation System [22].

2.5.5 Components of drilling fluid Circulation System

The drilling circulation system consists of various components in the circulation system for effective drilling mud flow. The major components of the drilling fluid flow circulation system are;

1. Mud Pump: This is the core component for effective drilling fluid flow system. This equipment generates the pressure necessary to pump the fluids at various pressure into the wellbore through the standpipe and the rotary hose which connect the pipe to the drilling equipment via the swivel [23].
2. Drilling string: This consist of the Kelly, drill pipe and the drill collar. The drilling fluid flows at high velocity and pressure through the Kelly, drill pipe, drill collar and then out of the nozzle of the bit to act against the bottom hole pressure (BHP). From the bottom of the well the mud returns up the annulus (between the drill string and borehole wall) degraded by the bottom hole conditions, dehydrated and carrying cuttings [21]. The ability of the fluid to transport cuttings out of the wellbore solely depends on the flow velocity (which must be greater than the settling velocity of the cuttings), density and viscosity of the fluids [23].
3. Cleaning system: As the drilling fluid returns to the surface through the flow line, it carries cutting and other substances, thus altering the mud density, rheology and other properties. Therefore to retain the original characteristics of the fluid, to achieve its original functions, the fluid is subjected to retreatment cleaning processes. Cleaning system may consist of the following;

- Shale shaker: This is responsible for removing larger solid formations in the fluid. It is made with a disperser plate, arranged either horizontally or vertically, as the mud flows through the plate, it shakes/vibrate and thus filtering out the mud from the cuttings/particles [23]. Figure 2- 12 shows an example of different shale shakers used in oil/gas rig.

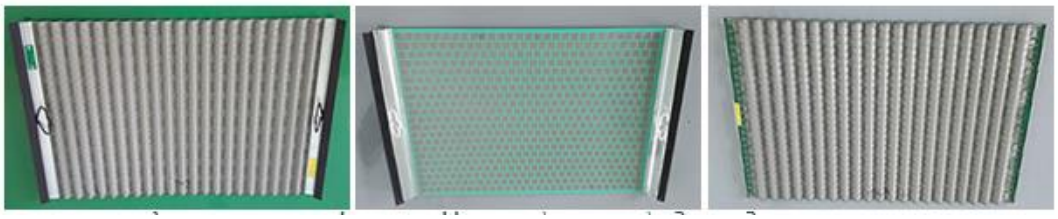

Figure 2- 12. Shale shakers [23]

- Desander and desilter: Particles that escape the shale shakers are picked up by the desander which is directly located below the shale shaker while desilter removes the particles which have to escape the desander.
- Degasser: This is responsible for removing small entrained gas bubbles such as hydrogen sulphide, carbon dioxide and natural gas left in the mud.

4. Mud tank: This is where the fluids are stored and prepared for the next circulation into the well. Fresh additives are added and mud weight is adjusted before the mud is pumped back into the well.

2.5.6 Monitored measurands on drilling fluid flow system

During drilling, measurements are taken both below and above the wellbore for safe and efficient drilling operation. Smart reliable sensors and transmitters are used to enable drilling Engineers to take important decisions when necessary. Figure 2- 13 shows a P&ID diagram of the variables that can be monitored during drilling operations.

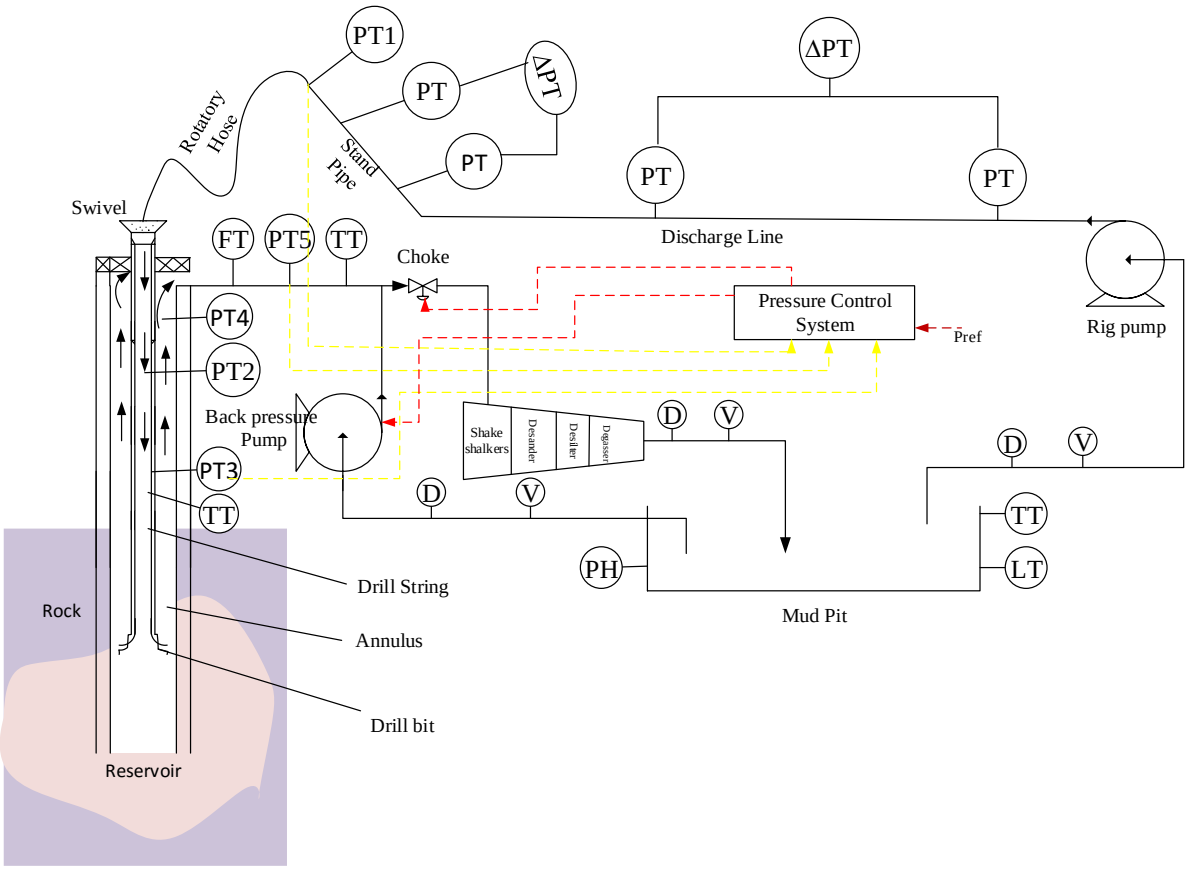

Figure 2- 13. P&ID diagram of monitored measurands during drilling as used in the oil and gas industry

- Pressure (PT): Pressure is the first requirements to be considered for every drilling operation. The pore pressure and the fracture pressure must be kept within the drilling window, therefore, accurate pressure measurement must be taken throughout the circulating system.

$$\text{BHP} = H_p + F_p + B_p \tag{2.3}$$

Where H_p is the hydrostatic pressure which is proportional to drilling fluid density, F_p is the frictional pressure which is dependent on the flow regime and B_p is the back pressure which can be controlled with a choke valve. The mud pump produces pressure needed for the fluid flow throughout the entire system. This pressure produced by the pump together with the frictional pressure drop will give a pressure called the standpipe pressure which is measured at the standpipe [16].

From Figure 2- 13 the combination of annulus discharge pressure (PT_5) and standpipe pressure (PT_1) can be used for early kick detection, wellbore breathing and drill string sticking. Bottom hole pressure (PT_3) can be measured with the help of electromechanical device located down the hole through a high strength bi-directional coaxial cable.

- Temperature (TT): This affects the conditions of the drilling fluids and drilling equipment during drilling. In order to minimize the effect of temperature, adequate measurement and control must be provided at all times during the operations. Since drilling fluids perform the function of both cooling and lubrications, measurements are taken both below and above the wellbore to correlate adequate temperature of the fluids needed while drilling. In the oil and gas drilling rig, cooling towers are always available to cool the fluids before it is used again.

- Flow rate (FT): Continuous flow measurement in the return flow line and the flow line into the well gives a general overview of what is going on in the wellbore, therefore helping drilling Engineers to take important decisions during operations. Venturi flow meter can be used to measure the outflow from the annulus, but currently, Coriolis, peddler and sometimes electromagnetic flowmeter are installed in the return flow line to measure the flow rate out from the well.

- Density (D): This is the weight of the drilling fluid which is directly proportional to the hydrostatic pressure. Drilling fluid must have the right density in order to keep the hydrostatic pressure in check. The density of the fluid is usually measured along the flow line and additive such as calcium carbonate, barite, and hematite are added when required to control the density of the drilling fluids. The fluid density can also be estimated using the pressure at the standpipe [23].

- Viscosity (V): This determines the lifting ability and the preventing nature of drilling fluids to sink back into the wellbore. High viscosity is desired for cutting lifting, just as low viscosity is also desired at the surface of the wellbore for cutting filtration, thus there must be a reference point on the viscosity of the fluid. The viscosity of the fluid is usually measured along the flow line and additive such as bentonite or polymer are added to control fluid viscosity.

- PH: This indicates the acidic or alkalinity of a drilling fluid. A low pH indicates acidic fluids which incite corrosion of drilling equipment which is not desirable. The pH of drilling fluids are usually measured at the fluid tank or pit and a normal pH of drilling fluid is 9.5 -10.5 which is alkaline in nature [16].

- Level: Drilling Engineers sometimes uses the level of the fluid in the tank to determine kick or wellbore breathing. Measuring the level of the fluid in the tank helps in determining the total volume of the fluid available in the tank. For the purpose of safety, it is recommended that the total volume of the fluid in the tank should be three times the volume of the well [16].

2.6 Measurement techniques for Newtonian and Non-Newtonian fluids

The flow rate measurement of drilling fluids is critically important for safe and efficient drilling operations. Accurate information from the flow rate will help driller, mud specialist and mud engineers detect early kick or well breathing, thus preventing blowout or loss of drilling fluids [24]. There are various flow meters which have been developed for measuring drilling mud, but the selection of the flow meters solely depends on measurement principles, capability, construction, maintenance, cost and accuracy of the meter.

Traditionally, drilling fluids are measured by monitoring the flow rate of fluids in and out of the well. During drilling the fluids flowing into the well are indirectly measured by counting the pump strokes[8] which is then compared with the measurement from a paddle wheel flow meter which measures the fluid flowing out from the well [25]. Figure 2- 14 shows the traditional paddle flow meter installed to measure outflow from the well.

[8] Stroke counter counting the number of strokes of the pump piston per minutes to determine flow rate

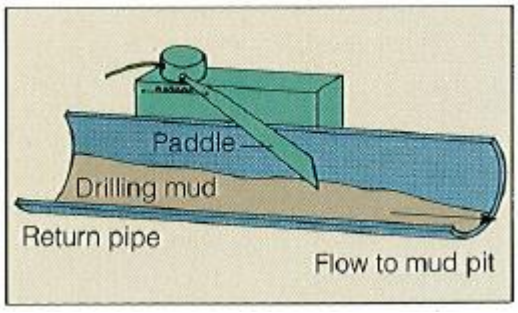

Figure 2- 14. Paddle wheel flow meter [25]

However this measurement technique is slow and sometimes inaccurate, thus impeding early kick detection. The inefficiency of the devices may be as follows;

- Pump efficiency: Factors such as valve seal, fluids compositions and discharge pressure affect the efficiency of the pump.
- Paddle flow meter: This flow meter is inaccurate and prone to damages due to contacts from cuttings and drilling fluids. It varies according to viscosity, density and level of the flow line. Calibrated paddle flow meter are only accurate up to 10 to 15 percent while the uncalibrated accounts for 40% error [25].
- Human Error: They is always the possibility of miscounting the pump strokes.
- Reactive approach: They is always difficulties in identifying potential problems since the flow rate is not measured in real time [24].

Sometimes electromagnetic flow meters is used for measuring the mud flow rate, but it has limitation based on its measurement principles which only measures conducting fluids [26]. Preference is going to Coriolis flow meter based on its ability to cope with all drilling fluids, but still it also have a limitation of operating pressure,can not measure two phase-flow(gas entrained mud) and requires heavy installations.

The limitation of the current flow meters has driven recent studies to focus on model-based flow rate estimation using open channel venturi for intelligent drilling operation since the flow rate out from the well flows into an open channel in the oil and gas rig.

2.6.1 Features of non-Newtonian flow metering

Non-Newtonian fluids are very viscous and highly dependent on many properties such as temperature, vibrational motion, and pressure. These fluids also have complexity in its

rheology, thus, fluid measurement of non-Newtonian fluids is a great challenge but also the most successful fluid used for drilling. Various empirical models have been developed to model non-Newtonian fluids under different flow conditions based on curve fittings [27, 23] with accuracy been a very critical challenge. Figure 2- 15 shows the different models that describe non-Newtonian fluids in relation to the linear Newtonian model.

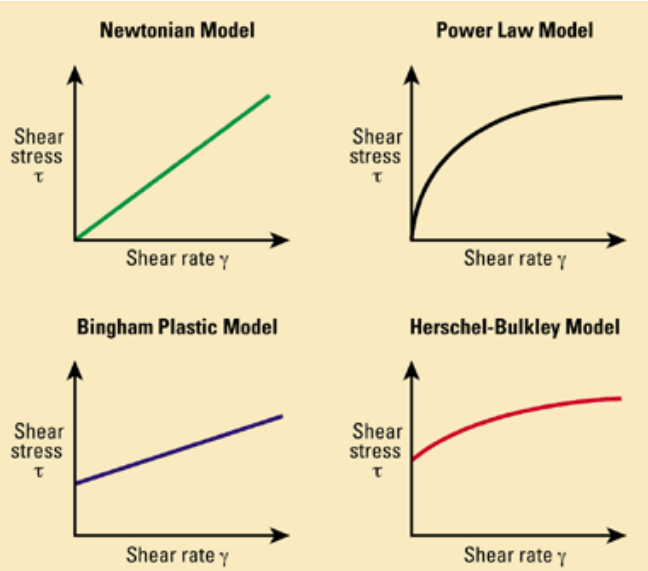

Figure 2- 15. Drilling fluids different viscosity models [21]

2.6.1.1 Power law model

This is a non-linear model that describes the behavior of non-Newtonian fluids to some extent by exploring the relationship between shear stress and shear rate. The model only describes fluid behavior within a range of shear rates of which the coefficient is fitted [23, 28]. The relationship between viscosity and shear rate is described as;

$$\tau = k\gamma^n \tag{2.4}$$

Where τ is the shear stress, K is the flow consistency index, γ is the shear rate and n is the flow behavior index.

This model predicts that effective viscosity of the fluid will decrease, with an increase in shear rate [21, 29].

2.6.1.2 Bingham plastic model

This model describes fluids of higher shear rates. It is described mathematically as;

$$\tau = Y_p + P_v\gamma \tag{2.5}$$

Where Y_p is the yield point which is the threshold stress and P_v is the plastic viscosity of the fluid. In a situation where we have a fast drilling fluid, it is recommended that the yield point should be as low as possible while the plastic viscosity must be high to some extent for easy carrying of the cuttings from the wellbore [21].

2.6.1.3 Herschel-Bulkley model

This model describes fluid viscosity at a higher shear rate, thus solving the problem of power law viscosity model. It is also called the modified power law model [29]. The relationship between shear stress and shear rate of this model is described as;

$$\tau = \tau_o + k\gamma^n \tag{2.6}$$

Where τ_o the yield stress and τ is the shear stress.

When the shear stress is less than the yield stress Herschel- Bulkley fluids turns to solid states, thus fluids cannot flow and when yield stress is zero the model becomes a Newtonian fluid model. This model is mostly used to describe drilling fluids behaviors and is mostly preferred to power law model or Bingham plastic model because of its accuracy [29, 21].

2.6.2 Groups of Non-Newtonian fluids

Non-Newtonian fluids are broadly divided into three major groups; this are the time dependent fluids, time independent fluids and viscoelastic fluids [27].

2.6.2.1 Time dependent fluids

These are fluids whose viscosity changes with time at a given shear rate and constant temperature. The longer a time dependent fluid is subjected to shear stress the more the viscosity of the fluid varies [27]. The two main type of time dependent fluids are the

thixotropic[9] and rheopectic[10] fluids. An example of thixotropic fluid is pseudoplastic fluids while rheopectic fluid is gypsum paste.

2.6.2.2 Time Independent fluids

There are fluids whose viscosity is solely dependent on the instantaneous stress at that particular point. The apparent viscosity of time-independent fluid varies with increased stress. The two main type of time independent fluids are the shear thickening or dilatant[11] fluid and shear thinning or pseudoplastic[12] fluids. The Prominent model used to model this group of fluids are the power of law and Herschel-Bulkley model [27].

2.6.2.3 Viscoelastic fluids

These are fluids with both elastic and viscous properties, there include shear thinning, extension thickening, and time dependent fluids. These fluids can be modeled by combining Newton's law of viscous fluid and Hooks law of elastic material [27].

2.6.3 Challenges of non-Newtonian flow metering

If viscosity is one of the input parameters for any flow metering, the major challenges that will be encountered are the lack of a general model that can describe the behavior of non-Newtonian fluids. [27]. The Power of law and Herschel-Bulkley are mainly used to describe dilatant and pseudoplastic fluids. Moreover, most of the methods used in developing modern flow meters require the addition of correction factor to the initial viscosity of the fluids to avoid unnecessary errors of the flow meters [30].

In using ultrasonic flow meters (single beam) in measuring non-Newtonian fluids, variation in the velocity profile and change in flow regime will lead to variation of the fluids temperature, therefore leading to an unacceptable errors in the flow measurement [30].

However, the use of electromagnetic flowmeter to measure non-Newtonian fluids is also a big challenge due to the fact that it can only measure conducting drilling fluids [26].

In using open Channel Venturi for flow measurement, it poses a great challenge due to the fact that it is not pressurized, but rather the level measurement of the flow is used to estimate

[9] fluids where the apparent viscosity decreases with time
[10] Fluids where the apparent viscosity increases with time
[11] Fluids where apparent viscosity increase with increased stress.
[12] Fluids where apparent viscosity decreases with increased stress.

the flow rate of the fluid. In other to achieve high accuracy, attention must be given to the position of the level measurements, the position of the venturi flume and the type of level sensors used to measure flow height.

2.7 Venturi flow metering

Venturi flow meter is a differential based flow meter whose principle is based on Bernoulli principle and continuity equation. It is classified as one of the obstruction flow meters with a lesser pressure drop as compared to orifice plate flow meter. Venturi flow meter consist of an inlet section which is of equal area as the pipe, a converging section from the initial pipe which causes an increase in velocity and decrease in pressure, a minimized area section called the throat where velocity is constant so that the decreased pressure can be measured and then it gradually increasing section (diverging) to the initial pipe area. This flowmeter has no moving parts, less sensible to wear and can be used to measure both liquid and gas.

The volume flow rate of a venturi flow meter is given mathematically as;

$$Q = \frac{CA_2}{\sqrt{1 - \left({}^{A_2}/_{A_1}\right)^2}} \sqrt{\frac{2[(P_1 + g\rho z_1) - (P_2 + g\rho z_2)]}{\rho}} \qquad (2.7)$$

Where P is the fluid pressure, g is the acceleration of gravity A_1 is the initial cross sectional area, A_2 is the throat cross sectional area, ρ is the fluid density, z is the pipe elevation relative to a specific reference elevation and C is the discharge coefficient factor which is a function of Reynolds number and diameter of the pipe ratio.

It is also interested to note that if the pipe laid horizontally, the elevation term z_1 and z_2 are the same and thus cancels out. Figure 2- 16 shows a venturi flow meter.

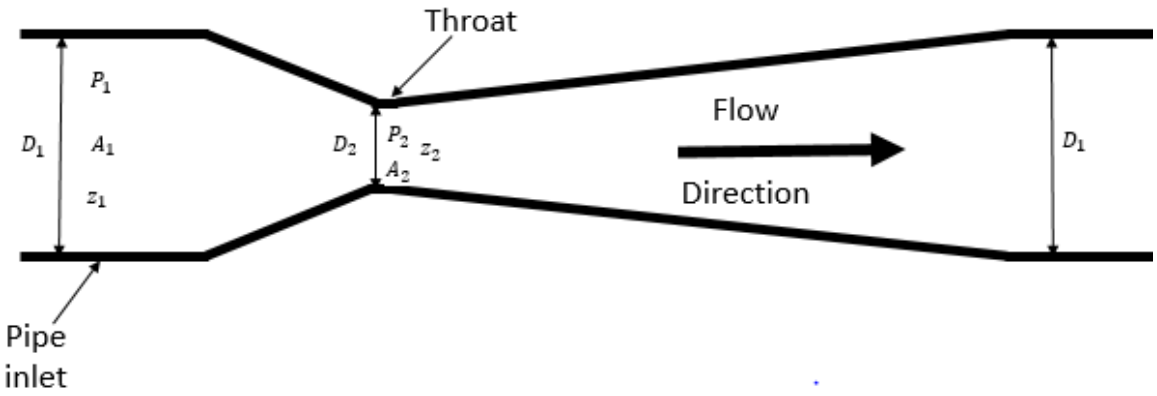

Figure 2- 16. Venturi flow meter

There are various designed construction of venturi flow meter which depends on the head loss (pressure drop). The most popular designed flumes are the classical Herschel venturi and Parshall (short throated).

2.7.1 Classical Venturi

This is also called the Herschel venturi, it was designed in 1887 by Clemens Herschel. This flow meter has a flow coefficient of 0.984 with an uncertainty of ±0.75% of the flow rate [31]. In measuring the pressure, six to eight pressure taps connects the throat, which is then connected to an annular chamber, thus providing an average pressure reading [31]. Figure 2-17 show the classical venturi flow meter.

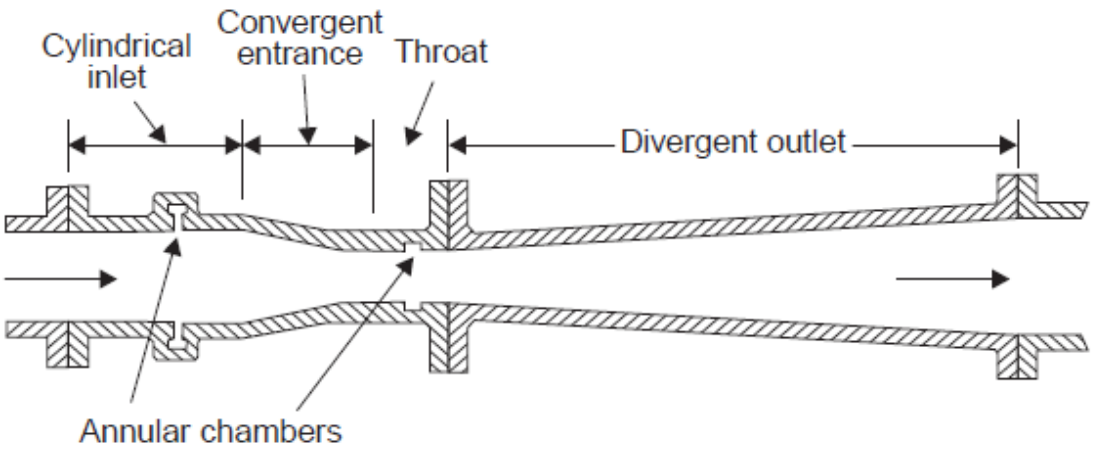

Figure 2- 17. Classical Venturi flow meter [31]

2.7.2 Short form Venturi

This type of venturi maintains all the advantage of the classical venturi with a reduced cost, shorter length, increased entrance angle from 7° to 21° and the annular chamber replaced by a single pressure tap. The flow coefficient of the short throated venturi is 0.985 with an uncertainty of ±1.5% of flow rate [31]. In measuring the pressure, the pressure tap is located at one-quarter to one-half pipe diameter upstream of the inlet cone and at the middle of the throat section [31]. Figure 2- 18 show the short throated venturi flow meter.

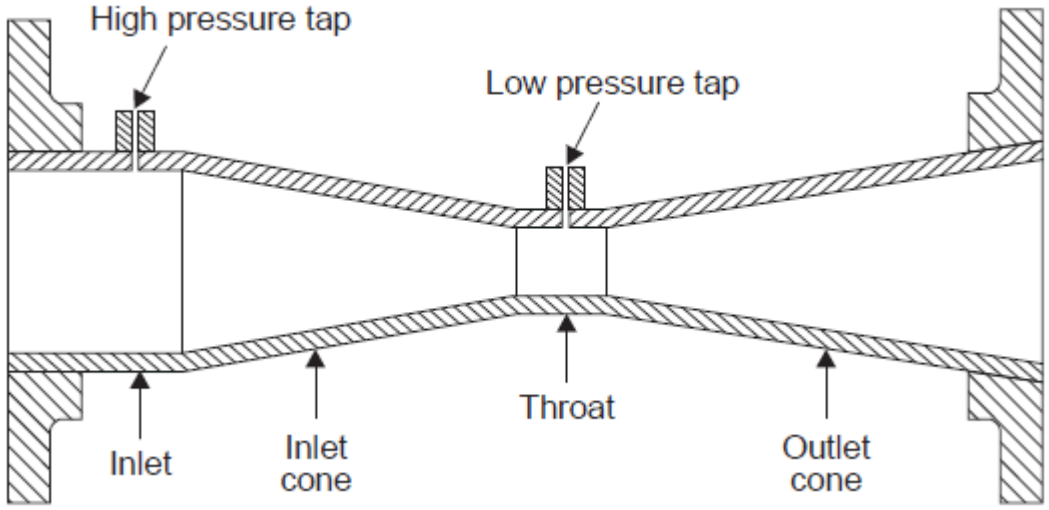

Figure 2- 18. Short form venturi flow meter [31]

2.8 Venturi Secondary monitoring device

They are various secondary measuring devices which are used with the venturi flow meter for adequate measurement. These devices can be subdivided based on open channel venturi and closed conduit venturi.

2.8.1 Open channel Venturi

An open channel venturi is a flow meter open to the atmosphere. It uses level measurements instead of pressure measurements to correlate for the flow measurement. They are various ways of estimating flow rate in an open channel, some of which includes, the dilution method, timed gravitational method, velocity method, and hydraulic structure method. The most used method is the hydraulic structure method where measurement of the fluid depth in the throat and the upstream section are done in order to correlate the flow rate. Open channel venturi is characterized as a self-cleaning flow meter which enables measurement of solid

impurities like industrial waste, sewage and irrigation systems. Figure 2- 19 show an open channel venturi flow meter.

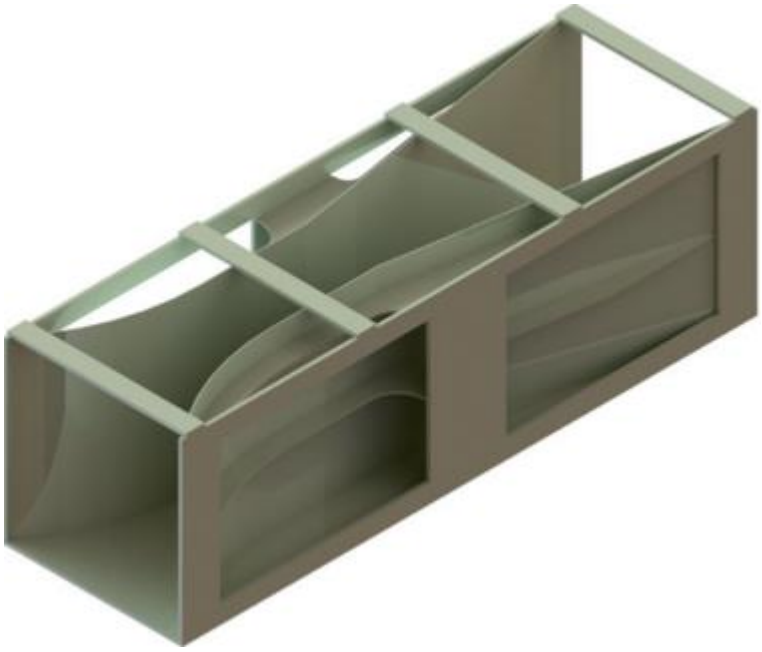

Figure 2- 19. Open channel Venturi [31]

In order to estimate the change in fluid depth, various level measurements do exist which are based on some unique characteristic such as the design, accuracy and construction. Examples of level measurement devices used in the open venturi channel are; Ultrasonic level sensors, level gauges and gamma level measurement.

2.8.1.1 Ultrasonic level sensor

This sensor does not have any direct contact with the fluids. Its measurement principle is based on high frequency sound pulse which is directed toward the surface of the fluid, the time of reflection and receiving the pulse signal is used to correlate the level of the fluid, that is,

$$L = \frac{c_f T}{2} \tag{2.8}$$

Where c_f is the speed of sound, T is the time of travel and L is the level.

Since the speed of sound is a function of chemical composition and temperature, thus foam or change in gas density is a major challenge that affects the accuracy of this type of level sensor [32].

2.8.1.2 Gamma level measurement

This is a nuclear based sensor with a unique characteristic of non-contact with the fluid. Its operating principle is based on gamma source emitting radiations and a detector mounted on the opposite side of the source which absorbed the gamma ray. This level measurement economically compensates for the disadvantages of the ultrasonic sensor but requires high safety check in its operations.

2.8.1.3 Staff gages

This is the easiest level measurement, it gives a quick level measurement and definitely not reliable based on human error. It helps the field operators to have a quick visual indication of the level. It is usually designed with a heavy metal, has a direct contact with the fluid and is directly mounted on the body of the open channel venturi.

2.8.2 Closed conduit venturi

A closed conduit venturi is a venturi with boundaries, hence, also call pressure flow conduit. The surface of a closed conduit venturi is not exposed to the atmosphere as compared with the open channel venturi. The measurement is done by determining the differential pressure drop between the throat and the upstream section. In measuring the pressure a suitable differential pressure device is used as a secondary measuring device to determine this pressure difference which is then used to correlate the flow rate. An example of the pressure transducer that can be used in a closed conduit venturi based on different principles of operation are; the capacitive pressure sensor, strain-gage pressure sensor, and linear variable differential transformer pressure transducer (LVDT). Figure 2- 20 show a closed conduit venturi with positions where the sensors can be installed.

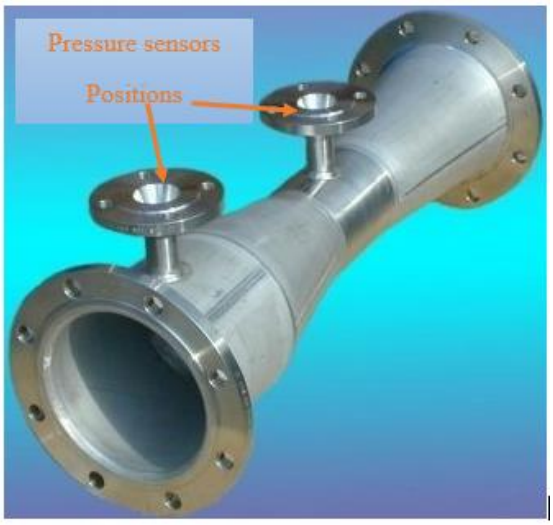

Figure 2- 20. Closed Conduit Venturi [33]

2.9 Flow regime

This shows the relationship between velocity and the mode in which the substances are transported in the pipe or channel. Adequate information about the flow regime is very important in measuring the pressure or level, stability and safety of a flow system [34]. Reynolds discovered during an experimental procedure with a dye that, as the velocity of the fluid increases, the flow sequence changes from laminar to turbulent flow [35, 36]. Figure 2-21 shows the flow regime categories.

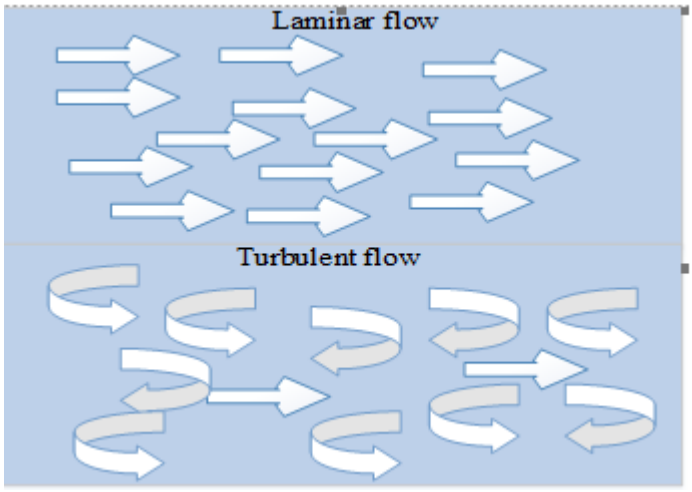

Figure 2- 21. Flow regime

2.9.1 Laminar flow

This is also called a streamline flow, here fluids flow at a low velocity and in an orderly manner without any macroscopic change in layers. The velocity profile of a laminar flow is parabolic with a pressure or level proportional to the flow rate [35]. A simple analytical solution is always used to estimate the pressure or level difference during laminar flow in order to correlate the flow rate. For the laminar flow, the discharge flow is simply determined by measuring the pressure or level at the throat [37]. Also based on Reynolds research laminar flow has a value of Reynolds number[13] less than or equal to 2000 [36].

2.9.2 Turbulent flow

This is usually observed when the flow rate is increased and characterized by an irregular fluctuating flow structure. The velocity profile of a turbulent flow is flattened at the end with a pressure or level which increases more rapidly almost as the square of the flow rate [34]. Empirical correlations are used in estimating the pressure or level difference during turbulent flow in order to correlate the flow rate. Measuring the pressure or level differences at the upstream and the throat of the venturi can be used to estimate the discharged turbulent flow [36]. Turbulent flow has a value of Reynolds number of 4000 and above [35].

2.10 Computational Fluid Dynamics (CFD)

This is the science of analyzing a system, and solving mathematical equations such as conservation of mass, momentum and energy balance for quick efficient prediction of the fluid flows, heat transfer, mass transfer, chemical reactions and all other related phenomena. CFD can be used in many industries such as electric power plant, chemical process plant, marine engineering and lots more. The simulation results of CFD design is very crucial in taking the final decision during the conceptual studies of new design, product development and troubleshooting of existing systems [38].

[13] Reynolds number describes how a meter will react to a variation in fluids from gaseous state to liquid state

$$\mathrm{R}e = \frac{\rho D v}{\mu}$$

where D is the diameter of the flow channel, v is the average flow velocity, ρ is the fluid density and μ is the fluid viscosity

2.10.1 An overview of CFD model dedicated to non-Newtonian fluids

In [39] the flow of time independent non-Newtonian fluid through a vibrated tube was modeled both experimentally and with CFD based on SIMPLEC process and differential scheme (Quadratic upwind scheme). The flow rate was solved as a two dimensional problem in cylindrical coordinates using the power law model with high viscous carboxyl-methyl-cellulose sodium salt in dilute water, density of $1000kgm^{-3}$, a consistency index of $1.47kgs^{n-1}m^{-1}$ and flow behavior index of 0.57. The effect of flow rate on various amplitude change, frequency of sinusoidal vibration and rheological parameter on the tube was investigated.

From the result of [39] the vibrational force at the wall of the tube affect the fluid viscosity thereby affecting the fluid flow. Figure 2- 22 shows the effect of vibration frequency and amplitude, as the frequency or amplitude of vibration increases so is the enhancement ratio[14]. This confirms that cuttings can be easily separated from viscous drilling fluids at the surface of the wellbore by subjecting the fluids to some shaking (shale shakers).

[14] Ratio of flow rate when tube was vibrating to the steady state flow rate

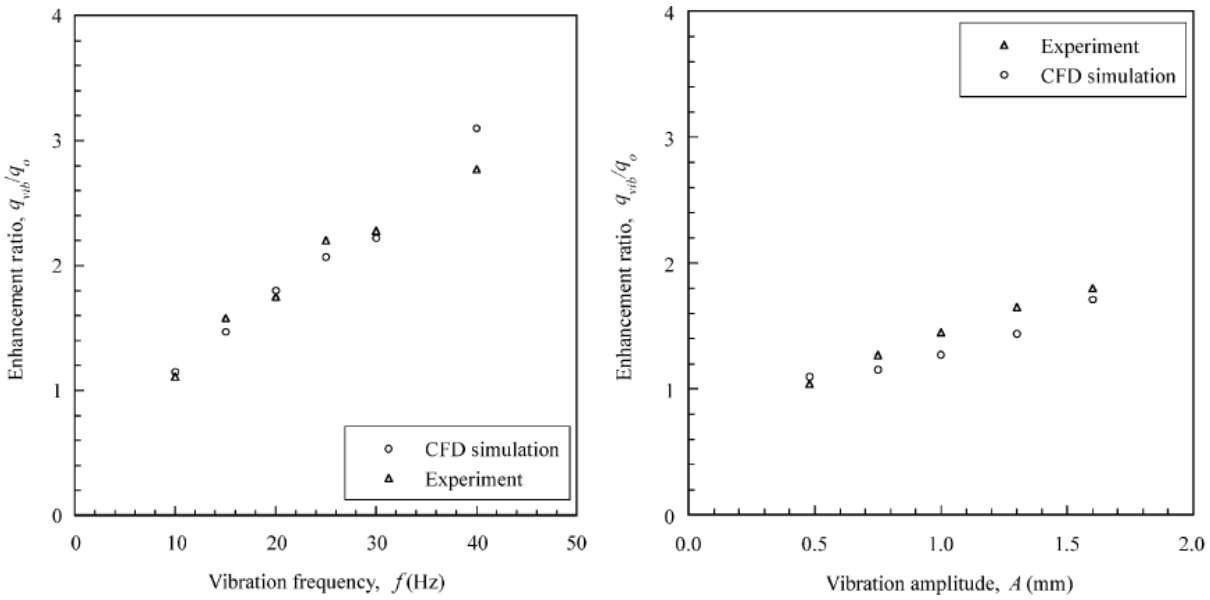

Figure 2- 22. Effect of Vibration frequency and amplitude on flow rate [39]

It is also seen in [39], the rheological parameter using a Herschel-Bulkley fluid shows higher the value of the consistency index with higher flow rate and the behavior index changes with flow rate as shown in Figure 2- 23. When a shear thinning or pseudoplastic fluid (n<1) is subjected to vibration, flow rate of the fluid increases while with shear thickening or dilatant fluids (n>1) reduced flow rate is been experienced.

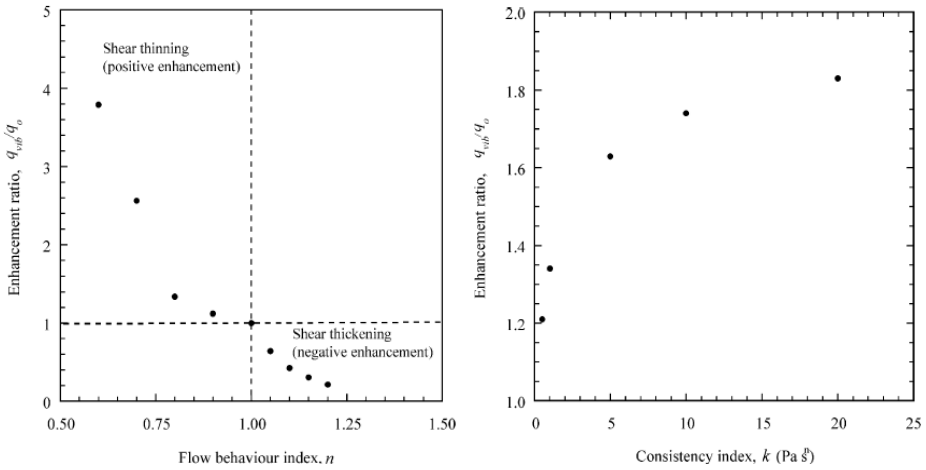

Figure 2- 23. Effect of Consistency Index and Flow behavior index on flow rate: Herschel-Bulkey fluid: k = 1, n = 0.8, ρ = 1000kgm-3 [39].

In [40], a CFD model using FLUENT 6.3 to predict the velocity and pressure drop across an elbow of non-Newtonian and gas non –Newtonian liquid flow through an elbow was investigated.Table 1 shows the range of parameters used in the model.

Table 1. CFD Parameters used in [40] to predict velocity and pressure drop

Measurement Type	Range
Liquid and Flow properties	
Concentration of SCMC Solution (kg/m^3)	0.2 to 0.8
Flow behavior index	$0.6015 \leq n' \leq 0.9013$
Consistency index (Ns$^{n'}$/m^2)	$0.0142 \leq K' \leq 0.7112$
Density (kg/m^3)	$1001.69 \leq \rho \leq 1003.83$
Liquid Flow Rate $Q_l \times 10^5$(m^3/s)	3.75 to 29.83
Gas Flow Rate $Q_g \times 10^5$(m^3/s)	2.90 to 44.75
Reynolds Number	$47.51 \leq R_e \leq 2234.21$
Dean Number	$32.41 \leq D_e \leq 2130.23$
Pressure Drop (Experimental) (kPa)	$0.1333 \leq \Delta P \leq 45.46$
Elbow	
Angle of Elbow	45° to 135°
45^0 elbow	Radius of curvature = 0.011m Linear length of the elbow = 0.014m
90^0 elbow	Radius of curvature = 0.022m Linear length of the elbow = 0.011m
135^0 elbow	Radius of curvature = 0.017m Linear length of the elbow = 0.016m

The result in [40] reveals that due to centrifugal force the location of the maximum velocity of non- Newtonian liquid flow through an elbow is at the inner wall of the elbow while the maximum pressure is at the outer wall and more away from the center of curvature. **Error! Reference source not found.**CFD contour plot of the pressure and velocity inside the pipe of

135^{o} elbow.

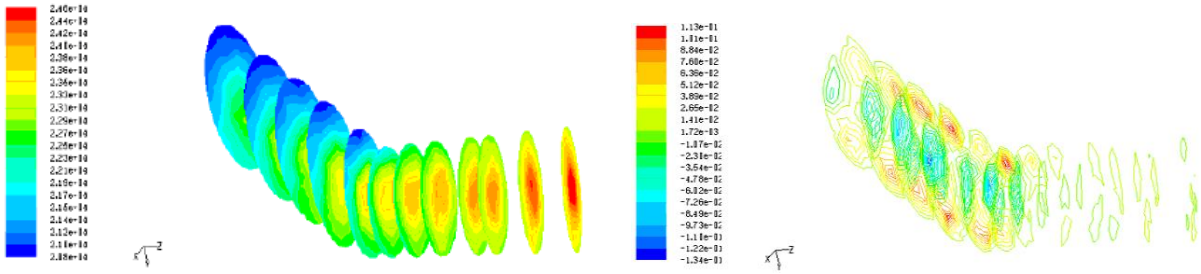

Figure 2- 24. Contour plot of pressure inside of 135^{o} elbow at flow rate of 21.94×10^{-5} (left) and Contour plot of velocity inside of 135^{o} elbow at flow rate of 21.94×10^{-5}(Right) [40]

In the case of gas non-Newtonian liquid flow, according to [40] as the mixture of gas and SCMC solution enters the elbow, due to centrifugal force, lower velocity and higher static pressure exist in the outer wall, thus higher density liquid moves to the outer wall while gas with less low density fluids moves to the inner wall where lower pressure exists. Figure 2- 25 shows that the air velocity at the inner wall is higher while the pressure lower.

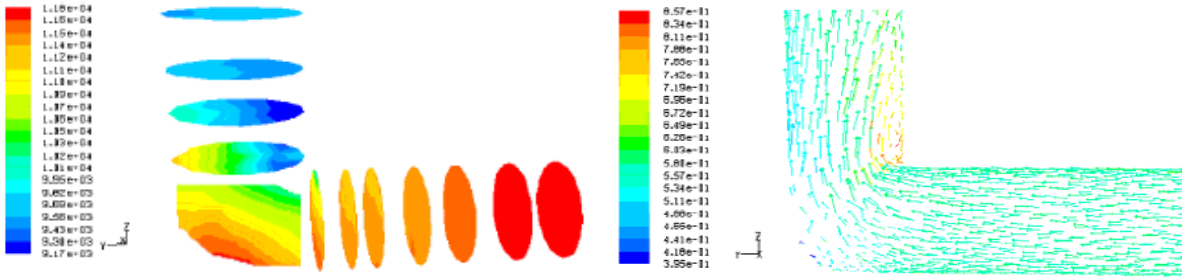

Figure 2- 25. Contour plot of pressure of air of 90^{o} elbow at SCMC velocity 1.733ms^{-1} gas velocity 2.3933ms^{-1}(Left) and Contour plot of velocity of air of 90^{o} elbow at SCMC velocity 1.733ms^{-1} gas velocity 2.3933ms^{-1} (Right) [40]

In [41], the possibility of transporting highly viscous non-Newtonian fluid using core-annular fluid lubrication method was studied using CFD ANSYS FLUENT 14.5 in a horizontal pipe of diameter 0.003m and length of 0.025m. The pressure drop and the force exerted on the fluid flow was analysed. Shear thickening fluid with a consistency index (μ) of 10 Pa.s^n, power of law index (n) of 1.2 and density of 1100kgm^{-3} was used as the core fluid while Newtonian fluid (water) of consistency index of 1.003 × 10^{-3}Pa.$s^n$and density 998.2kgm^{-3} which is added into the annular space through a nozzle was considered as the annular fluid.

From the result in [41], it is observed that when only non-Newtonian fluid is present in the pipe with a constant inlet velocity, showing higher pressure drop and a slug flow velocity profile as compared to the core- annular fluid which demonstrated a lower pressure drop, thus reducing the pumping power and reduced energy loss. Figure 2- 26 shows the significant pressure drop when ever fluids mixed together.

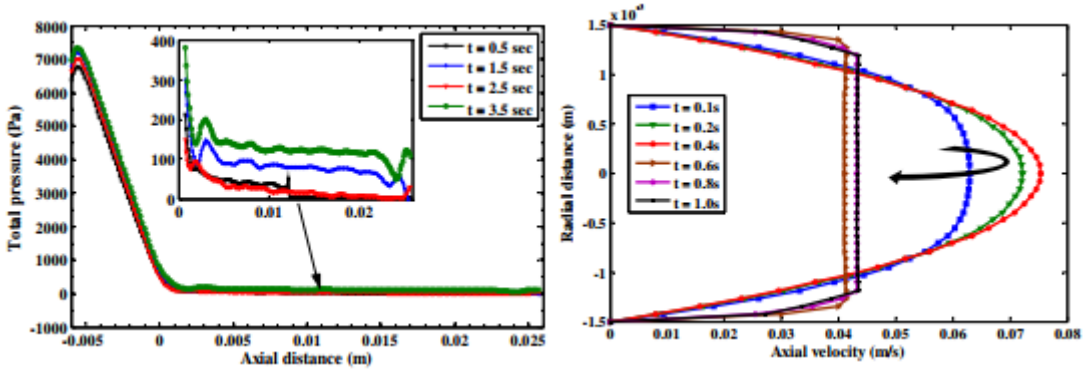

Figure 2- 26. Axial pressure variation at different time (Left) and Velocity profile in the region (Right) [41]

3 Overview of University College of Southeast Norway rig with open Venturi-channel

Appendix 2 shows the updated P&ID diagram of the rig in university college of southeast Norway. The instruments and sensors installed with measurement capabilities are discussed here.

3.1 Temperature Transmitter (TT-13)

This is a resistance thermometer with platinum resistance as the sensing element used to measure fluid temperature. According to [42], this sensor has a very short response time with operating temperature of 0℃ to 100℃ and uncertainty class A $\pm$0.19℃ at 20℃.

3.2 Ultrasonic level sensors (LT-15, LT-17 and LT-18)

These sensors are installed at the top of the open channel venturi used to measure the level of the fluids. In using these sensors for estimating other parameters like flow rate, the sensors can be re-positioned to find the optimal positions for best estimations. According to the data sheet [43], the sensor can measure both the level of liquid and solids up to a distance of 15meters with an accuracy of 0.25% full span with temperature compensation. It uses 4-20mA DC analog output with HART7 communication protocol. The temperature range of this sensor is between -20℃ to 65℃.

3.3 Angle Inclination Sensor (ZT-27)

This sensor measures the angle of inclination of the venturi channel. According to [44], this sensor can measure angle between ranges of -15 to 15^o with an absolute accuracy of $\pm$0.2^o and high shock resistance. The sensor has an analog output signal of 4-20mA and a temperature influence of $\leq$ 0.004^o/k.

3.4 Differential Pressure Transmitter (PDT-14)

The position of installation of the differential pressure together with the Coriolis flow meter in the rig is intended for the purpose of estimating the fluid viscosity.

According to the data sheet [45], the sensor uses HART communication protocol and can withstand both overload and pressure surge of up to 250 – 420bar, at a nominal pressure

range 0 – 70bar. The accuracy of the sensor is ±0.1% of calibrated range and a response time of 500ms. The operating temperature range of this sensor is -25 to 80℃ ambient temperature. At a temperature above 120℃ , impulse line or diaphragm seal will be used for the measurements.

3.5 Pressure Transmitters (PT-11)

This measures the pump pressure, the transmitter is configured in such a way that when the discharge pressure of the pump is too high the pump shut down.

According to the data sheet [46] a piezoresistance silicon is used as the sensing element separated from the medium (gas, vapour or liquid) with a diaphragm and manometric liquid. The sensor uses the standard HART communication protocol and measures between the range of 0 -1000bar with 1200bar as the overpressure limit without hysteresis at an accuracy of ±0.1% of calibrated range.

The operating temperature of the sensor is -40 to 85℃ ambient temperature with an extended version of -40 - 85℃ and -40 to 120℃. At temperature above 120℃ , impulse line or diaphragm seal will be used for the measurements.

3.6 Gama sensor (DT-900)

This sensor is used to measure the density of all liquid and suspensions. According to the data sheet [47], the sensor can measure both liquid and slurries density with an accuracy ±0.2% of the highest density at a time constant of 20s and sensitivity of 0.001g/cm^3. It uses 4-20mA superimposed HART and RS-485 protocol for communications. It has a temperature stability of ±0.001%/℃ of highest density.

3.7 Level Switches

They are numerous level switch installed in the system, at the buffer tank (LSH 20) and the mixer (LSL 21 and LSH 22) tank to automatically shut down the pump when the level of the fluid is beyond a specific level. According to the data sheet [48], the sensor is capable of measuring both level and temperature of liquid with an operating temperature range of -20℃ to 120℃ at a temperature sensing accuracy of ±0.2℃. In measuring level, the switch action may be reversed by rotating the switch at an angle of 180°.

3.8 Old Coriolis flow meter (FT-14)

This act as the reference meter when using venturi with other variables to estimate flow rate. According to the data sheet [49], the flow meter can measure mass flow rate, density and temperature of liquid and gas in a closed pipe. The measuring range of this flow meter is between 0-3000kg/min with mass flow rate accuracy for liquids as ±0.1% and for gas ±0.5% of the full scale value with excellent repeatability. The density and temperature accuracies are ±0.0005g/cm^3 and ±0.5℃ respectively of the measured values. The flow meter uses either HART, Rackbus Rs485, or PROFIBUS PA/DP protocol for communications.

3.9 New Coriolis flow meter (FT-20)

This is the new flow meter installed in summer 2015, it also acts as a reference flow meter when estimating flow rates according to the data sheet [50], the flow meter can measure mass flow rates, density, temperature and viscosity of liquid and gas with low pressure loss. It uses PROFIBUS PA/DP, Modbus, HART, Ethernet/IP, and foundation field bus for communication. The measuring range of this flow meter in measuring liquid 0-3000kg/min with an accuracy of ±0.1% of the measured value. The density and temperature accuracy are ±0.5kg/m^3 and ±0.5℃ respectively of the measured values.

3.10 Fluid Pump (P-001)

This has a nominal capacity of 1000kg/min, according to [7] after testing with water the pump has an effective capacity of about 800kg/min.

3.11 Fluid Tanks

This comprises of the mixing tank (TK-001) and the buffer tank (TK-002). The buffer tank is made of plastic and used to ensure an even flow into the venturi channel while the mixing tank consist of two steel tanks that are connected together to form a single tank. The agitator (M-002) is connected to one of the mixing tank to ensure homogenous fluids mixing before running the rig. The tank capable of holding 1000liters of fluid.

4 Experimental Procedures

The scope of this chapter is to present the experimental procedures used for the flow rate estimation and comparison between the outputs of two Coriolis flow meters installed in the rig of University College of southeast Norway. It contains a brief theory of the analytical method that will be used for the comparisons.

4.1 Statistical Analysis Concept

Statistical analysis concept is used for experimental planning and interpretation of data gotten from experimental procedures. In every measurement process, errors are one of the essential features that are always observed which is caused by controlled or uncontrolled variables affecting the measurement system or process. Errors in experiment degrade the validation of data, and this errors can be classified into systematic and random errors [51].

- Systematic errors: This is sometimes referred to as fixed or bias errors. When a measuring system is not properly calibrated and used properly (loading errors) systematic error will develop in the measurement process. Moreover, this error can be easily be reduced by calibration.
- Random errors: This is caused by lack of uncontrolled variables and repeatability in the measurement system. The total elimination of the uncontrolled variable can minimize random errors. The concept of statistical analysis is usually used for random error analysis [51].

4.1.1 Definitions and formulas Used for the Analysis

Some common definitions that are useful for the purpose of this analysis are discussed here.

- Coriolis flow meter: This measures mass flow rate and density directly, its principle is based on measuring the rate of oscillation of the tube through which the fluid or substances passes through. When there is no fluid flowing through the tube, the tube vibrates in parallel, thus causing no phase shift. With the presence of fluid, the tube is forced to swing, causing a phase shift proportional to the mass flow rate and density measured by the Coriolis meter.
- Hysteresis: This is the difference between the rising and falling measurements values from a system. This phenomenon degrades the accuracy of the measurement system and is often classified as a systematic error [51].

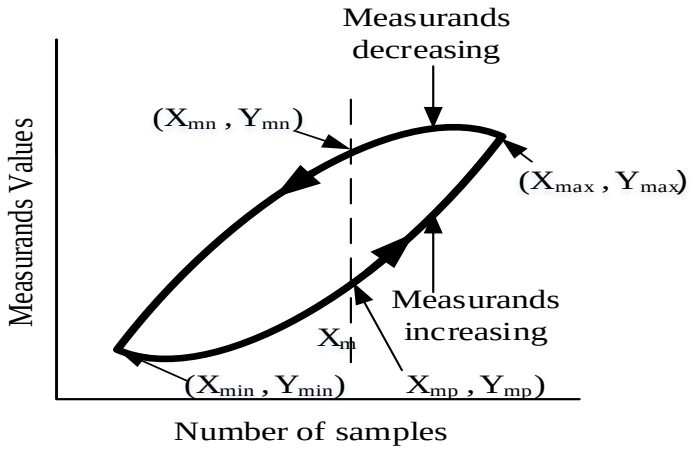

Figure 4- 1. Hysteresis curve

Figure 4- 1 shows a hysteresis curve of a measurement system, it can be calculated with the formula described as;

$$\text{Hysteresis} = \frac{\text{Y}_{\text{mn}} - \text{Y}_{\text{mp}}}{\text{Y}_{\text{max}} - \text{Y}_{\text{min}}} \tag{4.1}$$

Where Y_{mn} and Y_{mp} are the measurands midpoint values while $Y_{max}\ and\ Y_{min}$ are the minimum and maximum measurands values.

- Confidence level: This represent how the true population will fall within the specified confidence interval, it is usually expressed in terms of the level of significance (α) [51]. Mathematically it is expressed as;

$$\text{confidence level} = 1 - \alpha \tag{4.2}$$

Where α is the probability that the mean value will fall outside the confidence interval.

- Uncertainty interval of measurement: This is simply called uncertainty, it is the best estimate with some confidence level of the limit of an error in a measurement system. In calculating the uncertainty of any measurement system, the source of the uncertainty must be identified before estimating the size of the uncertainty from the source [51]. According to ASME, it suggests that student's t distribution can be used for analyzing continuous symmetrical experimental data with sample size less than

30, while for sample size greater than 30 normal distribution can be used. The percentage uncertainty can be expressed as

$$\text{Percentage uncertainty} = \frac{uncertainty\ in\ measurement}{\text{Measurement}} \times 100 \tag{4.3}$$

In estimating random uncertainty using student's t distribution for a measured variable (x), the random uncertainty is calculated with the following formula;

Random uncertainty of the mean ($P_{\bar{x}}$) is expressed as

$$P_{\bar{x}} = \pm t\frac{S_x}{\sqrt{n}} \tag{4.4}$$

Random uncertainty of each measurement (P_x) is expressed as

$$P_x = tS_x \tag{4.5}$$

For a given confidence level the value of t can be obtained from the standard student's t distribution table as shown in Appendix 4B for the degree of freedom ($v = n - 1$)

Where n is the number of samples and S_x is the population standard deviation expressed as

$$S_x = \sqrt{\sum_{i=1}^{n} \frac{(x_i - \bar{x})^2}{n-1}} \tag{4.6}$$

In estimating random uncertainty using normal distribution for a measured variable (x), the random uncertainty is calculated with the following formula;

Random uncertainty of the mean ($P_{\bar{x}}$) is expressed as

$$P_{\bar{x}} = \pm z\frac{\sigma}{\sqrt{n}} \tag{4.7}$$

Random uncertainty of each measurement (P_x) is expressed as

$$P_x = z\sigma \tag{4.8}$$

For a given confidence level the value of z can be obtained from the standard normal distribution table as shown in Appendix 4A while σ is the sample standard deviation expressed as

$$\sigma = \sqrt{\sum_{i=1}^{n} \frac{(x_i - \bar{x})^2}{n}} \tag{4.9}$$

- Total uncertainty: This is the combination of systematic and random uncertainty. According to ASME (1998) and ISO (1993), in estimating the total uncertainty of a measurement system both uncertainty need to be evaluated at the same confidence level, usually at 95% confidence level. Total uncertainty of the mean can be determined mathematically from;

$$W_{\bar{x}} = \left(B_x{}^2 + P_{\bar{x}}{}^2\right)^{1/2} \tag{2.10}$$

And the total uncertainty of each measurements can be determined from

$$W_x = \left(B_x{}^2 + P_x{}^2\right)^{1/2} \tag{4.11}$$

Where $P_{\bar{x}}$ and P_x are calculated from equation (4.4) or (4.7) and equation (4.5) or (4.8) respectively while B_x is the systematic uncertainty.

4.2 Open Venturi Channel mud flow Rig loop description

The trapezoidal open venturi rig flow loop at the University college of Southeast Norway was commissioned in May 2014, Section 3 highlighted all the instruments installed with their measurement capabilities. 1000liters tank is used to supply the flow loop with fluid which is pumped by a screw pump through the venturi flume and back again into the tank. The model

of the rig is built to emulate the circulation system used in the real drilling operation. The updated P&ID diagram and the physical views of the open venturi channel flow rig are given in Appendix 2A

4.2.1 Venturi Rig Experimental Procedures

The experiment was performed with three different fluids, Table 2 shows the characteristic of the fluids used for the experiments.

Table 2. Fluids characteristics

Fluid - 1	140 kg of K2CO3 in 1000 liters of water. The low density fluid with density 1165 kg/m^3 The fluid forms insignificant bubbles/foam as flow rate increase
Fluid - 2	1000 kg of K2CO3 in 1300 liters of water The high density fluid with density 1405 kg/m^3 The fluid forms enormous bubbles with increased flow rates
Water	Low density fluid with density 1000 kg/m^3 Forms no form/ bubbles

The experiment was performed by increasing the set point from 250kg/min to 400kg/min with 5 minutes intervals within every change to the next set point and then decreased again from 400kg/min to 250kg/min on an interval of 10kg/min.

While performing the experiment with Fluid-2 which shows enormous foam/bubble at high flow rate, a set point from 250kg/min to 300kg/min and down again to 250kg/min was used for the analysis. Table 3 shows the test matrix used for this experiments.

Table 3- Test matrix

Set point (kg/min)	Downstream Level (LT-18) (mm)	Middle Level (LT-17) (mm)	Upstream Level (LT-15) (mm)	Pressure drop (PDT-12) (mbar)	Discharge pressure (PT-11) Bar	New Coriolis Viscosity (FT-20C) (cP)	New Coriolis Massflow (FT-20A) kg/min	New Coriolis Density (FT-20B) (kg/m^3)	Old Coriolis Massflow (FT-14A) kg/min	Old Coriolis Density (FT-14B) (kg/m^3)	Temperature (TT-13) ℃

At each set points 51 data was generated after sorting out the data by neglecting the first 10 seconds of every data set to ensure a representative value base on stable flow conditions. The total number of data generated after sorting out the data is 1581 data for fluid -1 and water while for fluid-2 a total of 561 data was generated purpose of analysis.

4.3 Density Laboratory Based measurements

In order to compare results of the two Coriolis flow meter densities in the rig, a laboratory based experiment was performed. The laboratory density instrument (Anton paar DMA 4500 Density/specific gravity/concentration meter) at the University College of southeast Norway was used for the density measurement of fluid-1 and fluid-2. According to the data sheet [52], the meter has a measuring range of 0 – 3g/cm^3 with an accuracy of $\pm$0.000005g/cm^3 in a temperature range of 0 - 95℃. Appendix 3 shows the preparation and procedure for using the instrument. Table 4 below shows the test matrix for the laboratory based density measurement experiment.

Table 4. Laboratory density based measurement test matrix

Sample	Temperature (℃)	Density (kg/m^3)
Fluid -1 Top		
Fluid -1 Bottom		
Fluid -1 rig flow		
Fluid -2 Top		
Fluid -2 Bottom		
Fluid -2 rig flow		

The experiment was performed with fluid - 1 and fluid - 2, samples was taken at fluid tank top, bottom, and also when the fluid was running at the venturi flume. The experiment was done for the purpose of density comparison with the old and new Coriolis meter and also the best possible position for sample collection for future measurements in the laboratory. The procedure used for collecting samples and performing the experiment is described as follows;

- Use pipette to take sample fluid from the tank for measurement (for top and bottom samples).
- Use a beaker to take sample fluid from the venturi flume.
- Use magnetic stirrer [45] to stir the fluid for homogeneity.
- Clean the density equipment using degassed water (see Appendix 3B for instrument preparation and procedures)
- Use string and inject 5ml of the sample
- Start measurement.

5 Simulation results and analysis

The scope of this chapter is to present the experimental results carried out in the venturi rig and laboratory based measurement carried out at University College of southeast Norway. The main part of the chapter will be focusing on analyzing the experimental data to estimate the flow of non-Newtonian drilling fluid and comparing two Coriolis flow meter.The results obtained from the experimental procedures is presented and analyzed here. All the simulations are done in Matlab and the codes are presented in Appendix 5.

5.1 Comparing laboratory based viscosity measurement with new Coriolis viscosity measurement

In performing the laboratory based viscosity measurement, samples of fluid-1 and fluid-2 was taken to Statoil, Porsgrunn, Norway for laboratory measurement using MCR502 rheometer from Anton Paar. The results of the measurements are presented here to compare the measurement of the new Coriolis flow meter which also has the capability of measuring viscosity.

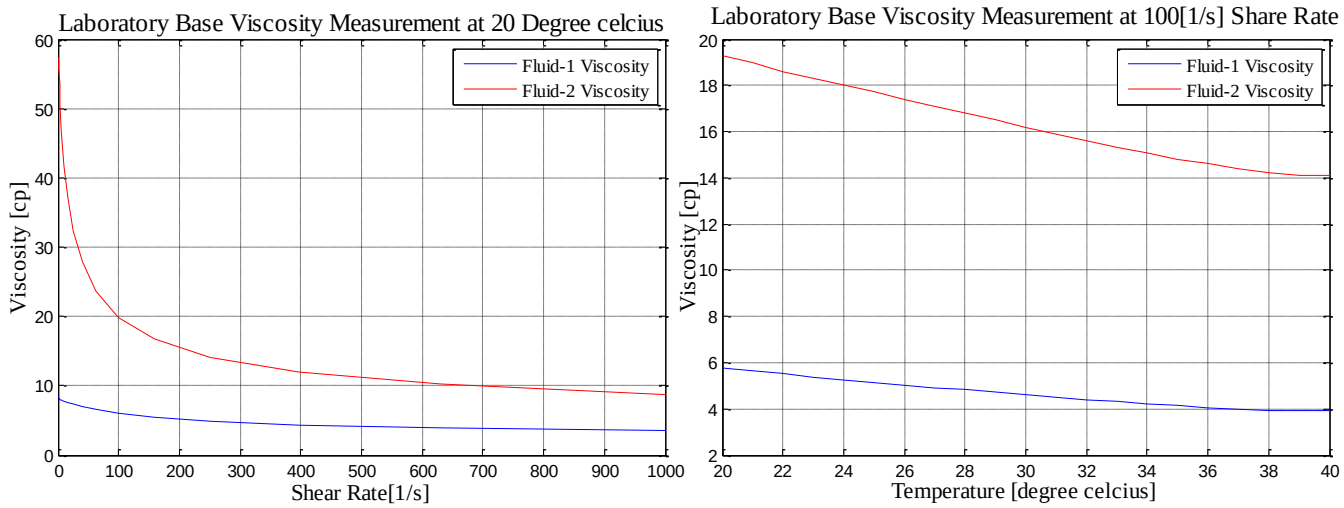

Figure 5- 1. Laboratory viscosity measurement of fluid-1 and fluid-2 at constant temperature of 20℃(left) and constant shear rate of 100s^{-1}(right)

Figure 5- 1 shows the viscosity of fluid-1 and fluid-2 as it changes with temperature and share rate. The results show that both fluids are non-Newtonian shear thinning fluids.

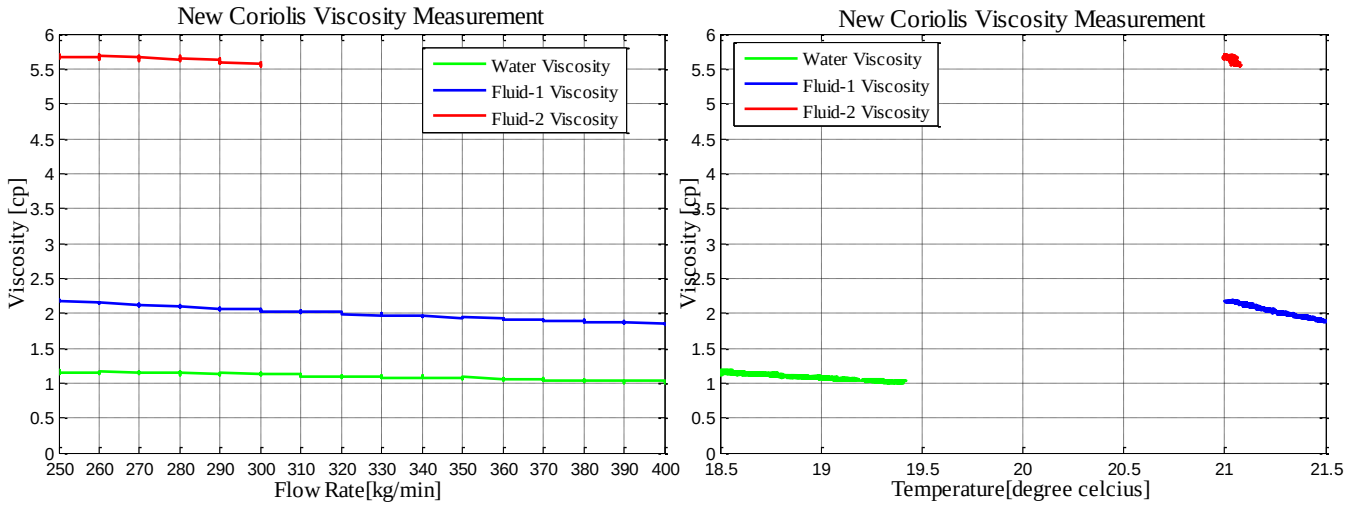

Figure 5- 2. Viscosity measurement of water, fluid-1 and fluid-2 from the new Coriolis flow meter

Figure 5- 2 shows the viscosity of water, fluid-1 and fluid-2 from the new Coriolis flow meter. Notice that the sensor measured the viscosity of water accurately while for both fluid-1 and fluid-2, the result also shows that the fluids are Newtonian in nature, contradicting the laboratory based measurement. This shows that the model used in designing the new Coriolis flow meter can only measure Newtonian fluids.

5.2 Laboratory based density measurement

The laboratory based density measurement was performed using fluids-1 and fluid -2. The fluids characteristic are described in Table 2, Section 4.2.1. The laboratory density measurement was performed for the purpose of determining the best possible position for sample collection and for comparison of old and new Coriolis flow meter.

5.2.1 Laboratory based density measurement for sample collection.

In order to determine the best possible positions for collecting samples for future laboratory measurement in the rig, the sample was collected at the fluid tank top, bottom and also when the fluids were flowing in the open venturi rig. The results of the density measurements presented here are within the temperature range of 15℃ to 60℃.

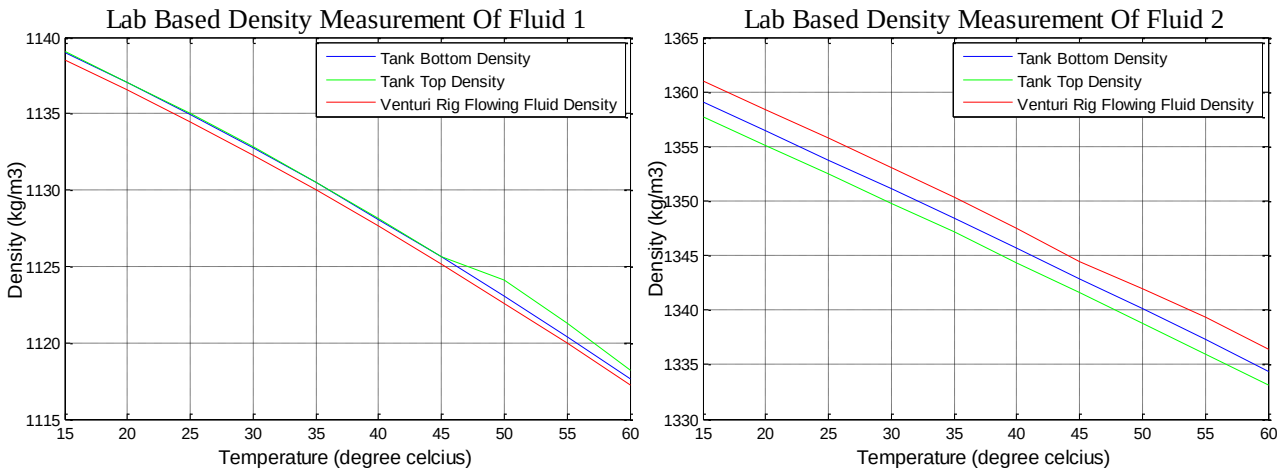

Figure 5- 3. Laboratory based density measurement for best possible position for collecting samples

As presented in Section 4.2.1, the actual density of the fluids are 1165 kg/m^3 and 1405 kg/m^3 for fluid-1 and fluid-2 respectively, therefore in comparing the density of the fluids for the best possible positions for sample collections the result from Figure 5- 3 shows that the fluids can be taken at any positions since it shows a very small deviation in the measurement positions. Moreover, the best possible position for fluid-1 is at the top of the tank while for fluid-2, taking the sample when the fluid is flowing at the venturi rig pose the best possible position.

5.2.2 Laboratory based density measurement for comparison purpose.

In order to compare the density of the Coriolis flow meter with laboratory measurements, the density measurement was done on a temperature range of 20℃ - 22℃ on an interval of 0.2℃ because the temperature in the process hall where the open venturi rig is installed varies within these range.

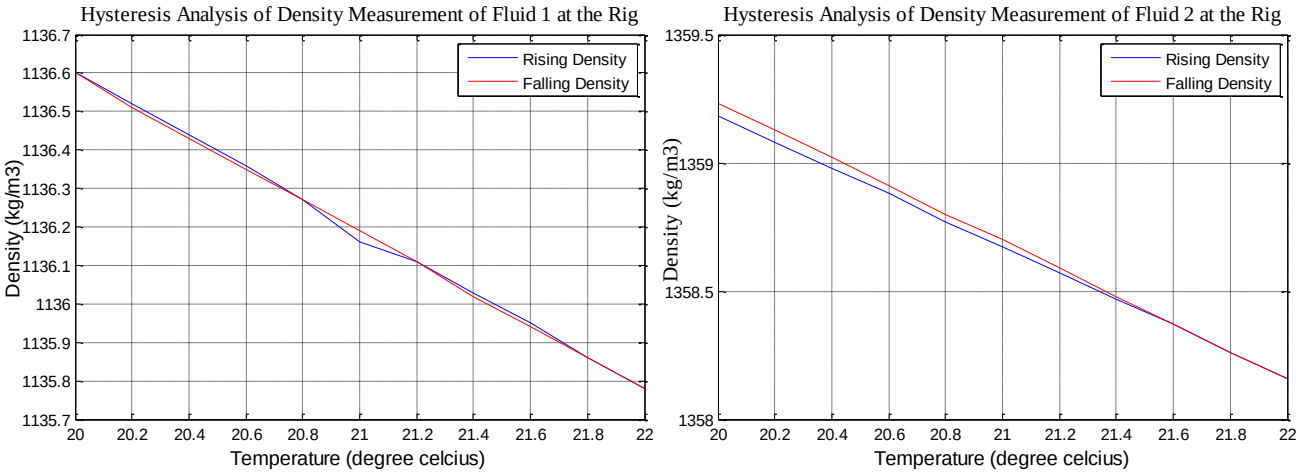

Figure 5- 4. Hysteresis plot of laboratory based density measurement of fluid -1 and fluid -2 flowing at the venturi rig

Hysteresis error correlates with the systematic error of a measuring instrument, Figure 5- 4 shows the hysteresis curve of the measuring instrument used for the measurement. The measurement process was repeated in exactly the same way by increasing the temperature from 20℃ to 22℃ and decreasing from 22℃ to 20℃. As shown in the figure, the instrument is a very accurate instrument.

5.2.3 Density comparison of using water

As discussed in Section 4.2.1 the experiment was performed by increasing the set point from 250kg/min to 400kg/min and decreasing from 400kg/min to 250kg/min on an interval of 10kg/min.

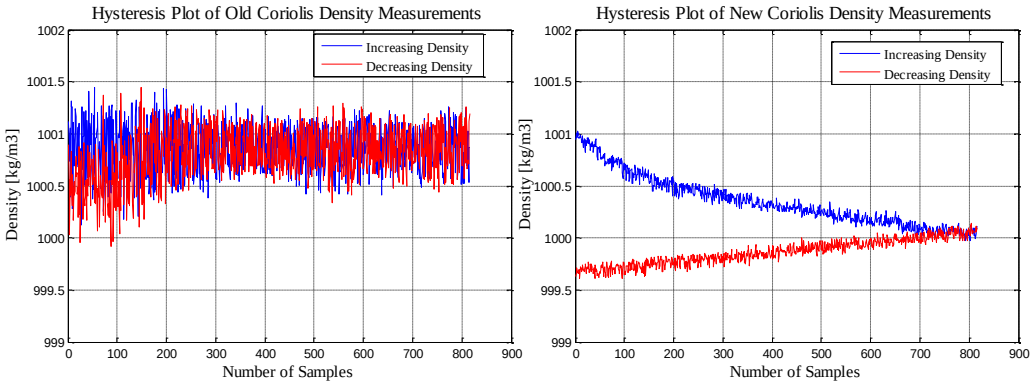

Figure 5- 5. Hysteresis density measurement of water from old Coriolis flowmeter(left) and new Coriolis flow meter(right)

The accuracy of the two flow meter in measuring density as given by the manufacturer is $\pm 0.5 kg/m^3$ [50, 49]. The result from Figure 5- 5, shows that the hysteresis curve of both

Coriolis flow meter falls more within the manufactures accuracy limits, notice the density intervals in the Y-axis is 0.5 kg/m^3.

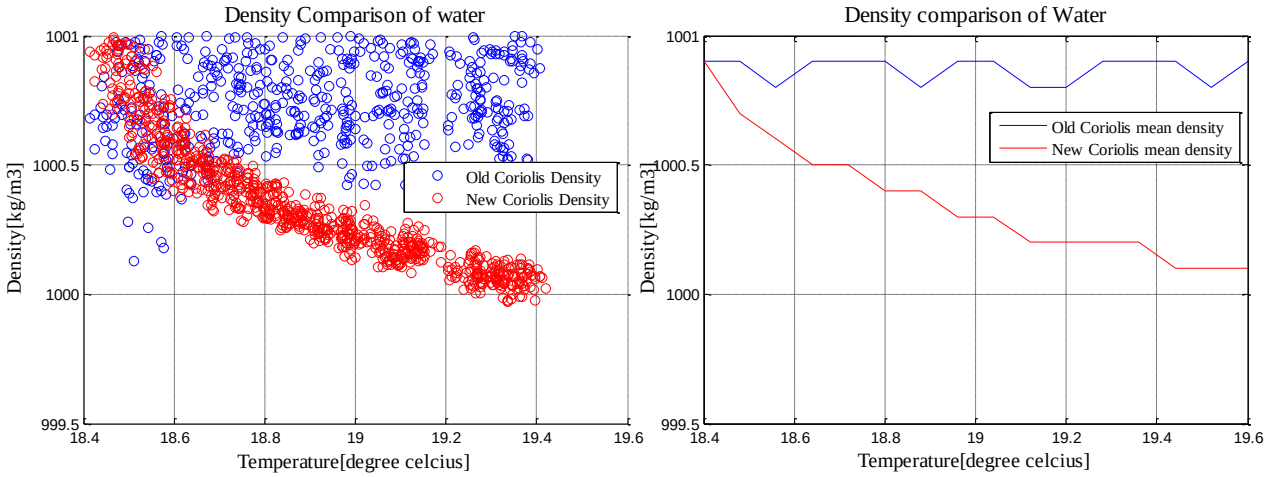

Figure 5- 6. Water density measurement from old Coriolis flowmeter(blue) and new coriolis flowmeter(red).

From Figure 5- 6, the figure at the left shows how all the density measurement values from the Coriolis flow meters changes with temperature as the flow rates is been increased while the right shows the mean density measurement. The result shows that both Coriolis flow meter measures density of water accurately within manufacturers accuracy limits of $\pm$0.5 kg/m^3. Considering 95% confidence level, the experimental uncertainty result when the flow rate of the fluid is increasing is shown in Table 5, using the equations discussed in Section 4.1.1. The results from the old and new flow meter are more or less the same.

Table 5.Uncertainty Experimental Results for Water Density at Various Flow Rates

Mass flow Rate (kg/min)	250	260	270	280	290	300	310	320	330	340	350	360	370	380	390	400
Uncertainty of Single Measurement Old Coriolis (kg/m^3)	0.59	0.59	0.58	0.57	0.52	0.45	0.39	0.38	0.35	0.43	0.41	0.44	0.37	0.32	0.36	0.41
Uncertainty of Single Measurement New Coriolis (kg/m^3)	0.11	0.09	0.09	0.10	0.08	0.09	0.08	0.07	0.07	0.06	0.08	0.08	0.07	0.07	0.07	0.08
Uncertainty of the mean Old Coriolis (kg/m^3)	0.08	0.08	0.08	0.08	0.07	0.06	0.05	0.05	0.05	0.06	0.06	0.06	0.05	0.05	0.05	0.06

Uncertainty of the mean New Coriolis (kg/m^3)	0.02	0.01	0.01	0.01	0.01	0.01	0.01	0.01	0.01	0.01	0.01	0.01	0.01	0.01	0.01	0.01
Total uncertainty of the mean(kg/m^3) Old Coriolis	0.51	0.51	0.51	0.51	0.51	0.50	0.50	0.50	0.50	0.50	0.50	0.50	0.50	0.50	0.50	0.50
Total uncertainty of the mean(kg/m^3) New Coriolis	0.50	0.50	0.50	0.50	0.50	0.50	0.50	0.50	0.50	0.50	0.50	0.50	0.50	0.50	0.50	0.50

5.2.4 Density comparison using fluid -1

In using fluid-1 for comparing the density measurement of the two Coriolis, the experiment was performed in the same procedures like that of water. It is also observed that as the flow rate increase, they are a slight increase in the density of fluid -1 and fluid-2 also as observed by [9].

As stated by the manufacturer, the density accuracy for the two flow meters is $\pm 0.5 kg/m^3$ [50, 49],

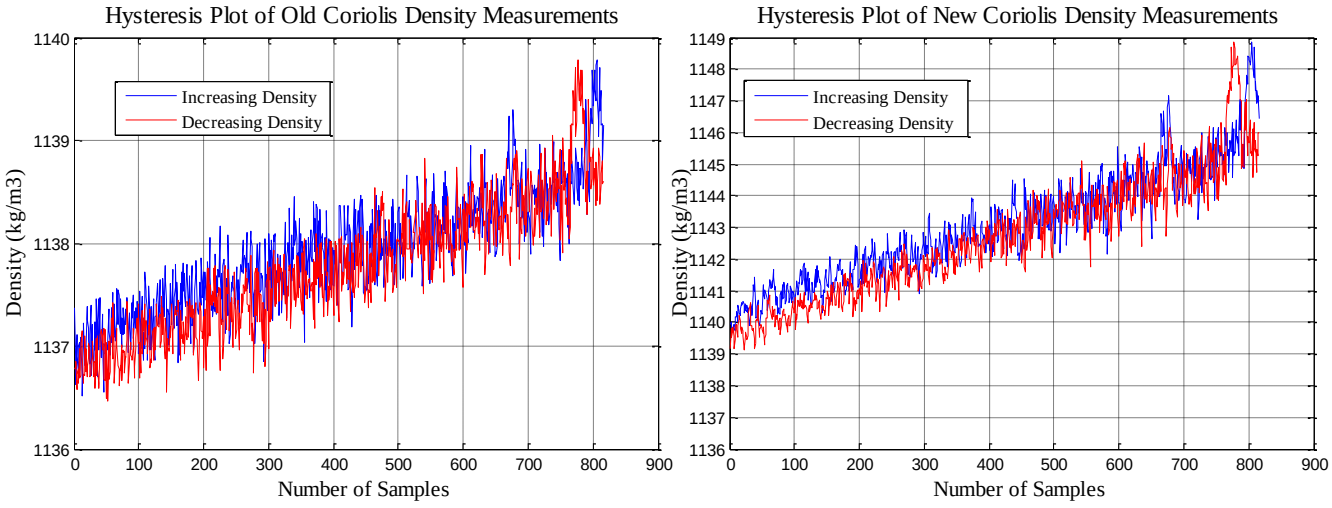

Figure 5- 7 shows the hysteresis plot of the two flowmeters using fluid-1.

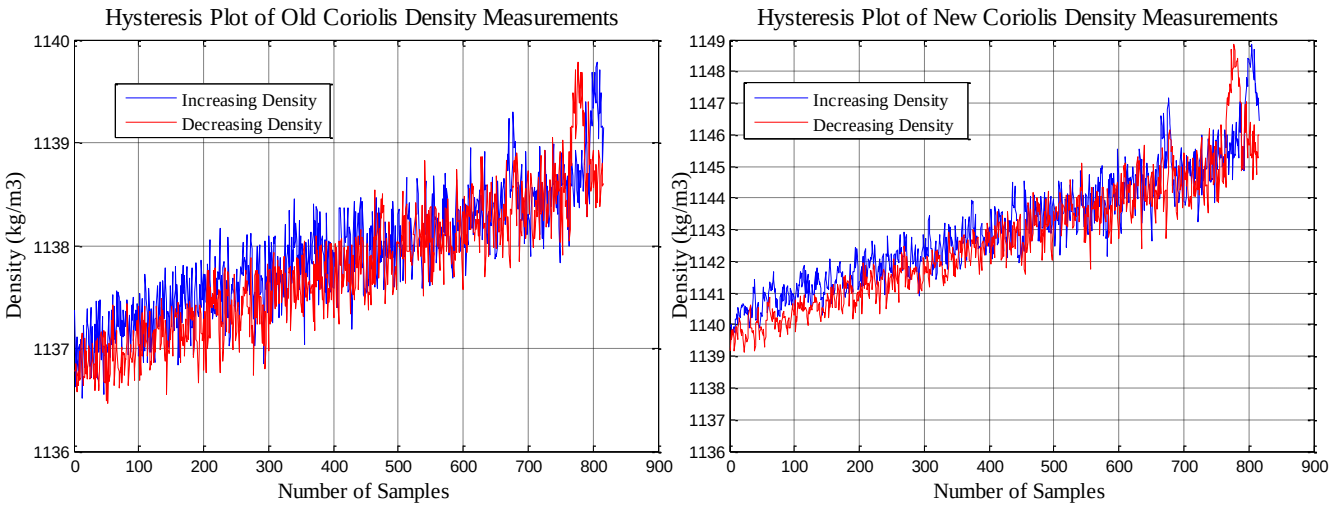

Figure 5- 7. Hysteresis density measurement of fluid-1 from old Coriolis flowmeter(left) and new Coriolis flow meter(right)

The result from figure 5- 7, shows that the density of both flow meters increases with increasing flow rates which conform to previous work done in [9].

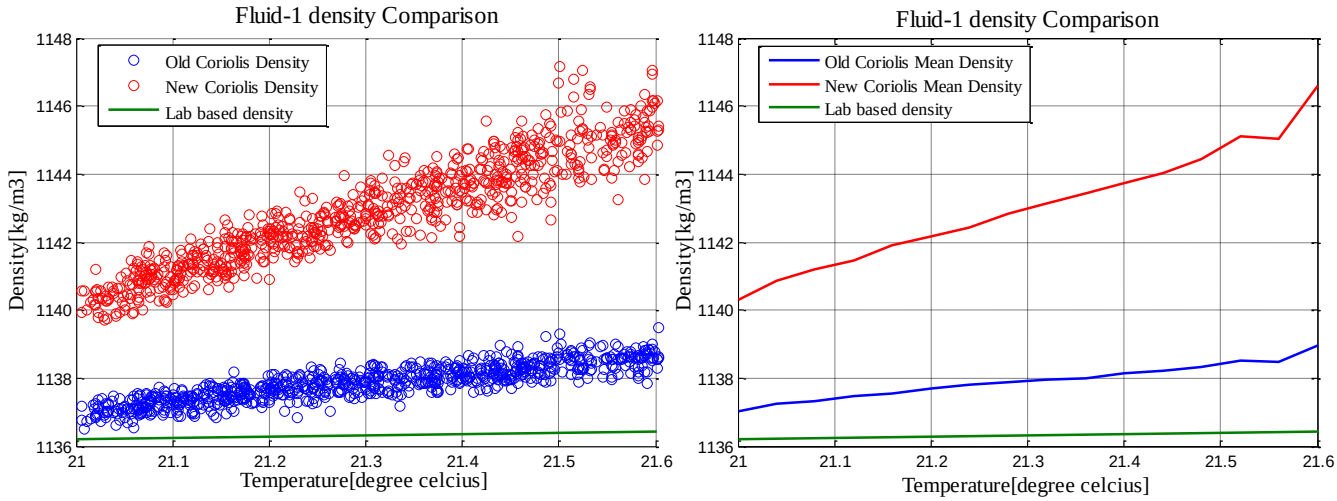

Figure 5- 8. Density of fluid-1 from old Coriolis flow meter(blue), new Coriolis flow meter (red) and laboratory based density measurement(green) as temperature changes.

From Figure 5- 8, the figure at the left shows the comparison of the laboratory-based density measurement and how all the density measurement from the Coriolis flow meters varies with temperature as the flow rates is been increased while the right shows the mean density measurement from the old and new Coriolis flowmeter. The results shows that the old Coriolis meter measures density more closely to the expected actual density value. The experimental uncertainty result shown in Table 6, considering 95% confidence level and using the equation discussed in Section 4.1.1 shows that the total uncertainty of the old

Coriolis flow meter is ±0.5 kg/m3 at lower flow rates but increases, as the flowrate increases as expected. The new Coriolis flow meter also shows a similar pattern but with higher errors as compared to the old Coriolis flow meter.

Table 6. Uncertainty Experimental Results for fluid-1 Density at Various Flow Rates

Mass flow Rate(kg/min)	250	260	270	280	290	300	310	320	330	340	350	360	370	380	390	400
Uncertainty of Single Measurement (kg/m^3) Old Coriolis	0.46	0.37	0.48	0.48	0.48	0.51	0.59	0.51	0.62	0.46	0.51	0.53	0.43	0.60	0.52	0.79
Uncertainty of Single Measurement (kg/m^3) New Coriolis	0.70	0.60	0.68	0.77	0.80	0.79	0.93	0.86	1.22	0.99	1.03	1.39	1.16	1.71	1.23	2.37
Uncertainty of the mean (kg/m^3) Old Coriolis	0.06	0.05	0.07	0.07	0.07	0.07	0.08	0.07	0.09	0.06	0.07	0.07	0.06	0.08	0.07	0.11
Uncertainty of the mean (kg/m^3) New Coriolis	0.10	0.08	0.10	0.11	0.11	0.11	0.13	0.12	0.17	0.14	0.14	0.19	0.16	0.24	0.17	0.33
Total uncertainty of the mean(kg/m^3) Old Coriolis	0.50	0.50	0.50	0.50	0.50	0.51	0.51	0.51	0.51	0.50	0.51	0.51	0.50	0.51	0.51	0.51
Total uncertainty of the mean(kg/m^3) New Coriolis	0.51	0.51	0.51	0.51	0.51	0.51	0.52	0.51	0.53	0.52	0.52	0.54	0.53	0.55	0.53	0.60

5.2.5 Density comparison using fluid -2

In using fluid-2 for comparing the density measurement of the two Coriolis flow meter, the experiment was performed by varying the flow rate from 250kg/min to 300kg/min and then decreased again to 250kg/min because of the effect of more bubbles that is generated by the fluid. It is also observed that as the flow rate increase, they are a slight increase in the density of the fluid also as observed by [9].

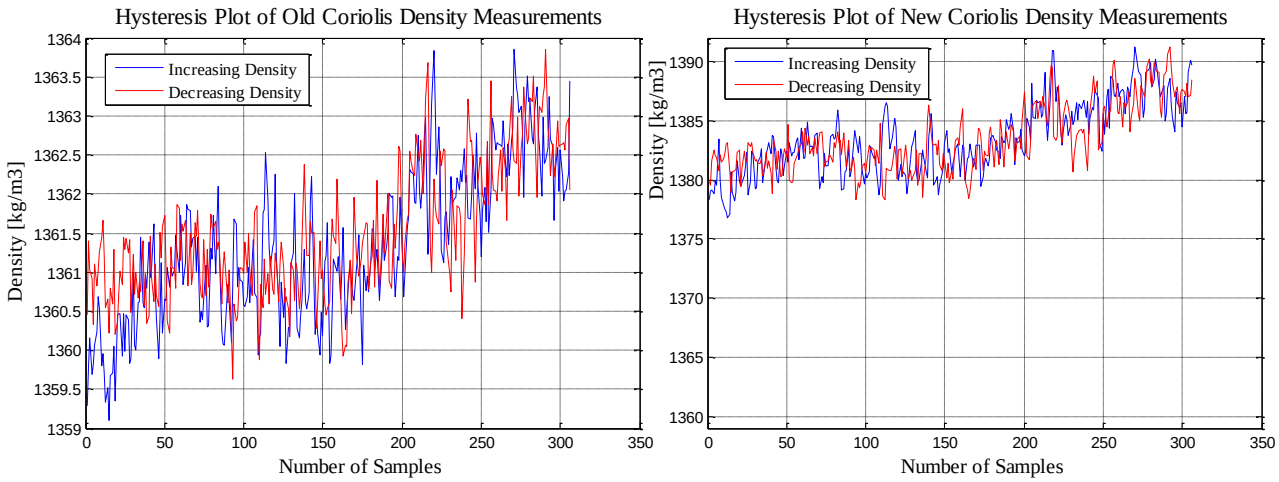

Figure 5- 9. Hysteresis density measurement of fluid-2 from old Coriolis flowmeter(left) and new Coriolis flow meter(right)

The result from

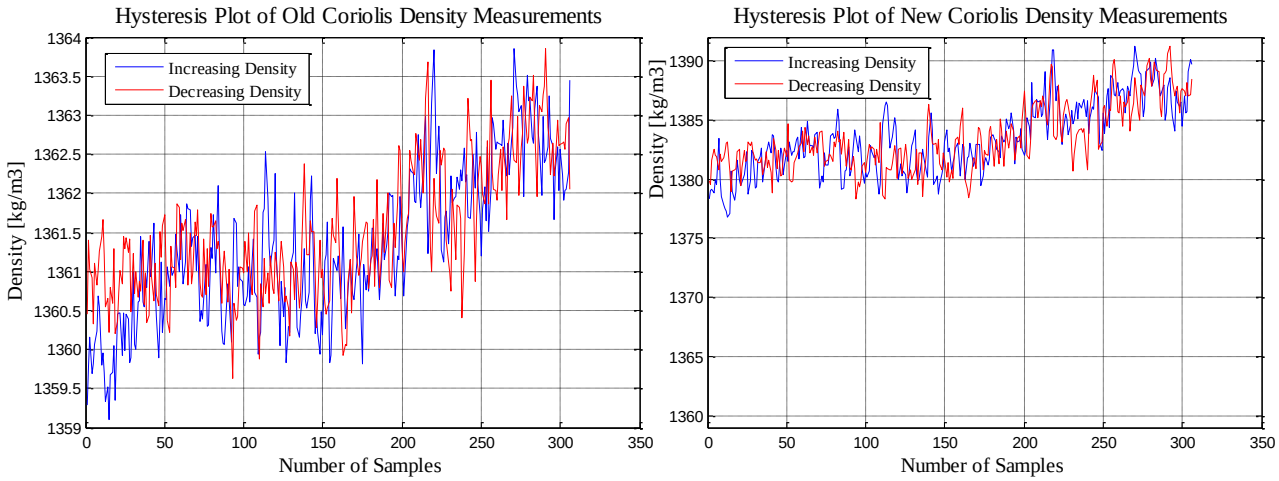

Figure 5- 9, shows that the density of both flow meters increases with increasing flow rates which conform to previous work in [9].

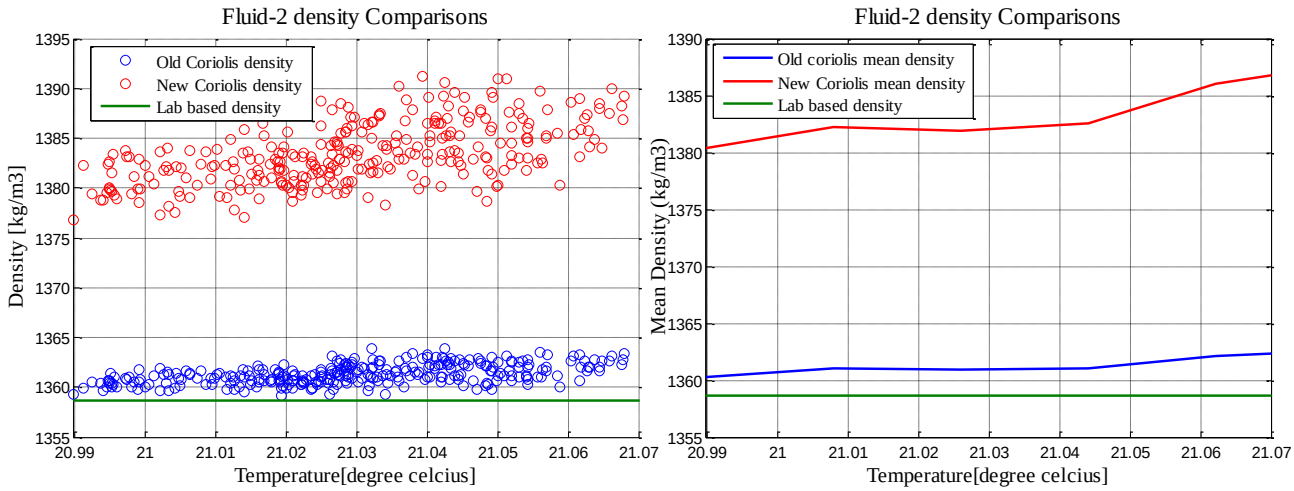

Figure 5- 10. Density of fluid-2 from old Coriolis flow meter(blue), new Coriolis flow meter (red) and laboratory based density measurement(green) as temperature changes.

From Figure 5- 10, the figure at the left shows the comparison of the laboratory-based density measurement and how all the density measurement values from the Coriolis flow meters varies with temperature as the flow rates is been increased, while the right shows the mean density measurement. The result shows that the old Coriolis meter measures density more closely to the expected actual density value. The experimental uncertainty result shown in Table 7, considering 95% confidence level and using the equation discussed in section 4.1.1 show that the total uncertainty of the old Coriolis flow meter is ± 0.5 kg/m^3 at lower flow rates but increases as the flow rate increases as expected. The new Coriolis flow meter also shows similar pattern but with higher errors as compared to the old Coriolis flow meter.

Table 7. Uncertainty experimental results for fluid-2 density at Various flow rates

Mass flow Rate (kg/min)	250	260	270	280	290	300
Uncertainty of Single Measurement (kg/m^3) Old Coriolis	1.12	0.99	1.31	1.00	1.06	0.92
Uncertainty of Single (kg/m^3) Measurement New Coriolis	3.55	3.14	4.02	2.65	3.54	3.22

Uncertainty of the mean (kg/m^3) Old Coriolis	0.16	0.14	0.18	0.14	0.15	0.13
Uncertainty of the mean (kg/m^3) New Coriolis	0.50	0.44	0.56	0.37	0.50	0.45
Total uncertainty of the mean(kg/m^3) Old Coriolis	0.52	0.52	0.53	0.52	0.52	0.52
Total uncertainty of the mean(kg/m^3) New Coriolis	0.71	0.67	0.75	0.62	0.70	0.67

5.2.6 Density comparison at higher flow rate

To investigate the effect of both Coriolis flow meter at higher flow rate, fluid-2 was used for the experiment. The flow rate set point was varied from 250kg/min to 550kgmin and then decreased again to 250kg/min. It is also observed that as the flow rate increase, they are a slight increase in the density of fluid -1 and fluid-2 also as observed by [9]. The hysteresis curve of both flow meter at higher flow rates is shown in Figure 5- 11 below.

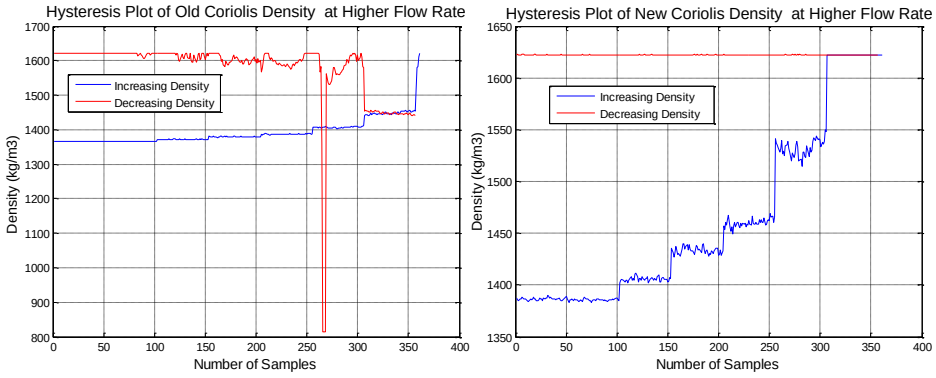

Figure 5- 11. *Hysteresis density measurement of fluid-2 from old(left) and new(right) Coriolis flow meter* at higher flow rate

From Figure 5- 11, the figure at the left shows the hysteresis of the old Coriolis flow meter while the right shows the hysteresis of the new Coriolis flow meter. It is seen that both flow meter got saturated at a particular but at the lower flow rates the flow meters measures density almost at the same values but with more errors with the new Coriolis flow meter.

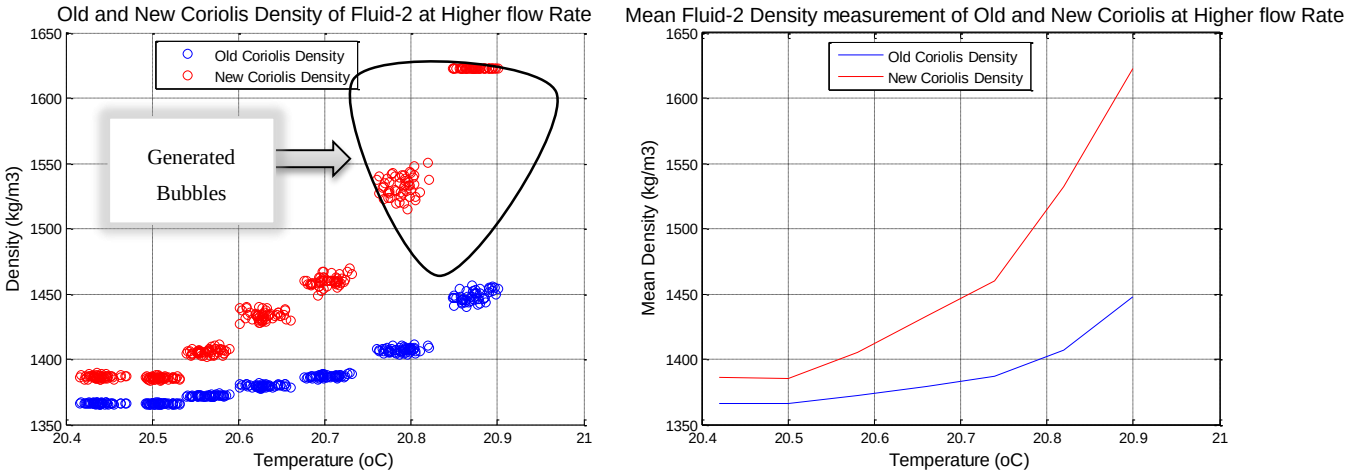

Figure 5- 12. Density of fluid-2 from old Coriolis flow meter(blue) and new Coriolis flow meter (red) at higher flow rate with generated bubbles.

As seen in Figure 5- 12, the figure at the left shows the how all the density measurement values from the Coriolis flow meters varies with temperature as the flow rate is been increased while the right show the mean density measurement as the flow rate increases. As seen in the figure at the left, more bubbles is been experienced as the flow rates increases and which is more greatly affected by the new Coriolis flow meter. In order words as the flow rates increases more bubbles are generated and the effect is greatly affected by the new Coriolis flow meter.

Table 8.Uncertainty experimental results for fluid-2 density at higher flow rates

Mass flow Rate (kg/min)	250	300	350	400	450	500	550
Uncertainty of Single Measurement (kg/m^3) Old Coriolis	0.86	0.73	1.17	1.80	1.91	3.56	8.43
Uncertainty of Single Measurement (kg/m^3) New Coriolis	2.35	1.92	4.04	6.64	7.52	15.32	0.04
Uncertainty of the mean (kg/m^3) Old Coriolis	0.12	0.10	0.16	0.25	0.27	0.50	0.18
Uncertainty of the mean (kg/m^3) New Coriolis	0.33	0.27	0.57	0.93	1.05	2.14	0.01
Total uncertainty of the mean(kg/m^3) Old Coriolis	0.51	0.51	0.53	0.56	0.57	0.71	1.28
Total uncertainty of the mean(kg/m^3) New Coriolis	0.60	0.57	0.75	1.06	1.17	2.20	0.50

5.3 Mass flow rate comparison of two Coriolis flow meter

This section describes the mass flow rate comparison of two Coriolis flow meter using three different fluids whose characteristic is described in Table 2 Section 4.2.1

5.3.1 Mass flow rate comparison using water

As discussed in Section 4.2.1 the experiment was performed by increasing the set point from 250kg/min to 400kg/min and decreasing from 400kg/min to 250kg/min on an interval of 10kg/min

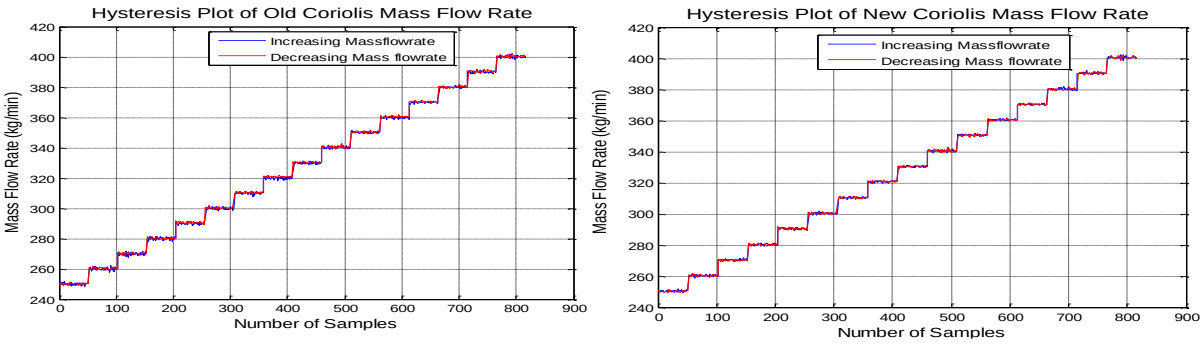

Figure 5- 13. Hysteresis mass flow rate measurement of water from old(left) and new(right) Coriolis flow meter

The accuracy of the flow meters for mass flow rate as given by the manufacturer is ±0.1% [50, 49]. Figure 5- 13 shows the hysteresis curve of the mass flow rate measurement readings of Coriolis flow meters (old Coriolis at the left and new Coriolis at the right). From Table 9 using equation (4.1), it is seen that the both flow meters measures flow rates within the manufactures specification.

Table 9. Mass flow rate of water hysteresis error

Flow meter	Hysteresis(kg/min)
Old Coriolis	± 0.07
New Coriolis	± 0.06

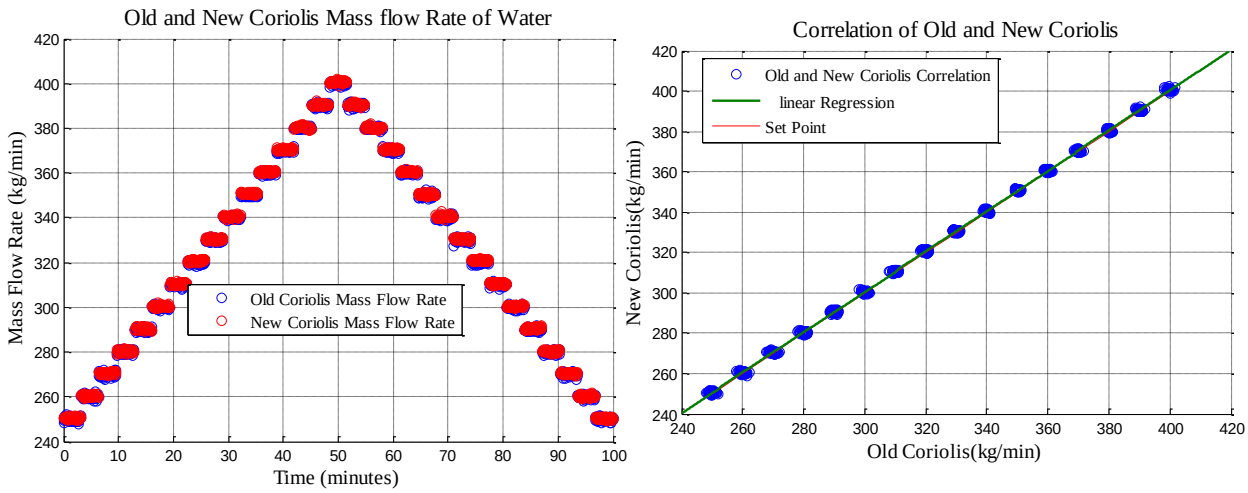

Figure 5- 14. Mass flow rate of water from Old(blue) and new(red) Coriolis flow meter as set point changes with time(left) and the correlation between the old and new Coriolis flow meter(right).

From Figure 5- 14 the flow rate of both Coriolis flow meter changing with time at the left and the correlation of both old and new Coriolis at the right. The results shows that the old and new flow meter are positively correlated with each other and measures the mass flow rate accurately.

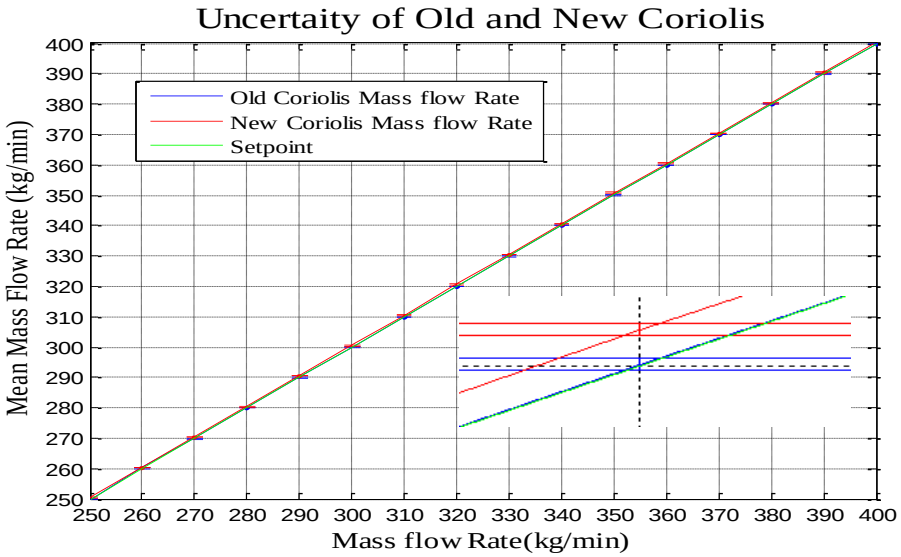

Figure 5- 15. Esimated uncertainty of old and new Coriolis flow meter using water

Considering 95% confidence level and using the equation discussed in Section 4.1.1. From Figure 5- 15, it can be clearly seen that both Coriolis flow meters agrees with the manufacturer's accuracy limits. Table 10 shows a detailed result of the analysis.

Table 10.Uncertainty experimental results for water mass flow rate at various flow rates

Mass flow Rate (kg/min)	250	260	270	280	290	300	310	320	330	340	350	360	370	380	390	400
Uncertainty of Single Measurement (kg/min) Old Coriolis	1.57	1.67	1.83	1.58	1.33	1.34	1.22	1.36	1.22	1.06	1.04	1.23	1.12	0.96	1.28	1.34
Uncertainty of Single Measurement (kg/min) New Coriolis	1.02	1.04	0.95	1.07	1.23	0.99	0.94	0.97	0.93	1.05	0.74	0.84	0.84	1.08	0.97	1.05
Uncertainty of the mean (kg/min) Old Coriolis	0.22	0.23	0.26	0.22	0.19	0.17	0.19	0.19	0.17	0.15	0.15	0.17	0.16	0.13	0.18	0.19
Percentage Uncertainty of the mean Old Coriolis	0.09	0.09	0.09	0.08	0.06	0.06	0.06	0.06	0.05	0.04	0.04	0.05	0.04	0.04	0.05	0.05
Uncertainty of the mean (kg/min) New Coriolis	0.14	0.15	0.13	0.15	0.17	0.14	0.13	0.14	0.13	0.15	0.10	0.12	0.12	0.15	0.14	0.15
Percentage Uncertainty of the mean New Coriolis	0.06	0.06	0.05	0.05	0.06	0.05	0.04	0.04	0.04	0.04	0.03	0.03	0.03	0.04	0.03	0.04
Total uncertainty of the mean(kg/min) Old Coriolis	0.13	0.13	0.14	0.13	0.12	0.12	0.11	0.12	0.11	0.11	0.11	0.11	0.11	0.11	0.11	0.11
Total uncertainty of the mean(kg/min) New Coriolis	0.12	0.11	0.11	0.11	0.12	0.11	0.11	0.11	0.11	0.11	0.10	0.11	0.10	0.11	0.11	0.11

5.3.2 Mass flow rate comparison Using Fluid – 1

In using fluid-1 for comparing the mass flow rate measurement of the two Coriolis, the experiment was performed in the same procedures like that of water. As stated by the

manufacturer, the density accuracy for the two flow meters is ±0.1% [50, 49]. In using fluid-1 for the experiment, a hysteresis plot of the two measuring instruments is as shown in Figure 5- 16 (old Coriolis at the left and new Coriolis at the right).

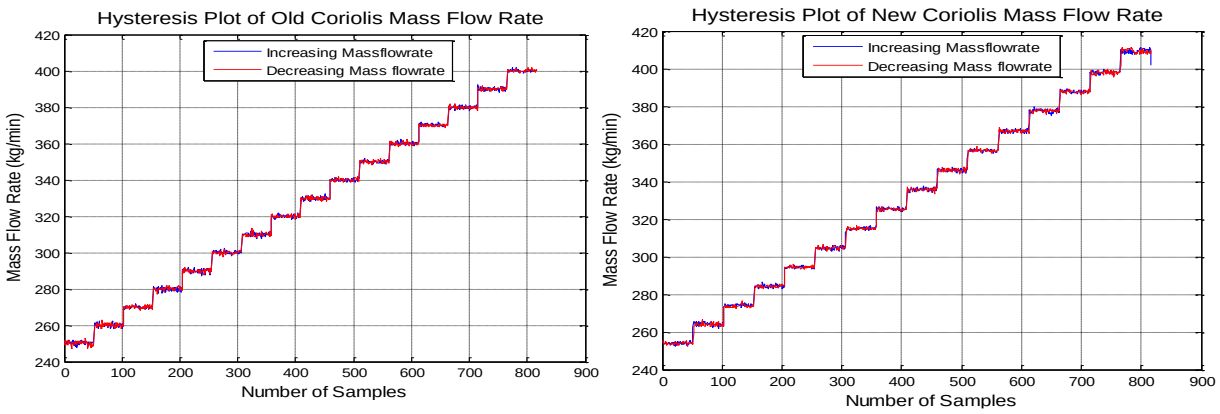

Figure 5- 16. Hysteresis mass flow rate measurement of fluid-1 from old(left) and new(right) Coriolis flow meter

The hysteresis plot of the flow measurement shows that both Coriolis flow meter show a similar pattern.

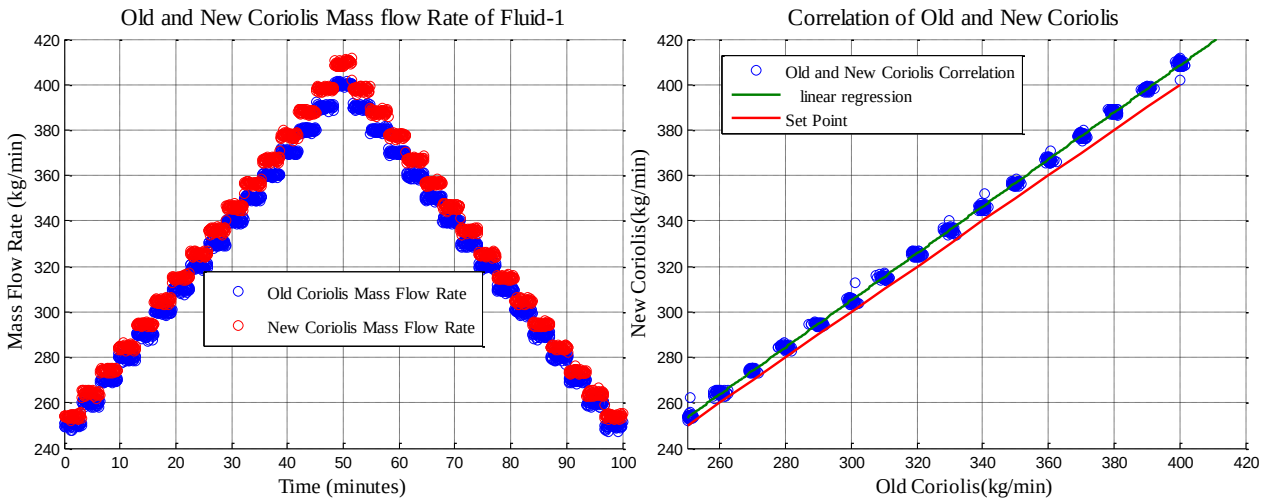

Figure 5- 17. Mass flow rate of fluid-1 from Old(blue) and new(red) Coriolis flow meter as set point changes with time(left) and the correlation between the old and new Coriolis flow meter(right).

From *Figure 5- 17*, the result shows that the old and new flow meter are positively correlated with each other.

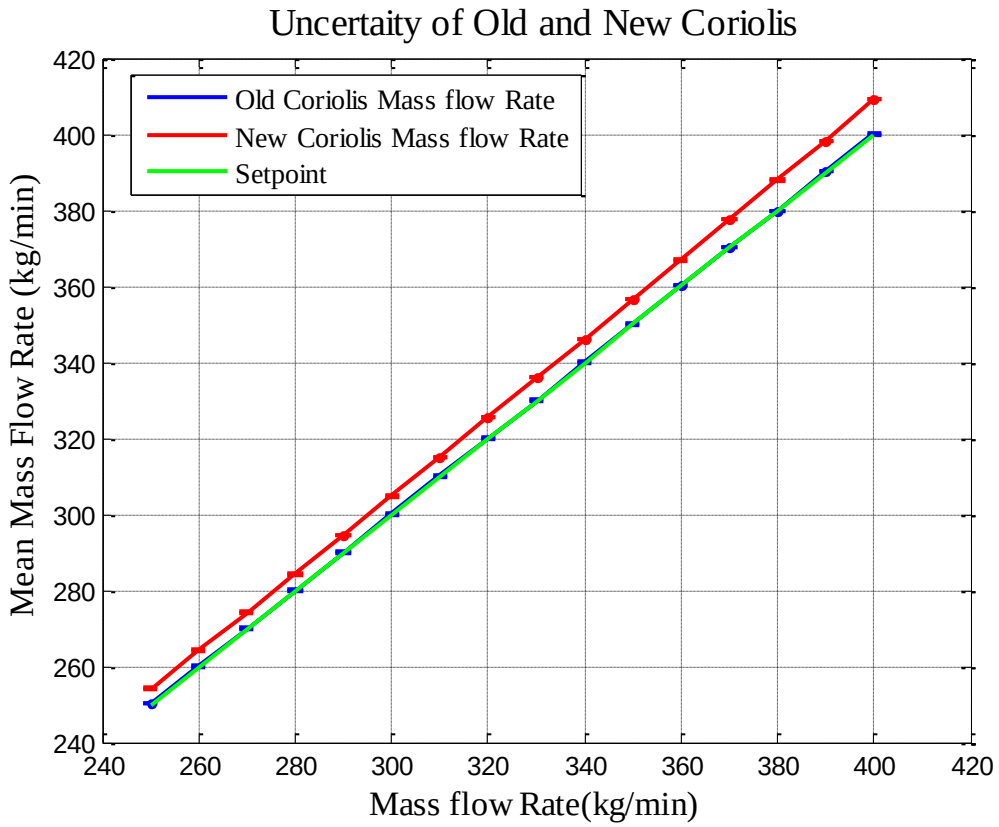

Figure 5- 18. Estimated Uncertainty of Old and new Coriolis Flow meter Using Fluid-1

Considering 95% confidence level and using the equation discussed in Section 4.1.1. The result from Figure 5- 18, shows that the new Coriolis flow meter has a higher error compared to the old Coriolis flow meters. Table 11 shows a detailed result of the analysis.

Table 11. Uncertainty Experimental Results for Fluid-1 Mass flow rate at Various Flow Rates

Mass flow Rate (kg/min)	250	260	270	280	290	300	310	320	330	340	350	360	370	380	390	400
Uncertainty of Single Measurement (kg/min) Old Coriolis	1.70	2.21	1.18	1.93	1.96	1.54	1.68	1.73	1.76	1.41	1.31	1.36	1.30	1.50	1.55	1.16
Uncertainty of Single Measurement (kg/min) New Coriolis	2.58	1.62	1.18	1.52	1.00	2.72	1.21	1.45	2.00	2.16	1.24	1.77	1.74	1.39	1.28	2.81
Uncertainty of the mean (kg/min) Old Coriolis	0.24	0.31	0.17	0.27	0.28	0.22	0.23	0.24	0.25	0.20	0.18	0.19	0.18	0.21	0.22	0.16

Percentage Uncertainty of the mean Old Coriolis	0.09	0.12	0.06	0.10	0.09	0.07	0.08	0.08	0.07	0.06	0.05	0.05	0.05	0.06	0.06	0.04
Uncertainty of the mean (kg/min) New Coriolis	0.36	0.23	0.17	0.21	0.14	0.38	0.17	0.20	0.28	0.30	0.17	0.25	0.24	0.19	0.18	0.39
Percentage Uncertainty of the mean New Coriolis	0.14	0.09	0.06	0.08	0.05	0.13	0.05	0.06	0.08	0.09	0.05	0.07	0.07	0.05	0.05	0.10
Total uncertainty of the mean(kg/min) Old Coriolis	0.14	0.16	0.12	0.14	0.14	0.12	0.13	0.13	0.12	0.12	0.11	0.11	0.11	0.11	0.11	0.11
Total uncertainty of the mean(kg/min) New Coriolis	0.18	0.13	0.12	0.13	0.11	0.16	0.11	0.12	0.13	0.13	0.11	0.12	0.12	0.11	0.11	0.14

5.3.3 Mass flow rate comparison Using Fluid – 2

In using fluid-2 for comparing the mass flow rate measurement of the two Coriolis flow meter, the experiment was performed by varying the flow rate from 250kg/min to 300kg/min and then decreased again to 250kg/min because of the effect of bubbles of the fluid at higher flow rates. The hysteresis curve of both flow meter at higher flow rates is shown in Figure 5- 19 below,

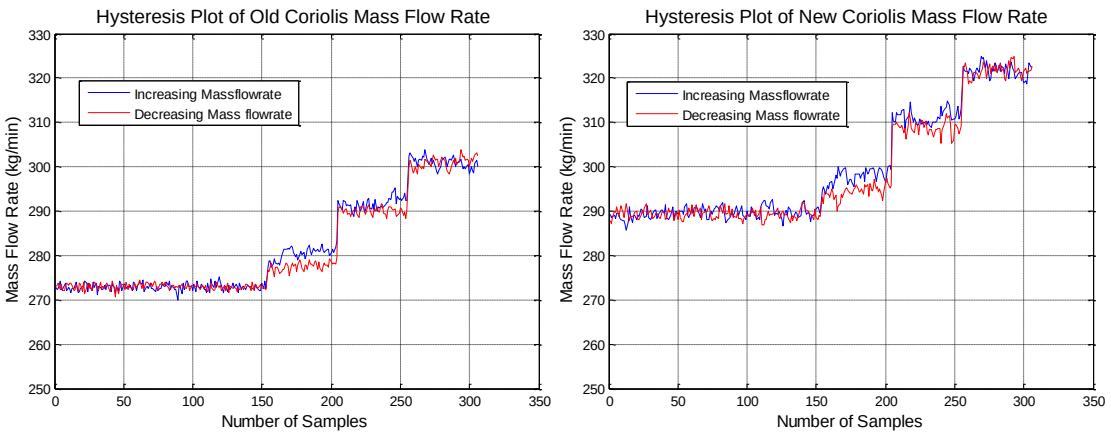

Figure 5- 19. Hysteresis mass flow rate measurement of fluid-2 from old(left) and new(right) Coriolis flow meter

From Figure 5- 19 (Old Coriolis at the left and new Coriolis at the right), noticed that the two Coriolis flow meters started measuring the mass flow rate at approximately 272kg/min due to the high density of the fluid.

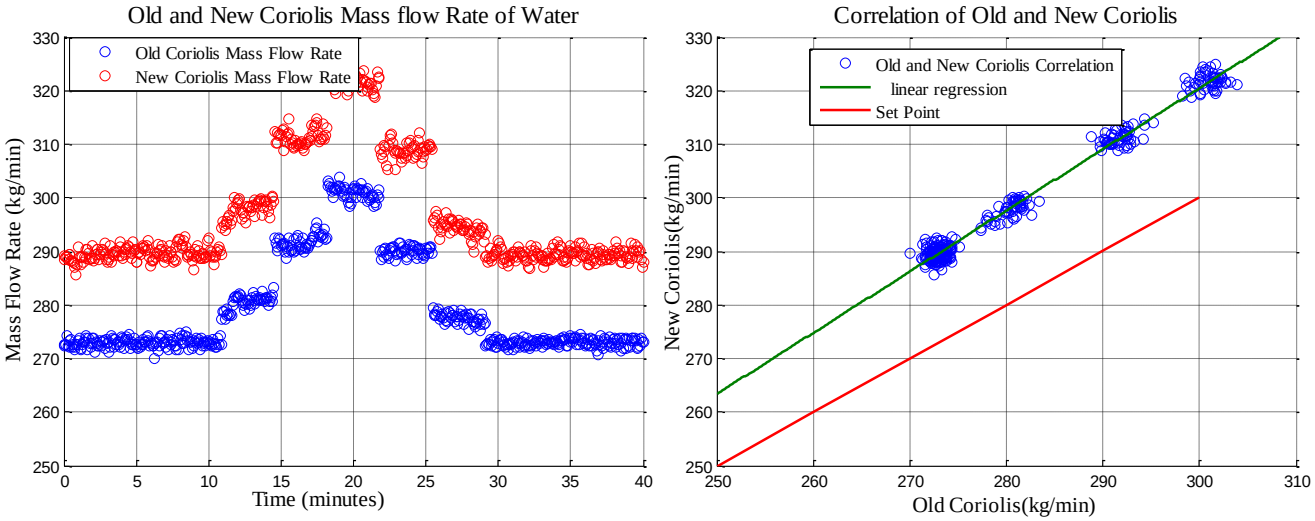

Figure 5- 20. Mass flow rate of fluid-2 from Old(blue) and new(red) Coriolis flow meter as set point changes with time(left) and the correlation between the old and new Coriolis flow meter(right).

From Figure 5- 20 the flow rate of both Coriolis flow meter changing with time at the left and the correlation of both old and new Coriolis at the right. The result shows that the old and new flow meter are positively correlated with each other.

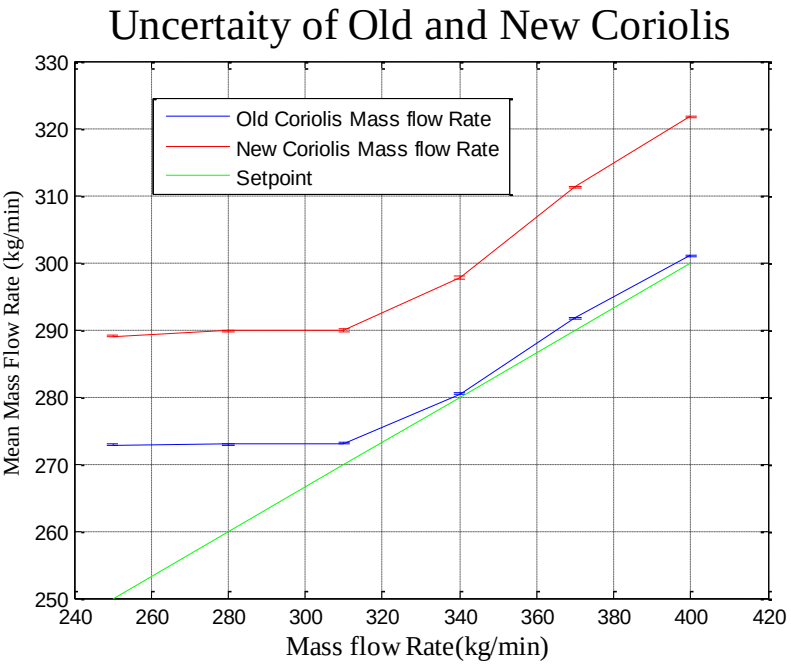

Figure 5- 21. Estimated Uncertainty of Old and New Coriolis Flow meter Using Fluid-2

Considering 95% confidence level and using the equation discussed in Section 4.1.1,

Figure 5- *21* shows the uncertainty of old and new Coriolis flow meter using fluid-2 for the experimental analysis. It can be clearly seen that the error in the new Coriolis flow meter is higher than the old Coriolis and as the flow rates increase the error also increases. Table 12 shows a detailed result of the analysis.

Table 12.Uncertainty experimental results for fluid-2 mass flow rate at various flow rates

Mass flow Rate (kg/min)	250	260	270	280	290	300
Uncertainty of Single Measurement (kg/min) Old Coriolis	1.52	1.62	1.56	2.68	2.59	2.40
Uncertainty of Single Measurement (kg/min) New Coriolis	2.14	2.12	2.60	3.26	2.88	2.77
Uncertainty of the mean Old (kg/min) Coriolis	0.21	0.23	0.22	0.38	0.36	0.34
Percentage Uncertainty of the mean Old Coriolis	0.09	0.09	0.08	0.13	0.13	0.11
Uncertainty of the mean (kg/min) New Coriolis	0.30	0.30	0.36	0.46	0.40	0.49
Percentage Uncertainty of the mean New Coriolis	0.12	0.11	0.14	0.16	0.14	0.13
Total uncertainty of the mean(kg/min) Old Coriolis	0.13	0.13	0.13	0.17	0.16	0.15

Total uncertainty of the mean(kg/min) New Coriolis	0.16	0.15	0.17	0.19	0.17	0.16

5.3.4 Mass flow rate comparison at higher flow rate

To investigate the effect of both Coriolis flow meter as the flow rate increases, fluid-2 was used for the experimental analysis. The flow rate set point was varied from 250kg/min to 550kgmin and then decreased again to 250kg/min on an interval of 50kg/min. The hysteresis curve of both flow meter at higher flow rates is shown in Figure 5- 22 below (old Coriolis at the left and new Coriolis at the right).

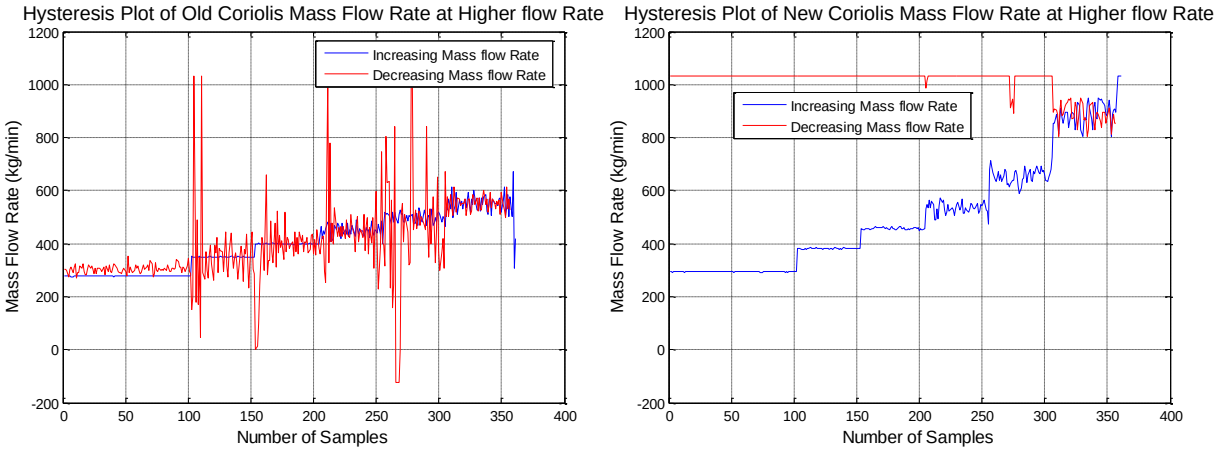

Figure 5- 22. Hysteresis mass flow rate measurement of fluid-2 from old(left) and new(right) Coriolis flow meter at higher flow rates

From Figure 5- 22 (old Coriolis at the left and new Coriolis at the right), noticed that as the flow rates increases more bubbles are generated, thereby creating more errors in both flow meters. However the new Coriolis flow meter is greatly affected by the bubbles and thus generating more errors.

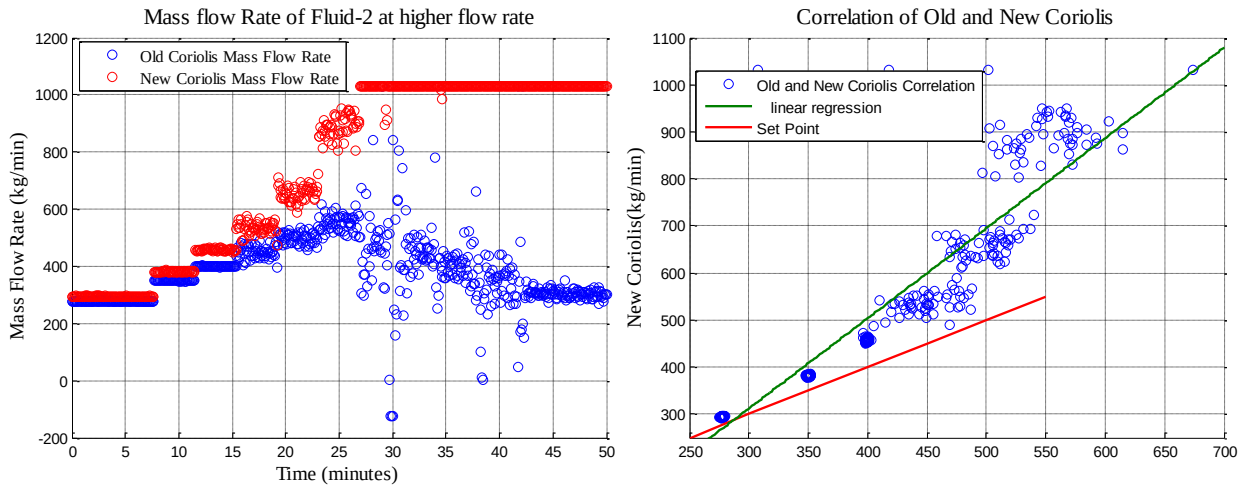

Figure 5- 23. Mass flow rate of fluid-2 from Old(blue) and new(red) Coriolis flow meter as set point changes with time(left) and the correlation between the old and new Coriolis flow meter(right) as flow rates increases

Figure 5- 23, the flow rate of both Coriolis flow meter changing with time at the left and the correlation of both old and new Coriolis at the right. The results show more bubbles are generated as the flow rates increases, thus affecting both Coriolis flow meter but more adversely by the new Coriolis flow meter.

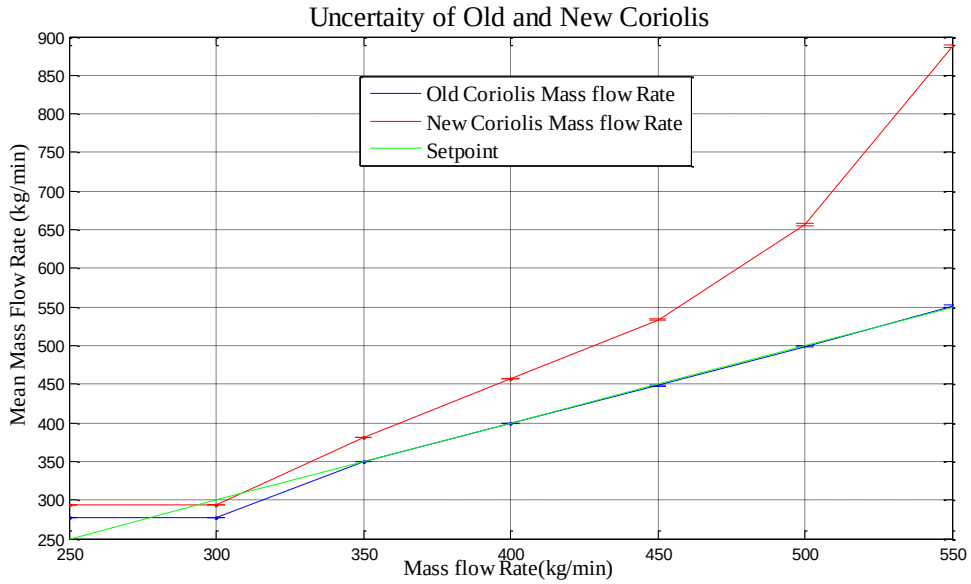

Figure 5- 24. Estimated Uncertainty of Old and new Coriolis Flow meter at higher flow rate Using Fluid-2

Considering 95% confidence level and using the equation discussed in Section 4.1.1, Figure 5- 24, Shows the uncertainty of old and new Coriolis flow meter at higher flow rates using fluid-2 for the experimental analysis. As seen in the figure, the higher the flow rates the more the errors in both Coriolis flow meter but with a more error in the new Coriolis flow meter. The old Coriolis flow meter has a lower error compared to the new Coriolis flow meter. Table 13 shows a detailed result of the analysis.

Table 13.Uncertainty Experimental Results for Fluid-2 at Higher Mass flow rate

Mass flow Rate (kg/min)	250	300	350	400	450	500	550
Uncertainty of Single Measurement (kg/min) Old Coriolis	1.79	1.50	2.15	2.45	42.49	38.99	56.41
Uncertainty of Single Measurement (kg/min) New Coriolis	1.79	1.57	3.10	6.76	41.45	52.09	74.28
Uncertainty of the mean (kg/min)Old Coriolis	0.25	0.21	0.30	0.34	5.95	5.46	7.90
Percentage Uncertainty of the mean Old Coriolis	0.10	0.7	0.09	0.09	1.32	1.09	1.44
Uncertainty of the mean (kg/min)New Coriolis	0.25	0.22	0.43	0.95	5.80	7.29	10.40

Percentage Uncertainty of the mean New Coriolis	0.10	0.07	0.12	0.24	1.29	1.46	1.89
Total uncertainty of the mean(kg/m^3) Old Coriolis	0.14	0.12	0.13	0.13	1.33	1.10	1.44
Total uncertainty of the mean(kg/m^3) New Coriolis	0.14	0.12	0.16	0.26	1.29	1.46	1.89

5.4 Mass flow rate model estimation

In order to make a model to estimate mass flow rate in the open venturi channel, Coriolis flow meter was used as a reference meter while other variables such as temperature, pressure, level measurement in the open venturi channel, differential pressure and density were used as an input. However before the model can be generated, we need to investigate how the variables are related to mass flow rate, thus, multivariate data analysis method is used to extract the variables of interest that have a higher correlation with mass flow rates in the open channel venturi flow meter.

5.4.1Multivariate data analysis (MDA)

Multivariate data analysis is a statistical method used to analyze more than one variables by finding the best possible model for predicting the parameter of interest from varieties of measurements. This method of analysis can be used for process optimization and control, research and development, quality control among others [53]. In using multivariate data analysis, various models can be generated, such as Principal component analysis, principal component regression and partial least square regression. However for the purpose of this thesis a partial least square regression model will be developed.

5.4.1.1 Partial least square regression model

This is the process of finding a linear relationship between any parameter of interest from variety measurements simultaneously. The objective here is to use a set of variables (level, temperature, pressure etc.) to predict the relationship of another variable (mass flow rate). Using the experimental data set discussed in Section 4, the old and new Coriolis flow meter will be our reference meter while the varieties measurements from the venturi rig will be our input to estimate mass flow rate. To investigate and visualize how these variables vary with each other Figure 5- 25 shows the sample variance line plot.

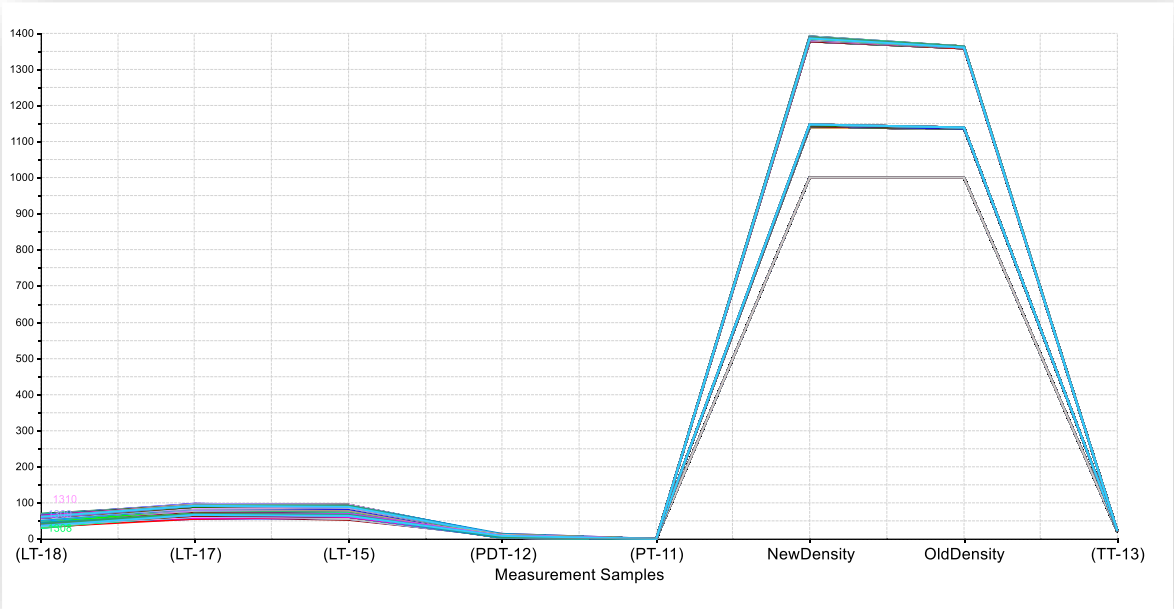

Figure 5- 25. Variations of samples measurements in the open channel venturi rig

The variations of this variables were due to the difference in measurements units. Therefore to standardize the data, the variables are multiplied with the inverse of standard deviation.

After the data has been standardized the model was made, using test set validation method. In using this validation method the data was divided into two data set, which is calibration data and test data. The test data is only used to test the model. Figure 5- 26 shows the generated model using four (4) components/factors. The first component is the most important component to describe mass flow rate because it used 78% of the variables to explain mass flow rates.

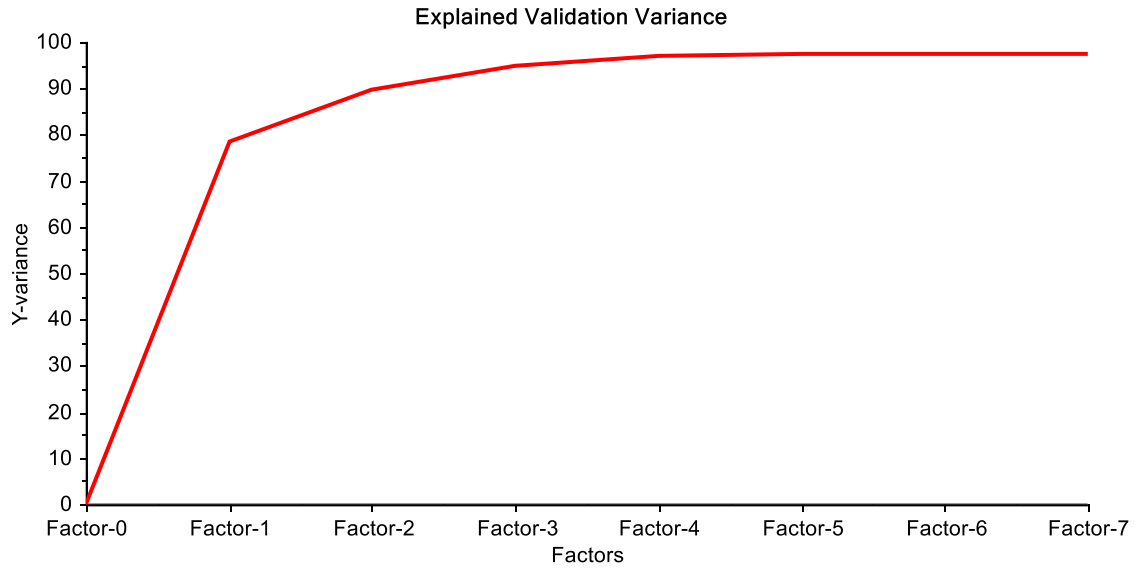

Figure 5- 26. Model Explained Validation Variance with factor -1 predicting mass flow rate mostly with 78% of all the variables

To investigate for the presence of outliers in the model in all the four (4) components/factors, Figure 5- 27 shows the score plots of all the four (4) components/factor.

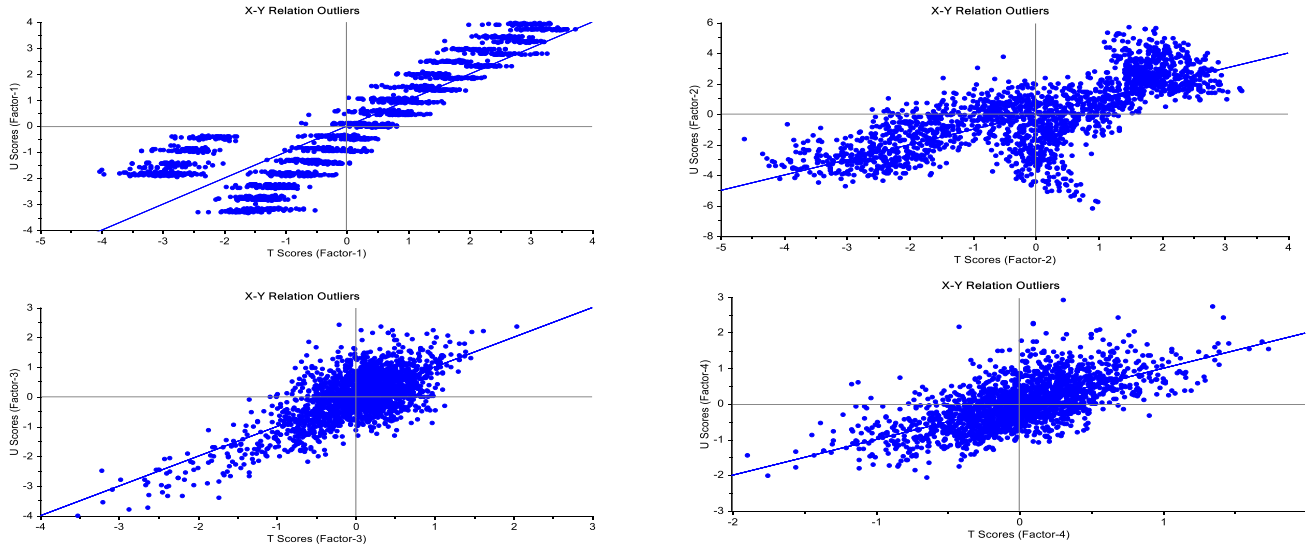

Figure 5- 27. Score plots showing no outliers in the model

Notice from Figure 5- 27 that the data are within a cluster, therefore, no outliers in the model, this was due to the careful sorting of the data by neglecting the first 10 seconds of every data set to ensure a representative value base on stable flow conditions as discussed in Section 4.

Therefore to investigate the relationship between the variables, Figure 5- 28 shows the loading plots of all the variables that will be investigated using only the first components.

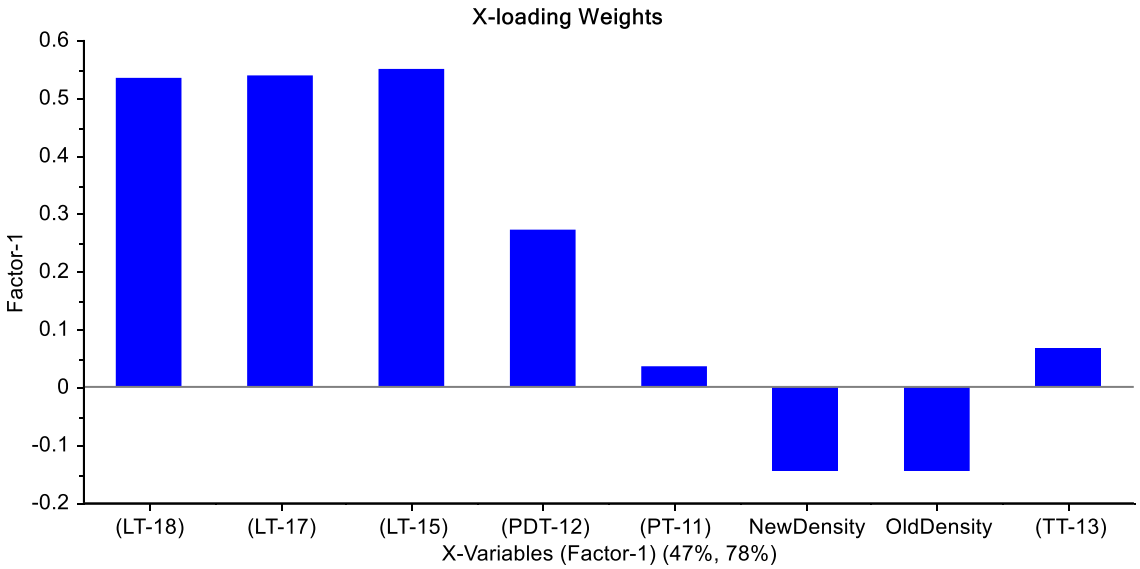

Figure 5- 28. Loading plots showing variables with higher correlation with mass flow rates

Notice that temperature (TT13) and discharge pressure (PT11) have a lower correlation in modeling mass flow rate compared to other variables which have a higher correlation. Therefore, downstream level (LT18), middle stream level (LT17), upstream level (LT15), differential pressure (PDT12) and density are the best parameters to estimate mass flow rate in the open venturi channel rig. The result of the predicted model in relation to the reference is shown in

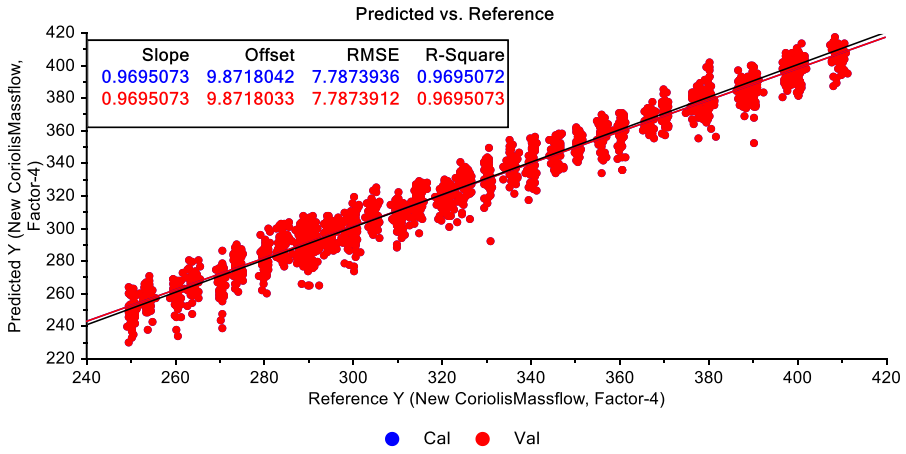

Figure 5- 29.

Figure 5- 29. Predicted vs. Reference plots

Notice the slope of the predicted model is almost close to unity with the target and regression line also almost the same. The result shows a root mean square error of 7.79kg/min (minimal error of 3.4% of the mass flow rate).

5.4.2 Artificial Neural Network

This is a soft sensor computational model, it is inspired by natural biological neurons and used to estimate parameters that depend on a variety of other parameters. It reduces the complexity involve in developing mathematical models based on numerous equations and higher computational time involved. The basic idea of neural network is to take measurements data, known as the training data and then develop a system of interconnected neurons which exchange messages between each other to learn from the training data. Neural network is used in varieties of systems such as character recognition (like handwritten), image compressions, stock markets predictions, aircraft control system, medical fields, oil and gas fields and lots more. The two basics type of network used in artificial neural network modeling are feed forward and recurrent or feedback network [54]. However for the purpose of this thesis, feed forward neural network will be used to predict the mass flow rate of fluids flowing in an open venturi rig using numerous data. The reasons behind the use of this method in modeling the flow rate of drilling fluid are based on the fact that in the real industrial system, the flow properties of the drilling fluids out from the well are not known exactly and the fluids properties changes with different environmental effects. Thus in using artificial neural network the model can be re-trained based on any changes that can occur.

5.4.2.1 Neural Network Model Formulation for mass flow Rate

The results of the model developed using multivariate data analysis reveals that some parameters do not have a high correlation in modeling mass flow rate, thus, it is then assumed not important for further analysis. Therefore, Table 14 shows the variables of interest used for the neural network model

Table 14. Variables of Interest for NN Model Estimation

Variables	**Input/output**
Downstream level (LT18)	Input
Middle level (LT17)	Input
Upstream level (LT15)	Input
Density	Input
Pressure drop (PDT12)	Input
Coriolis Mass flow	Output

The model is developed using neural network toolbox in MATLAB by using feed forward network architecture, which is just considering forward connections of neurons. The number of hidden layers in the network was determined by varying the number of hidden layer from 1-20 while looking at the minimum test performance error (mean square error). The Symmetric sigmoid transfer function is used as the activation function in the hidden layer.

Levenberg Marquart training algorithm is used with supervised training method. This choice is based on the fact that it has a characteristic feature of memory reduction and it is faster [54].

The experimental data used for the model was divided into three (3) data set, 60% for training, 20% for validation and 20% for testing. The training data is used to train the neural network model which is adjusted according to its error while the validation data is used to validate the trained model. However, the test data is only used to measure the model performance during and after training.

Considering the zero degrees (0°) inclination of the venturi rig, a total of twelve models were developed based on the parameter of interest derived from the multivariate data analysis. Table 15 shows the results of the model developed with their calculated errors. Their respective figures are also shown in **Error! Reference source not found.**, Figure 5- 31 and Figure 5- 32.

Table 15. NN Model Estimations Result

NN Result for Venturi Zero degree Inclination								
S/N	LT18	LT17	LT15	PDT12	DENSITY	No of Neurons in Hidden Layer	Test Performance Error (Mean Square Error)	Mean Absolute Error (kg/min)
1	OK	OK	OK	OK	OK	15	30.05	4.14
2	OK	OK	OK	OK	NO	16	90.70	5.58
3	OK	OK	OK	NO	OK	13	33.45	4.38
4	OK	OK	OK	NO	NO	15	125.52	8.19
5	OK	OK	NO	NO	NO	13	184.96	10.27
6	OK	OK	NO	NO	OK	12	60.68	5.77
7	OK	OK	NO	OK	OK	15	46.62	4.89
8	OK	OK	NO	OK	NO	11	82.81	6.7
9	NO	OK	OK	OK	NO	14	73.67	5.85
10	NO	OK	OK	OK	OK	12	26.97	4.26
11	NO	OK	OK	NO	NO	15	125.81	8.56
12	OK	NO	NO	OK	NO	14	180.36	10.35

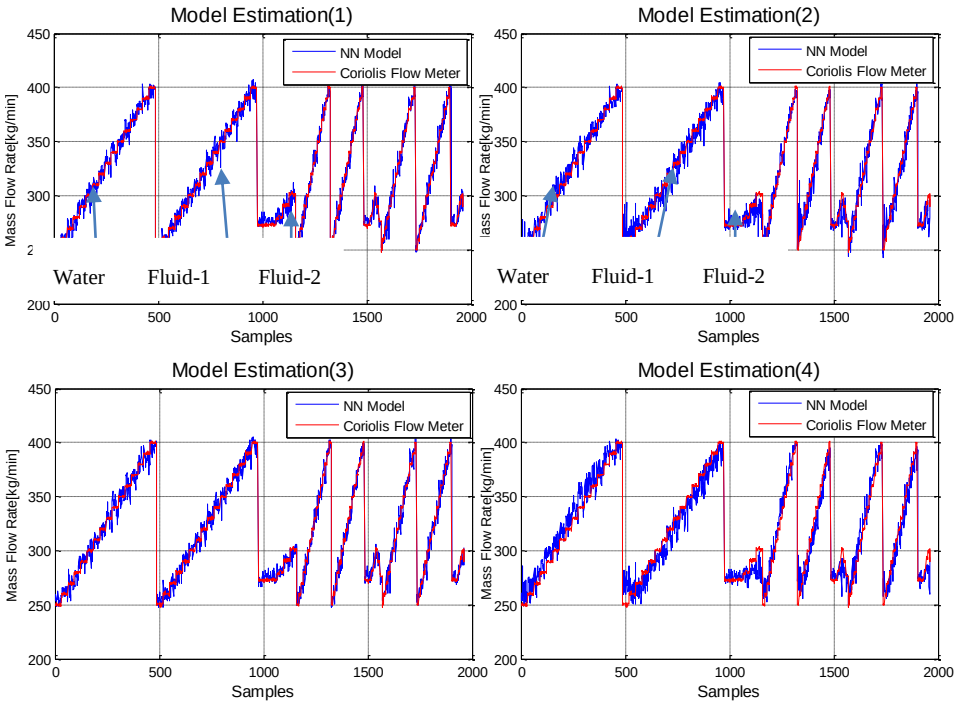

Figure 5- 30. NN model estimation of mass flow rate (1-4)

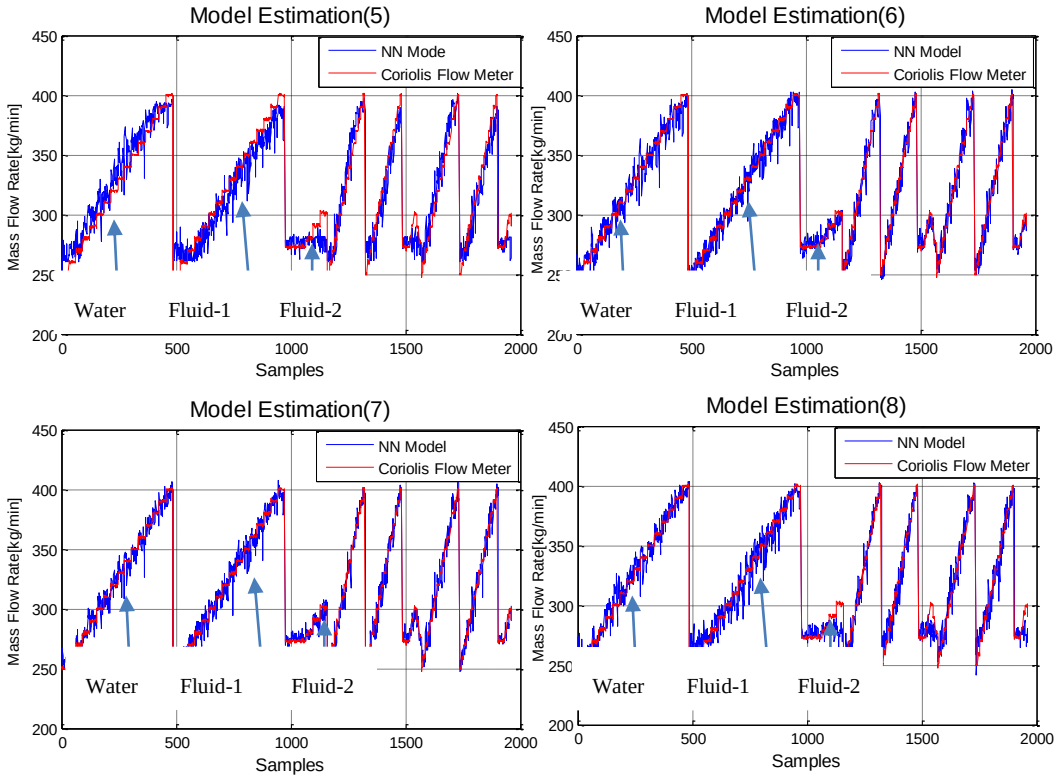

Figure 5- 31. NN model estimation of mass flow rate(5-8)

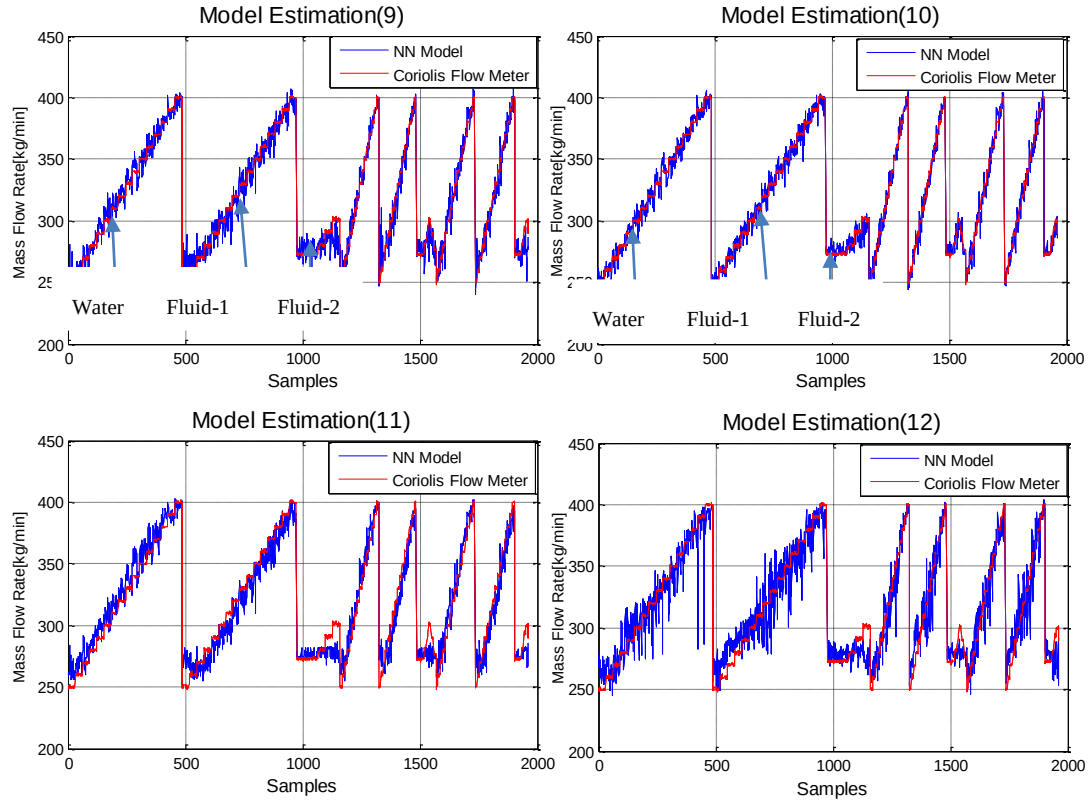

Figure 5- 32. NN Model Estimation of mass flow rate (5-12)

The result of the model in Table 15, shows that model number one with all the level measurements, density and pressure drop has the minimum mean absolute error forms the best model for predicting mass flow rate. It is also important to notes that density is a very important parameter when estimating mass flow rates of fluids with varying density. Notice in all the model when density is an input, the estimated error reduces.

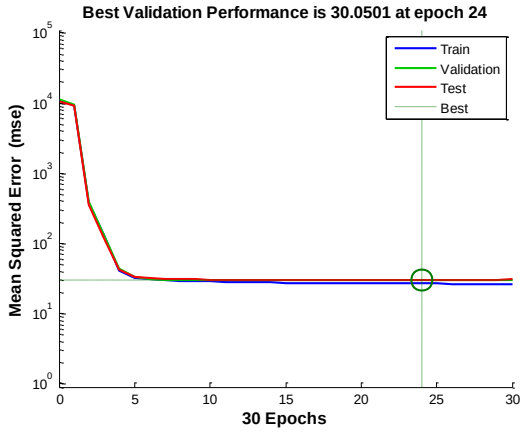

Figure 5- 33. Model-1 Performance Curve showing Mean square error of 30.05

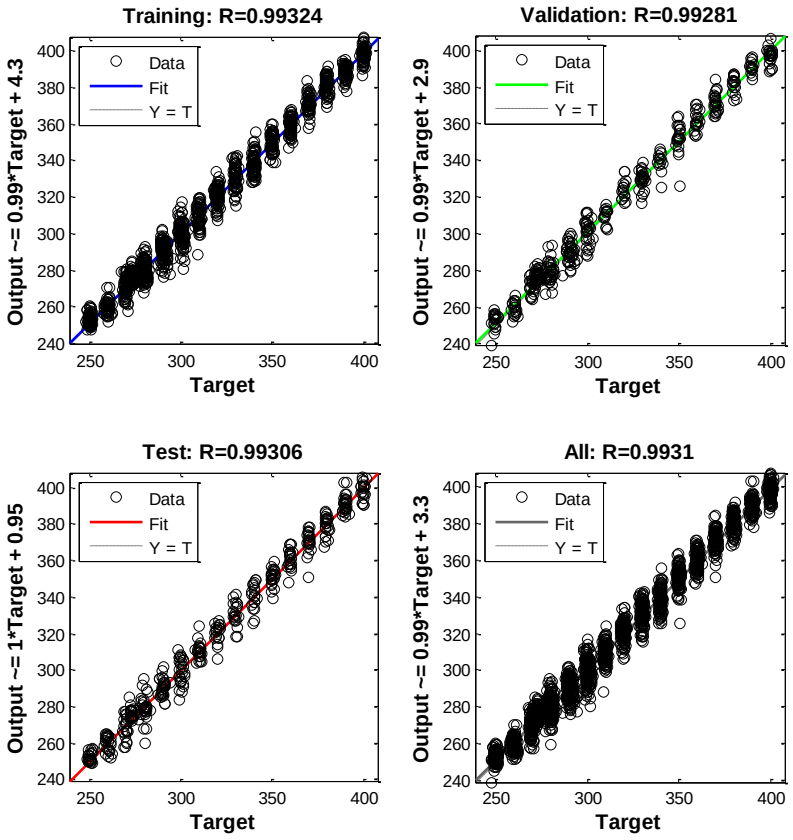

Figure 5- 34. Training Validation and Test Regression of Model-1

The model shows a very good prediction of mass flow rate using all the levels measurement in the open channel venturi rig, density and pressure with 24 iterations as presented in drop as illustrated inFigure 5- 33. The training, validation and test regression is almost at unity as shown in figure 5- 34.

6 Discussion

Whenever samples need to be taken for laboratory measurement in the rig as presented in Figure 5- 3, the best position for collecting samples is at the top of the tank for fluid -1 and at the venturi rig when the fluid is flowing for fluid-2.

The Viscosity measurement results presented in figure 5- 1 shows that the laboratory viscosity measurements for fluid-1 and fluid-2 are non-Newtonian in nature, characterized as a shear thinning fluids. However, the results from the new Coriolis flow meter as presented in figure 5- 2, contradicts the laboratory measurements, showing that the fluids are Newtonian in nature. Furthermore, the new Coriolis flow meter measured the viscosity of water accurately, proving the facts that the new Coriolis flow meter can only measure the viscosity of Newtonian fluids.

According to the manufacturer of the flow meter [50, 49], bubbles in the measuring tubes can result in increased measurement errors. Also according to the research performed by [9], it shows that whenever the agitator is in operation while measurements are been taken in the open venturi rig, more bubbles are generated thereby causing an increased measurement errors. The CFD simulation performed in [40], shows that maximum velocity of non-Newtonian fluids flowing through a bend is at the inner wall, therefore, a turbulent flow can be generated in the pipe thereby creating more bubbles for fluids which have the characteristic of generating bubbles (fluid-1 and fluid-2).

In comparing the density and mass flow rate measurement of the old and new Coriolis flow meter, the result of the measurements as presented in Figure 5- 6 shows that the old and new Coriolis flow meter can measure the density of water adequately. However in measuring the density of fluid-1 and fluid-2 as presented in Figure 5- 8 and Figure 5- 10, both Coriolis flow meter shows some deviation from the laboratory measurement. However the new Coriolis flow meter showed a higher error when compared to the old Coriolis flow meter. Also in comparing the mass flow rate, in using water, the result as presented in Figure 5- 14 and Figure 5- 15 shows that both Coriolis flow meters can measure the mass flow rate of water adequately. However in measuring the mass flow rate of fluid-1 and fluid-2 as presented Figure 5- 17, Figure 5- 18, Figure 5- 20 and

Figure 5- *21* the new Coriolis mass flow meter showed a higher error which also increases with increased flow rate as presented in Figure 5- 23 and Figure 5- 24. These errors generated by both flow meters is caused by the effect of bubbles generated by the fluids. The more error

generated by the new Coriolis flow meter is caused due to the position of installation of the flow meter(very close to a pipe bending of almost 90°).

In estimating the mass flow rate and extracting the parameter for improving estimation, the result from the multivariate data analysis reveals that temperature and pressure are not really important in estimating mass flow rate in the rig. However density, pressure drops, level measurements at the throat, downstream and upstream of the open venturi channel have a higher correlation with flow rate, thus, these parameters can be used to model mass flow rate in the open channel venturi rig.

The results from the neural network also reveal that density is another most important parameter very crucial in estimating mass flow rate with varying fluids density. Notice from the result in Table 15, whenever density is an input to the model , the estimated error reduces.

7 Conclusion and Recommendation

This thesis is mainly focused on the flow metering of non-Newtonian drilling fluid and the commissioning test of newly installed Coriolis flow meter in University College of Southeast Norway. It explains the design of an empirical model to estimate the flow rate of an emulated drilling fluids, the commissioning test of the newly installed Coriolis flow meter and comparison with the previously installed flow meter based on sampled data from the experiments carried out in the Open Channel venturi rig at University college of Southeast Norway.

In estimating the flow rate of the fluids, two different model were generated. The first model was obtained with a partial least squares approach in multivariate data analysis to find a linear relationship between mass flow rate and other variables. The result from the model gave an estimated error of 7.79kg/min of mass flow rate estimate and reveals that the open channel venturi level measurements at the throat, downstream, upstream, density and pressure drop are highly correlated with mass flow rate. These variables are the variables of interest used in designing an empirical model for mass flow rate estimation.

The second model was obtained with artificial neural network approach using feed forward network architecture. The input to the model are the results revealed from the multivariate data analysis. The output of the model is mass flow rate while the old Coriolis flow meter is used as a reference meter for the model. Twelve different neural network model was generated using the revealed variable of interest which are the density, pressure drop, level measurement of the open channel venturi throat, downstream and upstream. The best result from all the model was the model where all the four measurements were used as inputs with an estimated error of 4.14kg/min of mass flow rate using 15 hidden neurons in the hidden layer. The result from the neural network also revealed that density is an important parameter when estimating the flow rate of fluids with changing density. This is very important when making a model in the real life offshore drilling, where the actual density of drilling fluids flowing out from the well is varying. However when the drilling fluid density is constant, only the level measurement is adequate enough to estimate mass flow rate.

In the commissioning test of the newly installed Coriolis flow meter, the error generated due to the effect of the pipe bending for the emulated drilling can be reduced by re-positioning the newly installed Coriolis flow meter or otherwise an adding additive to the emulated drilling fluids to reduce the effect of the bubbles generated. However the previously installed Coriolis

flow meter as of today is more accurate in measuring mass flow rate than the newly installed Coriolis flow meter. It is also important to note that the modeled used in measuring the viscosity of newly installed Coriolis flow meter is only for Newtonian fluids. Therefore to measure the viscosity of Non-Newtonian fluids a model can be re-generated for the emulated drilling fluids.

Bibliography

[1] Geir Elseth, "State of the Art study - Kick and loss detection",Statoil, Porsgrunn, Telemark,pp.1-36, 2015.

[2] L.D. Maus, T.D. Tannich, W.T. Ilfrey,"Instrumentation Requirement for Kick Detection in Deep Water"Journal of *Petroleum Technology*, vol. 31, pp. 1029-1034, 1978.

[3] D.M. Schafer.et al, "Evaluation of Flow Meters for Detection of Kicks and Lost Circulation During Drilling",*SPE/IADC Drilling Conference*, New Orleans, Louisiana, 1992.

[4] C. E. Agu.et al "Simulation of open channel flow for Mass", TUC, Porsgrunn, 2013.

[5] C. E. Agu, "Model based estimation of drilling mud flow using a Venturi channel",TUC, Porsgrunn, 2014.

[6] S. J. Jonathan et al,"Production of model Fluid and Testing of Measuring Sensors for return drilling mud",TUC, Porsgrunn, 2015.

[7] S. Glittum et al, "Expansion of test facility for flow measurement on drilling fluid",TUC, Porsgrunn, 2015.

[8] J. Ejimofor et al, "Mud Flow Measurements in Open Venturi Channel",TUC, Porsgrunn, 2015.

[9] K. Chhantyal, "Drilling Fluids Design and the Density Adjustment Mechanism",TUC, Porsgrunn, 2015.

[10] Taher Elfakharany, "Comparison between underbalance and conventional overbalance drilling In the gulf of Suez using a Drilling Simulator", *Int. Journal of Advancement in Engineering, Technology and Computer,* Vol. 1, No. 1, pp. 43-51, 2014.

[11] D. B. Bennion et al, "Underbalanced drilling and Completion operations to minimize formation damage-reservoir screening criteria for optimum application", *The Journal of Canadian Petroluem Technology*, Vol. 37, No. 09, pp. 36-50, September 1998.

[12] Ahmad Nateghpour et al. (07 July 2011), "Investigation of Effective Parameters of Rotary drilling bits selector". [online]. Available: www.scribd.com/doc/59511434/Drilling-Bit-Selection

[13] Baker Hughes. (01 January 2016), "Drilling Bit Catalogs". [online]. Available: www.bakerhughes.com/news-and-media/resources/reference-guides/drill-bits-catalog.

[14] Shell. (2015) "www.shell.com/us/alaska". [Online]. Available: www.safetyinengineering.com/FileUploads/O&G%20offshore%20production_1414488606_2.pdf.

[15] Iain Caulfield et al. (2007) "Project Management of Offshore well Completion" [Online]. Available: www.slb.com/~/media/Files/resources/oilfield_review/ors07/spr07/p4_13.pdf.

[16] Sichei C. C. "Geothermal Drilling Fluids", Kenya Electricity Generating Company Ltd. 2011.

[17] Subhash N. Shah et al., "Future Challenges of Drilling Fluids and Their Rheological Measurements", *AADE,* Vol. 10, No. 41, pp. 1-16, 07 April 2010.

[18] Shyam Kumar, "Mud Engineering", Mud services ONGC.2001.

[19] Ryen Caenn, Darley H.C.H and George R.Gray, "Composition and properties of Drilling and Completion Fluid",6th ed. Oxford UK, Elsevier, 2011.

[20] Sience Stories (April 2010) "Drilling Fluids", [Online]. Available: sciencelearn.org.nz/Science-Stories/Strange-Liquids/Non-Newtonian-fluids.

[21] Schlumberger, (2013) "Oilfield Glossary",[Online]. Available: www.glossary.oilfield.slb.com.

[22] U.S. Dept. of Labour, "Oil and Gas Well Drilling and Seevicing eTool", [Online]. Available: www.osha.gov/SLTC/etools/oilandgas/drilling/mud_system.html.

[23] E. Hansen,"Evaluation of Drilling Fluids Properties", University of Stavanger,2012.

[24] Expro (2009),"Drilling Fluid flow measurements" [Online]. Available: www.exprogroup.com/products-and-services/meters/drilling-fluids-flow-measurement

[25] Trevor Burgess, A. Allen Starkey and David White, "Improvement for kick detection", *Schlumberger Oilfield Review, Vol.2 No.1* pp. 43-51.

[26] Le Blay F. et al, "A New Generation of Well Surveillance for Early Kick Detection of Gains and Losses When Drilling Very High Profile Ultradeep Water Wells, Improving Safety, and Optimizing Operation Procedures", *SPE,* Vol. 158373, 2012.

[27] S. Taha, "Polymer", *Elsevier,* Vol. 51, No. 22, pp. 5007-5023, 11 August 2010.

[28] A. Rao, "Rheology of Fluid, Semisolid and Solid Foods Principles and Applications", Springer, pp. 27-36, 2014.

[29] API, (2009)"API Recommended Practice 13D – Rheology and hydraulics of oil-well" . [Online]. Available: www.api.org.

[30] K.M. Kirillov et al., "An Ultrasonic Flowmeter for Viscous Liquid", Springer, vol. 57, No.5, pp. 533-536, August 2014.

[31] W.H. Wowe, L. D. Dinapoli and J.B. Arant, "Process Measurement and Analysis", 2003.

[32] K. Kadlec, "Level measurement System", *Measurement and Control,* pp.6, 2008.

[33] Indiamart, (1996) "Venturi Tube", [Online]. Available: www.indiamart.com/proddetail/venturi-tube-9637180073.html.

[34] Yunlong Zhou et al, "Identification method of gas-Liquid two phase flow regime based on Image Multifeature Fusion and support Vector Machines" *Chinese Journal of Chemical Engineer,* Vol.14, No.1, pp. 832-840, 2008.

[35] Holland F. A and Bragg R., "Fluid Flow for Chemical and Process Engineers" 2nd Ed, Butterworth-Heinemann, pp. 1-131, 1995.

[36] E. L. Upp and Paul J. LaNasa, "Fluid Flow Measurement : A Practical Guide to Accurate Flow Measurement" 2nd Ed, Woburn Gulf Publishing Company, pp. 24-255, 2002.

[37] Gertrudys B. Adkins, "Flow Measurement device", Division of Water Rights, 2006.

[38] H. K. Versteeg and W. Malalasekera, "An Introduction to Computational Fluids Dynamics (The Second Finite Method)", Pearson Education Limited, pp. 1- 517 2007.

[39] N. S. Deshpande and M. Barigou, "Vibrational flow of non-Newtonian fluids", *Chemical Engineering Science,* Vol. 56, No.12, pp.3845–3853, 25 July 2001.

[40] T. K. Bandyopadhyay and S. K. Das, "Non-Newtonian and Gas-non–Newtonian Liquid Flow through Elbows – CFD Analysis", *Journal of Applied Fluid Mechanics,* Vol. 6, No. 1, pp. 131-141, 2013.

[41] Sumit Tripathia et al.,"Lubricated Transport of Highly Viscous Non-Newtonian Fluid as Core-Annular Flow: A CFD Study", *ScienceDirect,* Vol. 15, pp. 278–285, 28 May 2015.

[42] Endress+Hauser,"RTD Thermometer omnigrad TST41N", [Online]. Available: https://portal.endress.com/wa001/dla/5000000/5566/000/00/TI232ten_1198.pdf.

[43] ABB,(23 May 2014), "LST400 Ultrasonic level / open channel flow transmitter LST400",. [Online]. Available: https://library.e.abb.com/public/c0b56699cecfef85c1257ce100366215/DS_LST400-EN%20Rev.%20C.pdf.

[44] Pepperl+FUCHS, "Inclination Sensor",[Online]. Available: http://files.pepperl-fuchs.com/selector_files/navi/productInfo/edb/222357_eng.pdf.

[45] Aplisens, "Smart Differential Pressure Transmitter Apre-2000",[Online]. Available: www.aplisens.com/dodatkowe_aplikacje_advertnet/pdf/produkty/APR-2000.pdf.

[46] Aplisens, "Smart Pressure Transmitter Pce-28.Smart",[Online]. Available: www.aplisens.com/dodatkowe_aplikacje_advertnet/pdf/produkty/PC-28Smart.pdf.

[47] S. T. S-Tech, "Density Transmitter DT-9300",[Online], Available: www.s-tec.no.217.171.192.197.xip.io/produkter/densitet-og-konsentrasjonsmalere/?sent=1&form=BestilldatabladD9300_05_1.

[48] C. Cynergy3,(2014), "Compact External Mount with Temperature Sensing",[Online]. Available: http://www.cynergy3.com/sites/default/files/product-data-sheets/Tsf70%202011.pdf.

[49] Endress+Hauser, "Promass 63 Mass Flow Measuring System",[Online]. Available: https://portal.endress.com/wa001/dla/5000000/3583/000/00/BA014DEN.pdf.

[50] Endress+Hauser, (01 April 2015)"Technical Information Proline Promass 80I, 83I Coriolis flowmeter",. [Online]. Available: https://portal.endress.com/wa001/dla/5000079/2114/000/04/TI00075DEN_1315.pdf

[51] A. R. Anthony J Wheeler, "Introduction to Engineering Experimentation", Pearson Education, pp. 5-210, 2001.

[52] Anton Paar,(04 May 2005), "DMA 4500 Density/Specific gravity/Concentration Meter",[Online]. Available: www.masterflex.com/assets/Manual_pdfs/DMA4500.pdf.

[53] Camo, "Multivariate Data Analysis", [Online]. Available: www.camo.com/multivariate_analysis.html.

[54] Siddique Nazmul and Adeli Hajjat, "Computational Intelligence",John Wileys & Sons Ltd, United Kingdom, pp. 103-180, 2013.

Appendix 1. Task description

University College of Southeast Norway

Campus Porsgrunn/Faculty of Technology
Department of Electrical Engineering, IT and Cybernetics

FMH606 Master's Thesis

Title: Open Venturi-Channel Flow metering of non-Newtonian Fluids –Case study with emulated drilling fluid

TUC supervisor(s): Prof. II, Geir Elseth STATOIL/ UCSN, Prof. Lars Hoff
Saba Mylvaganam, Håkon Viumdal, PhD Research Fellow Khim Chyyantal, UCSEN

External partner: STATOIL Dept. Intelligent Drilling, Porsgrunn.

Task description:

Drilling fluid with varying consistencies are used in the oil and gas industries in conjunction with drilling operations. One of the main functions is that the drilling mud is the first barrier against hydrocarbon blow out during drilling. The drilling fluid also called drilling mud used in such operations need to have the right density and viscosity before after its flow through the reservoir. This project focuses on the feasibility of the Venturi-channel as a stand-alone flowmeter facilitating continuous flow metering.

The goals for the present thesis project are the following:

1. Literature survey generally on drilling mud flow
2. An overview of the measurands monitored using a P&ID as used in the oil and gas industries (status quo).
3. A detailed overview of the UCSEN rig with open Venturi-Channel with all the instruments installed with a list of their measurement capabilities
4. Brief survey of measurement techniques used in monitoring flow with focus on Venturi flowmeters (both in open and closed conduits) for both Newtonian and non_Newtonian fluids
5. The main features and challenges of flow metering of non-Newtonian fluids
6. An overview of CFD work dedicated to non-Newtonian fluids with clear description of the parameters used and the outputs from the model. Status quo reaching to 2015.
7. Compare the viscosity, density data from Coriolis Meter (Serial number: K6071D02000) with lab base measurements
8. Compare and discuss the outputs of the two Coriolis meters focusing on any discrepancies.
9. Use the data and analyse them to extract parameters of interest including improving estimates of flow velocity.
10. Submit a report using the guidelines and template of UCSEN with systematically archived data sets and software

Task background

Non-Newtonian fluids like mud, paint, emulsions occur very frequently in the industries and research work. Characterising simultaneously the rheological parameters and the measurement of flow of non-Newtonian fluids is a demanding task. Continuous measurement of flow velocity of drilling fluid at selected locations in the drilling rig is the main task in this project. There is a dedicated measurement rig with many measurement devices in the Campus at Porsgrunn of UCSEN.

Student category:

This work is suitable for SCE and PEM students with experience in MATLAB /LabVIEW programming some CFD work. *As the work entails continuous lab work and program development, students need to be at UCSEN throughout the term. It is mandatory that students have weekly meeting with at least one of the supervisors in the lab.*

Practical arrangements:

Necessary hardware and software will be provided by UCSEN in collaboration with STATOIL. Work will be performed in Sensor Lab and Process Hall where the mud flow facilities are available. However, possible interaction research groups in Norway and abroad is also envisaged.

The modelling work, simulations and control algorithms will be implemented using MATLAB and/or LabVIEW. The work will be conducted mostly at UCSEN. This thesis work may be taken up by two students one with SCE background and the other with PEM background. In such a scenario, the tasks will be defined to cater to the background of the student and to complement each other's task.

Signatures:

Student (date and signature):

Supervisor (date and signature):

Appendix 2: Open channel Venturi rig Updated P&ID diagram

A. Open Channel Venturi Rig

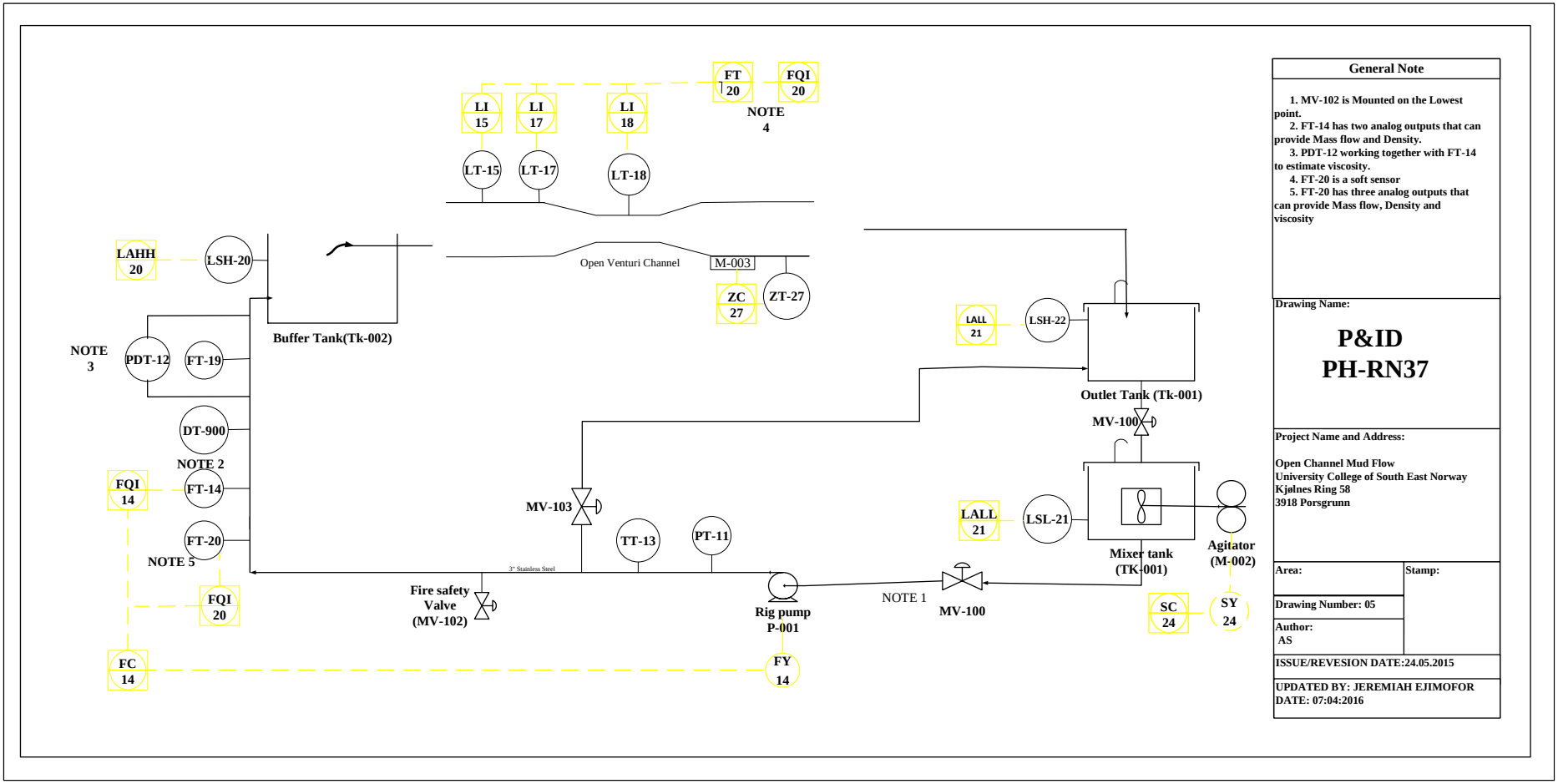

Figure- 2A. Open Channel venturi rig Updated P&ID diagram

B. Physical view of the venturi open channel flow meter

Figure 2B- 1. Venturi channel

Figure 2B- 2. Pump and Tank section

Figure 2B- 3. Position of Old and New Coriolis flow meter

Appendix 3. Lab based density measurement procedures

A: Density measurement preparation and procedures using Anton Paar DMA4500

Preparation:

- **Safety:** Use safety equipment rubber gloves. HSE datasheet must be available
- **Equipment:** Use de-gassed water. Ethanol and 10ml plastic syringe
- **Cleaning:** Use ethanol and de-gassed water for cleaning the instrument. Must be cleaned before and after use

Procedure:

- Start instrument by turning on the switch on the back side
- To prepare for density check Press menu ➡ Adjustment ➡ Density check ➡ check density.
- Inject 5ml of de-gassed water and press ok. Wait for the instrument to analyse the water density. If the deviation is less than or equal to ± 0.0002, then it is ready to start analysing by pressing save. If the deviation is greater, clean the instrument again.
- Inject 5ml of ethanol and 5ml of de-gassed water
- Insert the instrument air and start pumping air by pressing pump for quick drying and cleaning
- Stop the pump
- Inject 5ml of sample and press start. The instrument will use about 5 minutes for analysing depending on the sample temperature
- Clean the instrument by using de-gassed water and ethanol
- Perform density check with de-gassed water
- Leave the instrument on.

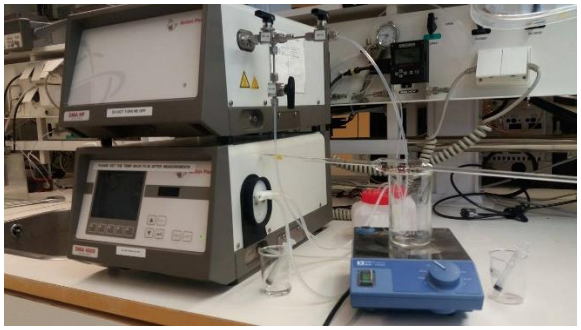

Figure 3A-1. Density measurement experiment station

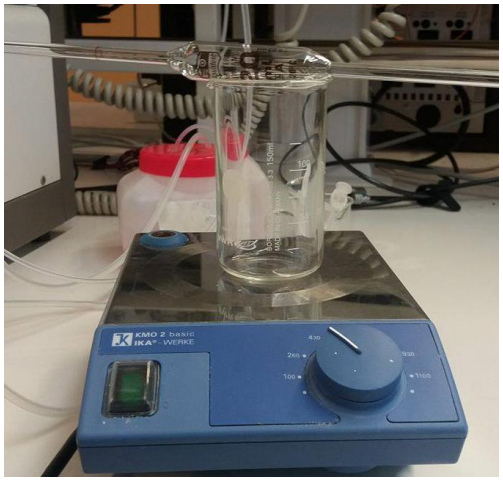

Figure 3A- 2. Process of stirring fluids using mmagnetic stirrer

Figure 3A- 3. Anton paar DMA 4500 Density/specific gravity/concentration meter

B: Preparation and procedures for degassing water

Preparation:

- **Safety:** Use safety equipment rubber gloves. HSE datasheet must be available
- **Equipment:** Buchi degasser and round-bottom flask with slip opening
- **Cleaning:** Normal cleaning after use

Procedure:

- Fill water into the water bath.
- Turn on the water bath.
- Set temperature of the heating bath.
- Pour the sample/water into the cool flask.
- Attach the flask into rotor vapour by screwing it on.
- Turn on the tap water.
- Turn on the rotor-vapour and set it to about 0.5
- Turn on the vacuum pump
- Study the boiling point table and then set a set point value of the pressure. Adjust the pressure by pressing the pressure set and rotary dial to adjust the pressure. ATTENTION! The table is for clean water.
- Press start to start the pump
- Allow the liquid to degas until it contains no more air.
- Turn off by pressing stop
- Turn off switches on the vacuum pump, rotor-vapour and water bath.

Appendix 4. Distribution tables

A. Standard Normal distribution Table

z	.00	.01	.02	.03	.04	.05	.06	.07	.08	.09
–3.4	.0003	.0003	.0003	.0003	.0003	.0003	.0003	.0003	.0003	.0002
–3.3	.0005	.0005	.0005	.0004	.0004	.0004	.0004	.0004	.0004	.0003
–3.2	.0007	.0007	.0006	.0006	.0006	.0006	.0006	.0005	.0005	.0005
–3.1	.0010	.0009	.0009	.0009	.0008	.0008	.0008	.0008	.0007	.0007
–3.0	.0013	.0013	.0013	.0012	.0012	.0011	.0011	.0011	.0010	.0010
–2.9	.0019	.0018	.0018	.0017	.0016	.0016	.0015	.0015	.0014	.0014
–2.8	.0026	.0025	.0024	.0023	.0023	.0022	.0021	.0021	.0020	.0019
–2.7	.0035	.0034	.0033	.0032	.0031	.0030	.0029	.0028	.0027	.0026
–2.6	.0047	.0045	.0044	.0043	.0041	.0040	.0039	.0038	.0037	.0036
–2.5	.0062	.0060	.0059	.0057	.0055	.0054	.0052	.0051	.0049	.0048
–2.4	.0082	.0080	.0078	.0075	.0073	.0071	.0069	.0068	.0066	.0064
–2.3	.0107	.0104	.0102	.0099	.0096	.0094	.0091	.0089	.0087	.0084
–2.2	.0139	.0136	.0132	.0129	.0125	.0122	.0119	.0116	.0113	.0110
–2.1	.0179	.0174	.0170	.0166	.0162	.0158	.0154	.0150	.0146	.0143
–2.0	.0228	.0222	.0217	.0212	.0207	.0202	.0197	.0192	.0188	.0183
–1.9	.0287	.0281	.0274	.0268	.0262	.0256	.0250	.0244	.0239	.0233
–1.8	.0359	.0351	.0344	.0336	.0329	.0322	.0314	.0307	.0301	.0294
–1.7	.0446	.0436	.0427	.0418	.0409	.0401	.0392	.0384	.0375	.0367
–1.6	.0548	.0537	.0526	.0516	.0505	.0495	.0485	.0475	.0465	.0455
–1.5	.0668	.0655	.0643	.0630	.0618	.0606	.0594	.0582	.0571	.0559
–1.4	.0808	.0793	.0778	.0764	.0749	.0735	.0721	.0708	.0694	.0681
–1.3	.0968	.0951	.0934	.0918	.0901	.0885	.0869	.0853	.0838	.0823
–1.2	.1151	.1131	.1112	.1093	.1075	.1056	.1038	.1020	.1003	.0985
–1.1	.1357	.1335	.1314	.1292	.1271	.1251	.1230	.1210	.1190	.1170
–1.0	.1587	.1562	.1539	.1515	.1492	.1469	.1446	.1423	.1401	.1379
–0.9	.1841	.1814	.1788	.1762	.1736	.1711	.1685	.1660	.1635	.1611
–0.8	.2119	.2090	.2061	.2033	.2005	.1977	.1949	.1922	.1894	.1867
–0.7	.2420	.2389	.2358	.2327	.2296	.2266	.2236	.2206	.2177	.2148
–0.6	.2743	.2709	.2676	.2643	.2611	.2578	.2546	.2514	.2483	.2451
–0.5	.3085	.3050	.3015	.2981	.2946	.2912	.2877	.2843	.2810	.2776
–0.4	.3446	.3409	.3372	.3336	.3300	.3264	.3228	.3192	.3156	.3121
–0.3	.3821	.3783	.3745	.3707	.3669	.3632	.3594	.3557	.3520	.3483
–0.2	.4207	.4168	.4129	.4090	.4052	.4013	.3974	.3936	.3897	.3859
–0.1	.4602	.4562	.4522	.4483	.4443	.4404	.4364	.4325	.4286	.4247
–0.0	.5000	.4960	.4920	.4880	.4840	.4801	.4761	.4721	.4681	.4641

z	.00	.01	.02	.03	.04	.05	.06	.07	.08	.09
0.0	.5000	.5040	.5080	.5120	.5160	.5199	.5239	.5279	.5319	.5359
0.1	.5398	.5438	.5478	.5517	.5557	.5596	.5636	.5675	.5714	.5753
0.2	.5793	.5832	.5871	.5910	.5948	.5987	.6026	.6064	.6103	.6141
0.3	.6179	.6217	.6255	.6293	.6331	.6368	.6406	.6443	.6480	.6517
0.4	.6554	.6591	.6628	.6664	.6700	.6736	.6772	.6808	.6844	.6879
0.5	.6915	.6950	.6985	.7019	.7054	.7088	.7123	.7157	.7190	.7224
0.6	.7257	.7291	.7324	.7357	.7389	.7422	.7454	.7486	.7517	.7549
0.7	.7580	.7611	.7642	.7673	.7704	.7734	.7764	.7794	.7823	.7852
0.8	.7881	.7910	.7939	.7967	.7995	.8023	.8051	.8078	.8106	.8133
0.9	.8159	.8186	.8212	.8238	.8264	.8289	.8315	.8340	.8365	.8389
1.0	.8413	.8438	.8461	.8485	.8508	.8531	.8554	.8577	.8599	.8621
1.1	.8643	.8665	.8686	.8708	.8729	.8749	.8770	.8790	.8810	.8830
1.2	.8849	.8869	.8888	.8907	.8925	.8944	.8962	.8980	.8997	.9015
1.3	.9032	.9049	.9066	.9082	.9099	.9115	.9131	.9147	.9162	.9177
1.4	.9192	.9207	.9222	.9236	.9251	.9265	.9279	.9292	.9306	.9319
1.5	.9332	.9345	.9357	.9370	.9382	.9394	.9406	.9418	.9429	.9441
1.6	.9452	.9463	.9474	.9484	.9495	.9505	.9515	.9525	.9535	.9545
1.7	.9554	.9564	.9573	.9582	.9591	.9599	.9608	.9616	.9625	.9633
1.8	.9641	.9649	.9656	.9664	.9671	.9678	.9686	.9693	.9699	.9706
1.9	.9713	.9719	.9726	.9732	.9738	.9744	.9750	.9756	.9761	.9767
2.0	.9772	.9778	.9783	.9788	.9793	.9798	.9803	.9808	.9812	.9817
2.1	.9821	.9826	.9830	.9834	.9838	.9842	.9846	.9850	.9854	.9857
2.2	.9861	.9864	.9868	.9871	.9875	.9878	.9881	.9884	.9887	.9890
2.3	.9893	.9896	.9898	.9901	.9904	.9906	.9909	.9911	.9913	.9916
2.4	.9918	.9920	.9922	.9925	.9927	.9929	.9931	.9932	.9934	.9936
2.5	.9938	.9940	.9941	.9943	.9945	.9946	.9948	.9949	.9951	.9952
2.6	.9953	.9955	.9956	.9957	.9959	.9960	.9961	.9962	.9963	.9964
2.7	.9965	.9966	.9967	.9968	.9969	.9970	.9971	.9972	.9973	.9974
2.8	.9974	.9975	.9976	.9977	.9977	.9978	.9979	.9979	.9980	.9981
2.9	.9981	.9982	.9982	.9983	.9984	.9984	.9985	.9985	.9986	.9986
3.0	.9987	.9987	.9987	.9988	.9988	.9989	.9989	.9989	.9990	.9990
3.1	.9990	.9991	.9991	.9991	.9992	.9992	.9992	.9992	.9993	.9993
3.2	.9993	.9993	.9994	.9994	.9994	.9994	.9994	.9995	.9995	.9995
3.3	.9995	.9995	.9995	.9996	.9996	.9996	.9996	.9996	.9996	.9997
3.4	.9997	.9997	.9997	.9997	.9997	.9997	.9997	.9997	.9997	.9998

B. Student T - Distribution Table.

df	*t:100*	*t:050*	*t:025*	*t:010*	*t:005*
1	3.078	6.314	12.706	31.821	63.657
2	1.886	2.920	4.303	6.965	9.925
3	1.638	2.353	3.182	4.541	5.841
4	1.533	2.132	2.776	3.747	4.604
5	1.476	2.015	2.571	3.365	4.032
6	1.440	1.943	2.447	3.143	3.707
7	1.415	1.895	2.365	2.998	3.499
8	1.397	1.860	2.306	2.896	3.355
9	1.383	1.833	2.262	2.821	3.250
10	1.372	1.812	2.228	2.764	3.169
11	1.363	1.796	2.201	2.718	3.106
12	1.356	1.782	2.179	2.681	3.055
13	1.350	1.771	2.160	2.650	3.012
14	1.345	1.761	2.145	2.624	2.977
15	1.341	1.753	2.131	2.602	2.947
16	1.337	1.746	2.120	2.583	2.921
17	1.333	1.740	2.110	2.567	2.898
18	1.330	1.734	2.101	2.552	2.878
19	1.328	1.729	2.093	2.539	2.861
20	1.325	1.725	2.086	2.528	2.845
21	1.323	1.721	2.080	2.518	2.831
22	1.321	1.717	2.074	2.508	2.819
23	1.319	1.714	2.069	2.500	2.807
24	1.318	1.711	2.064	2.492	2.797
25	1.316	1.708	2.060	2.485	2.787
26	1.315	1.706	2.056	2.479	2.779
27	1.314	1.703	2.052	2.473	2.771
28	1.313	1.701	2.048	2.467	2.763
29	1.311	1.699	2.045	2.462	2.756

30	**1.310**	**1.697**	**2.042**	**2.457**	**2.750**
32	**1.309**	**1.694**	**2.037**	**2.449**	**2.738**
34	**1.307**	**1.691**	**2.032**	**2.441**	**2.728**
36	**1.306**	**1.688**	**2.028**	**2.434**	**2.719**
38	**1.304**	**1.686**	**2.024**	**2.429**	**2.712**
1	**1.282**	**1.645**	**1.960**	**2.326**	**2.576**

Appendix 5. MATLAB codes for the simulation results

A. Laboratory based viscosity measurement and New Coriolis viscosity measurements MATLAB Code

```
% Laboratory based Viscosity at Temperature of 20 degree celcius
Shear_rate = [1000.00 631.00 398.00 251.00 158.00 100.00 63.10 39.80 25.10
15.80 10.00 6.31 3.98 2.51 1.59 1.00]; % [1/s]
fluid1_viscosity = [3.49 3.92 4.40 4.91 5.47 6.02 6.53 6.96 7.37 7.65 7.77
8.01 7.93 8.02 8.28 8.56]; % [cp]
fluid2_viscosity = [8.75 10.20 11.90 14.10 16.80 19.90 23.60 27.80 32.30
37.10 41.70 46.70 50.60 53.50 55.90 57.50]; % [cp]
subplot(1,2,1)
plot(Shear_rate,fluid1_viscosity)
hold on
plot(Shear_rate,fluid2_viscosity,'r')
legend('Fluid-1 Viscosity', 'Fluid-2 Viscosity')
title('Laboratory Base Viscosity Measurement at 20 Degree celcius')
xlabel('Shear Rate[1/s]')
ylabel('Viscosity [cp]')
grid on
subplot(1,2,2)
% shear Rate of 100
Viscosity_fluid2 = [14.10 14.10 14.20 14.40 14.60 14.80 15.10 15.30 15.60
15.90 16.20 16.50 16.80 17.10 17.40 17.70 18.00 18.30 18.60 19.00 19.30];
Viscosity_fluid1 = [3.90 3.90 3.93 3.99 4.06 4.14 4.22 4.31 4.40 4.50 4.60
4.71 4.82 4.93 5.04 5.15 5.27 5.39 5.51 5.63 5.76];
Temperature = [40 39 38 37 36 35 34 33 32 31 30 29 28 27 26 25 24 23 22 21
20];
plot(Temperature,Viscosity_fluid1)
hold on
plot(Temperature,Viscosity_fluid2,'r')
legend('Fluid-1 Viscosity', 'Fluid-2 Viscosity')
title('Laboratory Base Viscosity Measurement at 100[1/s] Share Rate')
xlabel('Temperature [degree celcius]')
ylabel('Viscosity [cp]')
grid on

 % New Coriolis viscosity
Flowrate = setpoints;
Temp_water = water_of_Temp;
Coriolis_Viscosity_water = waterviscosity;
Coriolis_Viscosity_fluid1 = fluid1;
Temp_fluid1 = fluid1temp;
Coriolis_Viscosity_fluid2 = fluid2_viscosity;
Temp_fluid2 = fluid2temp;
Flow2 = setpoint_fluid2;
subplot(1,2,1)
plot(Flowrate,Coriolis_Viscosity_water,'g')
hold on
plot(Flowrate,Coriolis_Viscosity_fluid1)
hold on
plot(Flow2, Coriolis_Viscosity_fluid2,'r')
legend('Water Viscosity','Fluid-1 Viscosity', 'Fluid-2 Viscosity')
title('New Coriolis Viscosity Measurement')
xlabel('Flow Rate[kg/min]')
ylabel('Viscosity [cp]')
grid on
subplot(1,2,2)
plot(Temp_water,Coriolis_Viscosity_water)
```

```
hold on
plot(Temp_fluid1,Coriolis_Viscosity_fluid1,'r')
hold on
plot(Temp_fluid2,Coriolis_Viscosity_fluid2,'g')
      legend('Water Viscosity','Fluid-1 Viscosity', 'Fluid-2 Viscosity')
      title('New Coriolis Viscosity Measurement')
      xlabel('Temperature[degree celcius]')
      ylabel('Viscosity [cp]')
      grid on
```

B. Laboratory based density measurement for sample collection and best position fpr sample collection MATLAB codes

```
clc
clear
%% Laboratory based Density measurement for sample collection
% Density measurement of fluid 1 and fluid 2 (Top, bottom and flowing fluid
on open venturi rig samples)
    Temp =[15,20,25,30,35,40,45,50,55,60]; % [degree celcius]
    Bottom_Density_fluid1 = [1138.99 1137.01 1134.93 1132.75 1130.46
    1128.08 1125.62 1123.05 1120.4 1117.66]; % [kg/m3]
    Top_Density_fluid1 = [1139.06 1137.08 1135.00 1132.82 1130.53 1128.15
    1125.67 1124.11 1121.23 1118.22]; % [kg/m3]
    Flowing_density_fluid1 = [1138.52 1136.55 1134.47 1132.29 1130.01
    1127.63 1125.16 1122.60 1119.95 1117.22]; % [kg/m3]
    Bottom_Density_fluid2 = [1359.00 1356.40 1353.78 1351.10 1348.40
    1345.68 1342.90 1340.09 1337.26 1334.39]; % [kg/m3]
    Top_Density_fluid2 = [1357.68 1355.08 1352.45 1349.79 1347.11 1344.38
    1341.61 1338.81 1336.00 1333.13];  % [kg/m3]
    Flowing_density_fluid2 = [1361.03 1358.4 1355.75 1353.06 1350.3
    1347.45 1344.39 1341.91 1339.29 1336.39]; % [kg/m3]
    subplot(1,2,1)
    plot(Temp,Bottom_Density_fluid1)
    hold on
    plot (Temp,Top_Density_fluid1,'g')
    hold on
    plot (Temp,Flowing_density_fluid1,'r')
    hold off
    legend('Tank Bottom Density', 'Tank Top Density', 'Venturi rig Flowing
fluid density')
    title('Lab Based Density Measurement of Fluid 1')
    xlabel('Temperature [degree celcius]')
    ylabel('Density (kg/m3)')
    grid on
    subplot(1,2,2)
    plot(Temp,Bottom_Density_fluid2)
    hold on
    plot (Temp,Top_Density_fluid2,'g')
    hold on
    plot (Temp,Flowing_density_fluid2,'r')
    hold off
    legend('Tank Bottom Density', 'Tank Top Density', 'Venturi rig Flowing
fluid density')
    title('Lab Based Density Measurement of Fluid 2')
    xlabel('Temperature [degree celcius]')
    ylabel('Density (kg/m3)')
    grid on

% Hysteresis plot of flowing fluid density for comparison purposes (since
best position is at the flowing venturi rig)
```

```
Temp_rising_fluid = [20 20.2 20.4 20.6 20.8 21 21.2 21.4 21.6 21.8
22]; % [degree celcius]
Temp_falling_fluid = [22 21.8 21.6 21.4 21.2 21 20.8 20.6 20.4 20.2
20]; % [degree celcius]
Flowing_density_rising_fluid1 = [1136.60 1136.52 1136.44 1136.36
1136.27 1136.16 1136.11 1136.03 1135.95 1135.86 1135.78]; % [kg/m3]
Flowing_density_falling_fluid1 = [1135.78 1135.86 1135.94 1136.02
1136.11 1136.19 1136.27 1136.35 1136.43 1136.51 1136.60]; % [kg/m3]
Flowing_density_rising_fluid2 = [1359.18 1359.08 1358.98 1358.88
1358.77 1358.67 1358.57 1358.47 1358.37 1358.26 1358.16]; % [kg/m3]
Flowing_density_falling_fluid2 = [1358.16 1358.26 1358.37 1358.48
1358.59 1358.70 1358.80 1358.91 1359.02 1359.13 1359.23]; % [kg/m3]
subplot(1,2,1)
plot(Temp_rising_fluid,Flowing_density_rising_fluid1)
hold on
plot (Temp_falling_fluid,Flowing_density_falling_fluid1,'r')
legend('Rising Density', 'Falling Density')
hold off
title('Hysteresis Analysis of Density Measurement of Fluid 1 at the
Rig')
xlabel('Temperature [degree celcius]')
ylabel('Density (kg/m3)')
grid on
subplot(1,2,2)
plot(Temp_rising_fluid,Flowing_density_rising_fluid2)
hold on
plot (Temp_falling_fluid,Flowing_density_falling_fluid2,'r')
legend('Rising Density', 'Falling Density')
hold off
title('Hysteresis Analysis of Density Measurement of Fluid 2 at the
Rig')
xlabel('Temperature [degree celcius]')
ylabel('Density (kg/m3)')
grid on

%% Statistical Analysis of Lab based density Experimental data for best
   positions
    %Estimating the random uncertainity with 95% confidence level.
    %% Given data for Density for sample collection
    confidence_level=0.95; %95%
    alfa=1-confidence_level; %level of significance
    Bottom_Density_fluid1 = [1138.99 1137.01 1134.93 1132.75 1130.46
    1128.08 1125.62 1123.05 1120.4 1117.66];
    Top_Density_fluid1 = [1139.06 1137.08 1135.00 1132.82 1130.53 1128.15
    1125.67 1124.11 1121.23 1118.22];
    Flowing_density_fluid1 = [1138.52 1136.55 1134.47 1132.29 1130.01
    1127.63 1125.16 1122.60 1119.95 1117.22];
    Bottom_Density_fluid2 = [1359.00 1356.40 1353.78 1351.10 1348.40
    1345.68 1342.90 1340.09 1337.26 1334.39];
    Top_Density_fluid2 = [1357.68 1355.08 1352.45 1349.79 1347.11 1344.38
    1341.61 1338.81 1336.00 1333.13];
    Flowing_density_fluid2 = [1361.03 1358.4 1355.75 1353.06 1350.3
    1347.45 1344.39 1341.91 1339.29 1336.39];
    n=length( Bottom_Density_fluid1);

    % Estimate population mean of bottom density measurement for fluid 1
    %Estimate confidence interval on the mean
    x_bar_Bottom_Density_fluid1=mean(Bottom_Density_fluid1)%sample mean
    sum=0;
    for i=1:length(Bottom_Density_fluid1)
        sum=(Bottom_Density_fluid1(i)-x_bar_Bottom_Density_fluid1)^2+sum;
```

```
    end
    sample_std_Bottom_Density_fluid1=sqrt((sum/(n-1)))%standard deviation
    of the sample
%% Estimate population mean of top density measurement for fluid 1
    %Estimate confidence interval on the mean
    x_bar_Top_Density_fluid1=mean(Top_Density_fluid1)%sample mean
    sum=0;
    for i=1:length(Top_Density_fluid1)
        sum=(Top_Density_fluid1(i)-x_bar_Top_Density_fluid1)^2+sum;
    end
    sample_std_Top_Density_fluid1=sqrt((sum/(n-1)))%standard deviation of
    the sample
%% Estimate population mean of flowing rig density measurement for fluid1
    %Estimate confidence interval on the mean
    x_bar_Flowing_density_fluid1=mean(Flowing_density_fluid1)%sample mean
    sum=0;
    for i=1:length(Flowing_density_fluid1)
        sum=(Flowing_density_fluid1(i)-x_bar_Flowing_density_fluid1)^2+sum;
    end
    sample_std_Flowing_density_fluid1=sqrt((sum/(n-1)))%standard
    deviation of the sample
%% Estimate population mean of bottom density measurement for fluid 2
    %Estimate confidence interval on the mean
    x_bar_Bottom_Density_fluid2=mean(Bottom_Density_fluid2)%sample mean
    sum=0;
    for i=1:length(Bottom_Density_fluid2)
        sum=(Bottom_Density_fluid2(i)-x_bar_Bottom_Density_fluid2)^2+sum;
    end
    sample_std_Bottom_Density_fluid2=sqrt((sum/(n-1)))%standard deviation
    of the sample
%% Estimate population mean of top density measurement for fluid 2
    %Estimate confidence interval on the mean
    x_bar_Top_Density_fluid2=mean(Top_Density_fluid2)%sample mean
    sum=0;
    for i=1:length(Top_Density_fluid2)
        sum=(Top_Density_fluid2(i)-x_bar_Top_Density_fluid2)^2+sum;
    end
    sample_std_Top_Density_fluid2=sqrt((sum/(n-1)))%standard deviation of
    the sample
%% Estimate population mean of flowing rig density measurement for fluid2
    %Estimate confidence interval on the mean
    x_bar_Flowing_density_fluid2=mean(Flowing_density_fluid2)%sample mean
    sum=0;
    for i=1:length(Flowing_density_fluid2)
        sum=(Flowing_density_fluid2(i)-
             x_bar_Flowing_density_fluid2)^2+sum;
    end
    sample_std_Flowing_density_fluid2=sqrt((sum/(n-1)))%standard
    deviation of the sample

      %% For t-distribution
          v=n-1;%Degree of freedom
          t_alfa_by_2=2.262; %from the standard table
      % calculating the random uncertainty of each sample
      D_i_Bottom_Density_fluid1=t_alfa_by_2*sample_std_Bottom_Density_fluid
      1;
      D_i_Top_Density_fluid1=t_alfa_by_2*sample_std_Top_Density_fluid1;
      D_i_Flowing_density_fluid1=t_alfa_by_2*sample_std_Flowing_density_flu
      id1;
      D_i_Bottom_Density_fluid2=t_alfa_by_2*sample_std_Bottom_Density_fluid
      2;
```

```
      D_i_Top_Density_fluid2=t_alfa_by_2*sample_std_Top_Density_fluid2;
      D_i_Flowing_density_fluid2=t_alfa_by_2*sample_std_Flowing_density_flu
      id2;
%calculating random uncertainty of the mean value
    D_x_bar_Bottom_Density_fluid1= D_i_Bottom_Density_fluid1/(n)^(1/2);
    D_x_bar_Top_Density_fluid1= D_i_Top_Density_fluid1/(n)^(1/2);
    D_x_bar_Flowing_density_fluid1= D_i_Flowing_density_fluid1/(n)^(1/2);
    D_x_bar_Bottom_Density_fluid2= D_i_Bottom_Density_fluid2/(n)^(1/2);
    D_x_bar_Top_Density_fluid2= D_i_Top_Density_fluid2/(n)^(1/2);
    D_x_bar_Flowing_density_fluid2= D_i_Flowing_density_fluid2/(n)^(1/2);
    fprintf('Random Uncertainty of each measurement of
    Bottom_Density_fluid1=%f\n', D_i_Bottom_Density_fluid1)
    fprintf('Random Uncertainty of each measurement of
    Top_Density_fluid1=%f\n', D_i_Top_Density_fluid1)
    fprintf('Random Uncertainty of each measurement of
    Flowing_density_fluid1=%f\n', D_i_Flowing_density_fluid1)
    fprintf('Random Uncertainty of each measurement of
    Bottom_Density_fluid2=%f\n', D_i_Bottom_Density_fluid2)
    fprintf('Random Uncertainty of each measurement of
    Top_Density_fluid2=%f\n', D_i_Top_Density_fluid2)
    fprintf('Random Uncertainty of each measurement of
    Flowing_density_fluid2=%f\n', D_i_Flowing_density_fluid2)
    fprintf('Random Uncertainty of the mean of the measurement of
    Bottom_Density_fluid1=%f\n', D_x_bar_Bottom_Density_fluid1)
    fprintf('Random Uncertainty of the mean of the measurement of
    Top_Density_fluid1=%f\n', D_x_bar_Top_Density_fluid1)
    fprintf('Random Uncertainty of the mean of the measurement of
    Flowing_density_fluid1=%f\n', D_x_bar_Flowing_density_fluid1)
    fprintf('Random Uncertainty of the mean of the measurement of
    Bottom_Density_fluid2=%f\n', D_x_bar_Bottom_Density_fluid2)
    fprintf('Random Uncertainty of the mean of the measurement of
    Top_Density_fluid2=%f\n', D_x_bar_Top_Density_fluid2)
    fprintf('Random Uncertainty of the mean of the measurement of
    Flowing_density_fluid2=%f\n', D_x_bar_Flowing_density_fluid2)
```

C. Comparison of Coriolis density measurement with lab based measurements MATLAB codes

```
%% Fluid -1 Density Comparison between old(serial:24520087 and New
Coriolis(Serial:K6071D02000') with lab based measurements

% Hysteresis Plot of Old and New Coriolis density Measurement
Number_of_samples_rising = linspace(1,816,816);
Number_of_samples_falling = linspace(816,1,816);
Old_coriolis_increase_density_fluid1 =
Old_coriolis_increasing_density_fluid1; % Density[kg/m3] measurement
at(250-400kg/min)
Old_coriolis_decrease_density_fluid1 =
Old_coriolis_decreasing_density_fluid1; % Density[kg/m3] measurement
at(400-250kg/min)
New_coriolis_increase_density_fluid1 =
New_coriolis_increasing_density_fluid1; % Density[kg/m3] measurement
at(250-400kg/min)
New_coriolis_decrease_density_fluid1 =
New_coriolis_decreasing_density_fluid1; % Density[kg/m3] measurement
at(400-250kg/min)
subplot(1,2,1)
```

```
plot(Number_of_samples_rising,Old_coriolis_increase_density_fluid1)
hold on
plot(Number_of_samples_falling,Old_coriolis_decrease_density_fluid1,'r')
hold off
legend('Increasing Density','Decreasing Density')
hold off
title('Hysteresis Plot of Old Coriolis Density Measurements ')
xlabel('Number of Samples')
ylabel('Density (kg/m3)')
grid on
subplot(1,2,2)
plot(Number_of_samples_rising,New_coriolis_increase_density_fluid1)
hold on
plot(Number_of_samples_falling,New_coriolis_decrease_density_fluid1,'r')
hold off
legend('Increasing Density','Decreasing Density')
hold off
      title('Hysteresis Plot of New Coriolis Density Measurements ')
      xlabel('Number of Samples')
      ylabel('Density (kg/m3)')
      grid on

      %Density Comparisons with Temperature plot
      Temperature_change_fluid1 = Temperature_fluid1;% degree celcius
      Old_Coriolis_Density_fluid1 = Old_coriolis_increasing_density_fluid1;
      New_Coriolis_Density_fluid1 = New_coriolis_increasing_density_fluid1;
      old_coriolis_mean_density_fluid1 = [1137.02 1137.24 1137.31 1137.47
      1137.55 1137.69 1137.79 1137.89 1137.96 1137.99 1138.14 1138.20
      1138.32 1138.53 1138.49 1138.97];
      new_coriolis_mean_density_fluid1 = [1140.32 1140.88 1141.21 1141.47
      1141.89 1142.15 1142.41 1142.82 1143.14 1143.43 1143.72 1144.03
      1144.44 1145.10 1145.04 1146.60];
      Flowing_density_fluid1_lab =      [1135.78 1135.86 1135.94 1136.02
      1136.11 1136.19 1136.27 1136.35 1136.43 1136.51 1136.60]; % [kg/m3]
      Temp_lab_fluid1 = [20 20.2 20.4 20.6 20.8 21 21.2 21.4 21.6 21.8 22];
      % [degree celcius]
      Temp_mean_fluid1 = linspace(21,21.6,16);
      subplot(1,2,1)
      scatter(Temperature_change_fluid1,Old_Coriolis_Density_fluid1)
      hold on
      scatter (Temperature_change_fluid1,New_Coriolis_Density_fluid1,'r')
      hold on
      plot(Temp_lab_fluid1,Flowing_density_fluid1_lab,'y')
      hold off
      legend('Old Coriolis Density', 'New Coriolis Density','Lab based
      density')
      hold off
      title('Fluid-1 density Comparison')
      xlabel('Temperature[degree celcius])')
      ylabel('Density[kg/m3]')
      grid on
      subplot(1,2,2)
      plot(Temp_mean_fluid1,old_coriolis_mean_density_fluid1)
      hold on
      plot (Temp_mean_fluid1,new_coriolis_mean_density_fluid1,'r')
      hold on
      plot(Temp_lab_fluid1,Flowing_density_fluid1_lab,'y')
      hold off
      legend('Old Coriolis Mean Density', 'New Coriolis Mean Density','Lab
      based density')
      hold off
```

```
        title('Density comparison of fluid-1')
        xlabel('Temperature[degree celcius]')
        ylabel('Density[kg/m3]')
        grid on

        % Fluid -2 Density Comparison between old (serial: 24520087 and New
        Coriolis (Serial: K6071D02000')
        % Hysteresis Plot of Old and New Coriolis Density Measurement
        Number_of_samples_rising = linspace(1,306,306);
        Number_of_samples_falling = linspace(306,1,306);
        Old_coriolis_increase_density_fluid2 =
        Old_coriolis_increasing_density_fluid2 ;% Density measurement at(250-
        400kg/min)
        Old_coriolis_decrease_density_fluid2 =
        Old_coriolis_decreasing_density_fluid2; % Density measurement at(400-
        250kg/min)
        New_coriolis_increase_density_fluid2 =
        New_coriolis_increasing_density_fluid2; % Density measurement at(250-
        400kg/min)
New_coriolis_decrease_density_fluid2 =
New_coriolis_decreasing_density_fluid2; % Density measurement at(400-
250kg/min)
subplot(1,2,1)
plot(Number_of_samples_rising,Old_coriolis_increase_density_fluid2)
hold on
plot(Number_of_samples_falling,Old_coriolis_decrease_density_fluid2,'r')
hold off
legend('Increasing Density','Decreasing Density')
hold off
title('Hysteresis Plot of Old Coriolis Density Measurements ')
xlabel('Number of Samples')
ylabel('Density [kg/m3]')
grid on
subplot(1,2,2)
plot(Number_of_samples_rising,New_coriolis_increase_density_fluid2)
hold on
plot(Number_of_samples_falling,New_coriolis_decrease_density_fluid2,'r')
hold off
legend('Increasing Density','Decreasing Density')
hold off
title('Hysteresis Plot of New Coriolis Density Measurements ')
xlabel('Number of Samples')
ylabel('Density [kg/m3]')
grid on

%Density with Temperature plot
Temperature_fluid2 = Temperature_fluid2;
lab_temp_fluid2 = [20 20.2 20.4 20.6 20.8 21 21.2 21.4 21.6 21.8 22];
lab_density_fluid2 = [1359.18 1359.08 1358.98 1358.88 1358.77 1358.67
1358.57 1358.47 1358.37 1358.26 1358.16];
Temperature_change_fluid2 = linspace(20.99,21.08,6);% degree celcius
Old_Coriolis_Density_fluid2 = Old_coriolis_increasing_density_fluid2;
old_coriolis_mean_fluid2 = [1360.30 1361.00 1360.90 1361.00 1362.10
1362.70];
New_Coriolis_Density_fluid2 = New_coriolis_increasing_density_fluid2;
new_coriolis_mean_fluid2 = [1380.40 1382.20 1381.90 1382.60 1386.00
1387.70];
subplot(1,2,1)
scatter(Temperature,Old_Coriolis_Density_fluid2)
hold on
scatter (Temperature,New_Coriolis_Density_fluid2,'r')
```

```
hold on
plot(lab_temp_fluid2,lab_density_fluid2,'y')
legend('Old Coriolis Density', 'New Coriolis Density','Lab Based Density')
hold off
hold off
title('Fluid-2 density Comparisons')
xlabel('Temperature[degree celcius]')
ylabel('Density [kg/m3]')
grid on
subplot(1,2,2)
plot(Temperature_change_fluid2,old_coriolis_mean_fluid2)
hold on
plot (Temperature_change_fluid2,new_coriolis_mean_fluid2,'r')
hold on
plot(lab_temp_fluid2,lab_density_fluid2,'y')
hold off
legend('Old coriolis mean density', 'New Coriolis mean density','Lab based
density')
title('Fluid-2 density Comparisons')
xlabel('Temperature[degree celcius]')
ylabel('Mean Density (kg/m3)')
      grid on

      %% Water Density Comparison betweeen old(serial:24520087 and New
      coriolis(Serial:K6071D02000')
      % Hysteresis Plot of Old and New Coriolis density Measurement
      Number_of_samples_rising = linspace(1,816,816);
      Number_of_samples_falling = linspace(816,1,816);
      Old_coriolis_increase_density_water =
      Old_coriolis_increasing_density_water; % Density[kg/m3] measurement
      at(250-400kg/min)
      Old_coriolis_decrease_density_water =
      Old_coriolis_decreasing_density_water; % Density[kg/m3] measurement
      at(400-250kg/min)
      New_coriolis_increase_density_water =
      New_coriolis_increasing_density_water; % Density[kg/m3] measurement
      at(250-400kg/min)
      New_coriolis_decrease_density_water =
      New_coriolis_decreasing_density_water; % Density[kg/m3] measurement
      at(400-250kg/min)
      subplot(1,2,1)
      plot(Number_of_samples_rising,Old_coriolis_increase_density_water)
      hold on
      plot(Number_of_samples_falling,Old_coriolis_decrease_density_water,'r
      ')
      hold off
      legend('Increasing Density','Decreasing Density')
      hold off
      title('Hysteresis Plot of Old Coriolis Density Measurements ')
      xlabel('Number of Samples')
      ylabel('Density (kg/m3)')
      grid on
      subplot(1,2,2)
      plot(Number_of_samples_rising,New_coriolis_increase_density_water)
      hold on
      plot(Number_of_samples_falling,New_coriolis_decrease_density_water,'r
      ')
      hold off
      legend('Increasing Density','Decreasing Density')
      hold off
      title('Hysteresis Plot of New Coriolis Density Measurements ')
```

```
        xlabel('Number of Samples')
        ylabel('Density (kg/m3)')
        grid on

        %Density Comparisons with Temperature plot
        Temperature_change_water = Temperature_water;% degree celcius
        Old_Coriolis_Density_water = Old_coriolis_increasing_density_water;
        New_Coriolis_Density_water =  New_coriolis_increasing_density_water;
        old_coriolis_mean_density_water = [1000.90 1000.90 1000.80 1000.90
        1000.90 1000.90 1000.80 1000.90 1000.90 1000.80 1000.80 1000.90
        1000.90 1000.90 1000.80 1000.90];
        new_coriolis_mean_density_water = [1000.90 1000.70 1000.60 1000.50
        1000.50 1000.40 1000.40 1000.30 1000.30 1000.20 1000.20 1000.20
        1000.20 1000.10 1000.10 1000.10];
        Temp_mean = linspace(18.4,19.6,16);
        subplot(1,2,1)
        scatter(Temperature_change_water,Old_Coriolis_Density_water)
        hold on
        scatter (Temperature_change_water,New_Coriolis_Density_water,'r')
        hold off
        legend('Old Coriolis Density', 'New Coriolis Density')
        title('Water density Comparison')
        xlabel('Temperature[degree celcius])')
plot(Temp_mean,old_coriolis_mean_density_water)
hold on
plot (Temp_mean,new_coriolis_mean_density_water,'r')
hold off
legend('Old Coriolis Mean Density', 'New Coriolis Mean Density')
hold off
title('Density comparison of Water')
xlabel('Temperature[degree celcius]')
ylabel('Density[kg/m3]')
grid on

%% Estimating the random uncertainity with 95% confidence level
%for Density Measurement of New coriolis flow meter of fluid-1.

%% given data
confidence_level=0.95; %95%
alfa=1-confidence_level; %level of significance
Density_250sp = density_250sp_new;% Kg/m3
Density_260sp = density_260sp_new; %kg/m3
Density_270sp = density_270sp_new; %kg/m3
Density_280sp = density_280sp_new; %kg/m3
Density_290sp = density_290sp_new; %kg/m3
Density_300sp = density_300sp_new; %kg/m3
Density_310sp = density_310sp_new; %kg/m3
Density_320sp = density_320sp_new; %kg/m3
Density_330sp = density_330sp_new; %kg/m3
Density_340sp = density_340sp_new; %kg/m3
Density_350sp = density_350sp_new; %kg/m3
Density_360sp = density_360sp_new; %kg/m3
Density_370sp = density_370sp_new; %kg/m3
Density_380sp = density_380sp_new; %kg/m3
Density_390sp = density_390sp_new; %kg/m3
Density_400sp = density_400sp_new; %kg/m3
n=length(Density_400sp); % number of samples 51

%% Estimate sample mean at 250 setpoint
%estimate confidence interval on the mean
```

```
x_bar_250 = mean(Density_250sp);%sample mean at 250setpoint
sum=0;
for i=1:length(Density_250sp)
    sum=(Density_250sp(i)-x_bar_250)^2+sum;
end
sample_std_250 = sqrt((sum/(n))); %standard deviation of the sample
%% Estimate sample mean at 260
%estimate confidence interval on the mean
x_bar_260 = mean(Density_260sp);%sample mean at 260setpoint
sum=0;
for i=1:length(Density_260sp)
    sum=(Density_260sp(i)-x_bar_260)^2+sum;
end
sample_std_260 = sqrt((sum/(n))); %standard deviation of the sample
%% Estimate sample mean at 270 setpoint
%estimate confidence interval on the mean
x_bar_270 = mean(Density_270sp);%sample mean at 270setpoint
sum=0;
for i=1:length(Density_270sp)
    sum=(Density_270sp(i)-x_bar_270)^2+sum;
end
sample_std_270 = sqrt((sum/(n))); %standard deviation of the sample
%% Estimate sample mean at 280 setpoint
%estimate confidence interval on the mean
x_bar_280 = mean(Density_280sp);%sample mean at 280setpoint
sum=0;
for i=1:length(Density_280sp)
        sum=(Density_280sp(i)-x_bar_280)^2+sum;
    end
    sample_std_280 = sqrt((sum/(n))); %standard deviation of the sample
    %% Estimate sample mean at 290 setpoint
    %estimate confidence interval on the mean
    x_bar_290 = mean(Density_290sp);%sample mean at 290setpoint
    sum=0;
    for i=1:length(Density_290sp)
        sum=(Density_290sp(i)-x_bar_290)^2+sum;
    end
    sample_std_290 = sqrt((sum/(n))); %standard deviation of the sample
    %% Estimate sample mean at 300 setpoint
    %estimate confidence interval on the mean
    x_bar_300 = mean(Density_300sp);%sample mean at 300setpoint
    sum=0;
    for i=1:length(Density_300sp)
        sum=(Density_300sp(i)-x_bar_300)^2+sum;
    end
    sample_std_300 = sqrt((sum/(n))); %standard deviation of the sample
    %% Estimate sample mean at 310 setpoint
    %estimate confidence interval on the mean
    x_bar_310 = mean(Density_310sp);%sample mean at 310setpoint
    sum=0;
    for i=1:length(Density_310sp)
        sum=(Density_310sp(i)-x_bar_310)^2+sum;
    end
    sample_std_310 = sqrt((sum/(n))); %standard deviation of the sample
    %% Estimate sample mean at 320 setpoint
    %estimate confidence interval on the mean
    x_bar_320 = mean(Density_320sp);%sample mean at 320setpoint
    sum=0;
    for i=1:length(Density_320sp)
        sum=(Density_320sp(i)-x_bar_320)^2+sum;
    end
```

```
        sample_std_320 = sqrt((sum/(n))); %standard deviation of the sample
        %% Estimate sample mean at 330 setpoint
        %estimate confidence interval on the mean
        x_bar_330 = mean(Density_330sp);%sample mean at 330setpoint
        sum=0;
        for i=1:length(Density_330sp)
            sum=(Density_330sp(i)-x_bar_330)^2+sum;
        end
        sample_std_330 = sqrt((sum/(n))); %standard deviation of the sample
        %% Estimate sample mean at 340 setpoint
        %estimate confidence interval on the mean
        x_bar_340 = mean(Density_340sp);%sample mean at 340setpoint
        sum=0;
        for i=1:length(Density_340sp)
            sum=(Density_340sp(i)-x_bar_340)^2+sum;
        end
        sample_std_340 = sqrt((sum/(n))); %standard deviation of the sample
        %% Estimate sample mean at 350 setpoint
        %estimate confidence interval on the mean
        x_bar_350 = mean(Density_350sp);%sample mean at 350setpoint
        sum=0;
        for i=1:length(Density_350sp)
            sum=(Density_350sp(i)-x_bar_350)^2+sum;
        end
        sample_std_350 = sqrt((sum/(n))); %standard deviation of the sample
        %% Estimate sample mean at 360 setpoint
        %estimate confidence interval on the mean
        x_bar_360 = mean(Density_360sp);%sample mean at 360setpoint
        sum=0;
        for i=1:length(Density_360sp)
    sum=(Density_360sp(i)-x_bar_360)^2+sum;
end
sample_std_360 = sqrt((sum/(n))); %standard deviation of the sample
%% Estimate sample mean at 370 setpoint
%estimate confidence interval on the mean
x_bar_370 = mean(Density_370sp);%sample mean at 370setpoint
sum=0;
for i=1:length(Density_370sp)
    sum=(Density_370sp(i)-x_bar_370)^2+sum;
end
sample_std_370 = sqrt((sum/(n))); %standard deviation of the sample
%% Estimate sample mean at 380 setpoint
%estimate confidence interval on the mean
x_bar_380 = mean(Density_380sp);%sample mean at 380setpoint
sum=0;
for i=1:length(Density_380sp)
    sum=(Density_380sp(i)-x_bar_380)^2+sum;
end
sample_std_380 = sqrt((sum/(n))); %standard deviation of the sample
%% Estimate sample mean at 390 setpoint
%estimate confidence interval on the mean
x_bar_390 = mean(Density_390sp);%sample mean at 390setpoint
sum=0;
for i=1:length(Density_390sp)
    sum=(Density_390sp(i)-x_bar_390)^2+sum;
end
sample_std_390 = sqrt((sum/(n))); %standard deviation of the sample
%% Estimate sample mean at 400 setpoint
%estimate confidence interval on the mean
x_bar_400 = mean(Density_400sp);%sample mean at 400setpoint
sum=0;
```

```
for i=1:length(Density_400sp)
    sum=(Density_400sp(i)-x_bar_400)^2+sum;
end
sample_std_400 = sqrt((sum/(n))); %standard deviation of the sample
%% for normal-distribution (since values is greater than 30)
alpha_by_2 = 0.025;
z_alfa_by_2 = 1.96; %value gotten from the standard normal distribution
table
%%
% calculating the random uncertainty of each measurement
P_x_250 = z_alfa_by_2*sample_std_250;
P_x_260 = z_alfa_by_2*sample_std_260;
P_x_270 = z_alfa_by_2*sample_std_270;
P_x_280 = z_alfa_by_2*sample_std_280;
P_x_290 = z_alfa_by_2*sample_std_290;
P_x_300 = z_alfa_by_2*sample_std_300;
P_x_310 = z_alfa_by_2*sample_std_310;
P_x_320 = z_alfa_by_2*sample_std_320;
P_x_330 = z_alfa_by_2*sample_std_330;
P_x_340 = z_alfa_by_2*sample_std_340;
P_x_350 = z_alfa_by_2*sample_std_350;
P_x_360 = z_alfa_by_2*sample_std_360;
P_x_370 = z_alfa_by_2*sample_std_370;
P_x_380 = z_alfa_by_2*sample_std_380;
P_x_390 = z_alfa_by_2*sample_std_390;
P_x_400 = z_alfa_by_2*sample_std_400;
%calculating random uncertainty of the mean value
P_x_bar_250 = P_x_250/(n)^(1/2);
P_x_bar_260 = P_x_260/(n)^(1/2);
P_x_bar_270 = P_x_270/(n)^(1/2);
P_x_bar_280 = P_x_280/(n)^(1/2);
P_x_bar_290 = P_x_290/(n)^(1/2);
P_x_bar_300 = P_x_300/(n)^(1/2);
      P_x_bar_310 = P_x_310/(n)^(1/2);
      P_x_bar_320 = P_x_320/(n)^(1/2);
      P_x_bar_330 = P_x_330/(n)^(1/2);
      P_x_bar_340 = P_x_340/(n)^(1/2);
      P_x_bar_350 = P_x_350/(n)^(1/2);
      P_x_bar_360 = P_x_360/(n)^(1/2);
      P_x_bar_370 = P_x_370/(n)^(1/2);
      P_x_bar_380 = P_x_380/(n)^(1/2);
      P_x_bar_390 = P_x_390/(n)^(1/2);
      P_x_bar_400 = P_x_400/(n)^(1/2);


      %% display
      fprintf('Standard deviation at 250sp=%f\n', sample_std_250)
      fprintf('Standard deviation at 260sp=%f\n', sample_std_260)
      fprintf('Standard deviation at 270sp=%f\n', sample_std_270)
      fprintf('Standard deviation at 280sp=%f\n', sample_std_280)
      fprintf('Standard deviation at 290sp=%f\n', sample_std_290)
      fprintf('Standard deviation at 300sp=%f\n', sample_std_300)
      fprintf('Standard deviation at 310sp=%f\n', sample_std_310)
      fprintf('Standard deviation at 320sp=%f\n', sample_std_320)
      fprintf('Standard deviation at 330sp=%f\n', sample_std_330)
      fprintf('Standard deviation at 340sp=%f\n', sample_std_340)
      fprintf('Standard deviation at 350sp=%f\n', sample_std_350)
      fprintf('Standard deviation at 360sp=%f\n', sample_std_360)
      fprintf('Standard deviation at 370sp=%f\n', sample_std_370)
      fprintf('Standard deviation at 380sp=%f\n', sample_std_380)
      fprintf('Standard deviation at 390sp=%f\n', sample_std_390)
```

```
        fprintf('Standard deviation at 400sp=%f\n', sample_std_400)
        fprintf('Random Uncertainty of each measurement at 250sp=%f\n',
        P_x_250)
        fprintf('Random Uncertainty of each measurement at 260sp=%f\n',
        P_x_260)
        fprintf('Random Uncertainty of each measurement at 270sp=%f\n',
        P_x_270)
        fprintf('Random Uncertainty of each measurement at 280sp=%f\n',
        P_x_280)
        fprintf('Random Uncertainty of each measurement at 290sp=%f\n',
        P_x_290)
        fprintf('Random Uncertainty of each measurement at 300sp=%f\n',
        P_x_300)
        fprintf('Random Uncertainty of each measurement at 310sp=%f\n',
        P_x_310)
        fprintf('Random Uncertainty of each measurement at 320sp=%f\n',
        P_x_320)
        fprintf('Random Uncertainty of each measurement at 330sp=%f\n',
        P_x_330)
        fprintf('Random Uncertainty of each measurement at 340sp=%f\n',
        P_x_340)
        fprintf('Random Uncertainty of each measurement at 350sp=%f\n',
        P_x_350)
        fprintf('Random Uncertainty of each measurement at 360sp=%f\n',
        P_x_360)
        fprintf('Random Uncertainty of each measurement at 370sp=%f\n',
        P_x_370)
        fprintf('Random Uncertainty of each measurement at 380sp=%f\n',
        P_x_380)
        fprintf('Random Uncertainty of each measurement at 390sp=%f\n',
        P_x_390)
        fprintf('Random Uncertainty of each measurement at 400sp=%f\n',
        P_x_400)
        fprintf('Random Uncertainty of the mean measurement at 250sp=%f\n',
        P_x_bar_250)
        fprintf('Random Uncertainty of the mean measurement at 260sp=%f\n',
        P_x_bar_260)
        fprintf('Random Uncertainty of the mean measurement at
        270spt=%f\n',P_x_bar_270)
        fprintf('Random Uncertainty of the mean measurement at 280sp=%f\n',
        P_x_bar_280)
        fprintf('Random Uncertainty of the mean measurement at 290sp=%f\n',
        P_x_bar_290)
        fprintf('Random Uncertainty of the mean measurement at 300sp=%f\n',
        P_x_bar_300)
        fprintf('Random Uncertainty of the mean measurement at 310sp=%f\n',
        P_x_bar_310)
        fprintf('Random Uncertainty of the mean measurement at 320sp=%f\n',
        P_x_bar_320)
        fprintf('Random Uncertainty of the mean measurement at 330sp=%f\n',
        P_x_bar_330)
fprintf('Random Uncertainty of the mean measurement at 340sp=%f\n',
P_x_bar_340)
fprintf('Random Uncertainty of the mean measurement at 350sp=%f\n',
P_x_bar_350)
fprintf('Random Uncertainty of the mean measurement at 360sp=%f\n',
P_x_bar_360)
fprintf('Random Uncertainty of the mean measurement at 370sp=%f\n',
P_x_bar_370)
fprintf('Random Uncertainty of the mean measurement at 380sp=%f\n',
P_x_bar_380)
```

```
fprintf('Random Uncertainty of the mean measurement at 390sp=%f\n',
P_x_bar_390)
fprintf('Random Uncertainty of the mean measurement at 400sp=%f\n',
P_x_bar_400)

%% Estimating the random uncertainty with 95% confidence level
%for Density Measurement of OLD Coriolis flow meter of fluid-1.

 %% given data
confidence_level=0.95; %95%
alfa=1-confidence_level; %level of significance
Density_250sp = density_250sp_old;% Kg/m3
Density_260sp = density_260sp_old; %kg/m3
Density_270sp = density_270sp_old; %kg/m3
Density_280sp = density_280sp_old; %kg/m3
Density_290sp = density_290sp_old; %kg/m3
Density_300sp = density_300sp_old; %kg/m3
Density_310sp = density_310sp_old; %kg/m3
Density_320sp = density_320sp_old; %kg/m3
Density_330sp = density_330sp_old; %kg/m3
Density_340sp = density_340sp_old; %kg/m3
Density_350sp = density_350sp_old; %kg/m3
Density_360sp = density_360sp_old; %kg/m3
Density_370sp = density_370sp_old; %kg/m3
Density_380sp = density_380sp_old; %kg/m3
Density_390sp = density_390sp_old; %kg/m3
Density_400sp = density_400sp_old; %kg/m3
n=length(massflow_400sp); % number of samples 51

%% Estimate sample mean at 250 setpoint
%estimate confidence interval on the mean
x_bar_250 = mean(Density_250sp);%sample mean at 250setpoint
sum=0;
for i=1:length(Density_250sp)
    sum=(Density_250sp(i)-x_bar_250)^2+sum;
end
sample_std_250 = sqrt((sum/(n))); %standard deviation of the sample
%% Estimate sample mean at 260
%estimate confidence interval on the mean
x_bar_260 = mean(Density_260sp);%sample mean at 260setpoint
sum=0;
for i=1:length(Density_260sp)
    sum=(Density_260sp(i)-x_bar_260)^2+sum;
end
sample_std_260 = sqrt((sum/(n))); %standard deviation of the sample
%% Estimate sample mean at 270 setpoint
%estimate confidence interval on the mean
x_bar_270 = mean(Density_270sp);%sample mean at 270setpoint
sum=0;
for i=1:length(Density_270sp)
    sum=(Density_270sp(i)-x_bar_270)^2+sum;
end
sample_std_270 = sqrt((sum/(n))); %standard deviation of the sample
%% Estimate sample mean at 280 setpoint
      %estimate confidence interval on the mean
      x_bar_280 = mean(Density_280sp);%sample mean at 280setpoint
      sum=0;
      for i=1:length(Density_280sp)
          sum=(Density_280sp(i)-x_bar_280)^2+sum;
      end
      sample_std_280 = sqrt((sum/(n))); %standard deviation of the sample
```

```
        %% Estimate sample mean at 290 setpoint
        %estimate confidence interval on the mean
        x_bar_290 = mean(Density_290sp);%sample mean at 290setpoint
        sum=0;
        for i=1:length(Density_290sp)
            sum=(Density_290sp(i)-x_bar_290)^2+sum;
        end
        sample_std_290 = sqrt((sum/(n))); %standard deviation of the sample
        %% Estimate sample mean at 300 setpoint
        %estimate confidence interval on the mean
        x_bar_300 = mean(Density_300sp);%sample mean at 300setpoint
        sum=0;
        for i=1:length(Density_300sp)
            sum=(Density_300sp(i)-x_bar_300)^2+sum;
        end
        sample_std_300 = sqrt((sum/(n))); %standard deviation of the sample
        %% Estimate sample mean at 310 setpoint
        %estimate confidence interval on the mean
        x_bar_310 = mean(Density_310sp);%sample mean at 310setpoint
        sum=0;
        for i=1:length(Density_310sp)
            sum=(Density_310sp(i)-x_bar_310)^2+sum;
        end
        sample_std_310 = sqrt((sum/(n))); %standard deviation of the sample
        %% Estimate sample mean at 320 setpoint
        %estimate confidence interval on the mean
        x_bar_320 = mean(Density_320sp);%sample mean at 320setpoint
        sum=0;
        for i=1:length(Density_320sp)
            sum=(Density_320sp(i)-x_bar_320)^2+sum;
        end
        sample_std_320 = sqrt((sum/(n))); %standard deviation of the sample
        %% Estimate sample mean at 330 setpoint
        %estimate confidence interval on the mean
        x_bar_330 = mean(Density_330sp);%sample mean at 330setpoint
        sum=0;
        for i=1:length(Density_330sp)
            sum=(Density_330sp(i)-x_bar_330)^2+sum;
        end
        sample_std_330 = sqrt((sum/(n))); %standard deviation of the sample
        %% Estimate sample mean at 340 setpoint
        %estimate confidence interval on the mean
        x_bar_340 = mean(Density_340sp);%sample mean at 340setpoint
        sum=0;
        for i=1:length(Density_340sp)
            sum=(Density_340sp(i)-x_bar_340)^2+sum;
        end
        sample_std_340 = sqrt((sum/(n))); %standard deviation of the sample
        %% Estimate sample mean at 350 setpoint
        %estimate confidence interval on the mean
        x_bar_350 = mean(Density_350sp);%sample mean at 350setpoint
        sum=0;
        for i=1:length(Density_350sp)
            sum=(Density_350sp(i)-x_bar_350)^2+sum;
        end
        sample_std_350 = sqrt((sum/(n))); %standard deviation of the sample
        %% Estimate sample mean at 360 setpoint
%estimate confidence interval on the mean
x_bar_360 = mean(Density_360sp);%sample mean at 360setpoint
sum=0;
for i=1:length(Density_360sp)
```

```
    sum=(Density_360sp(i)-x_bar_360)^2+sum;
end
sample_std_360 = sqrt((sum/(n))); %standard deviation of the sample
%% Estimate sample mean at 370 setpoint
%estimate confidence interval on the mean
x_bar_370 = mean(Density_370sp);%sample mean at 370setpoint
sum=0;
for i=1:length(Density_370sp)
    sum=(Density_370sp(i)-x_bar_370)^2+sum;
end
sample_std_370 = sqrt((sum/(n))); %standard deviation of the sample
%% Estimate sample mean at 380 setpoint
%estimate confidence interval on the mean
x_bar_380 = mean(Density_380sp);%sample mean at 380setpoint
sum=0;
for i=1:length(Density_380sp)
    sum=(Density_380sp(i)-x_bar_380)^2+sum;
end
sample_std_380 = sqrt((sum/(n))); %standard deviation of the sample
%% Estimate sample mean at 390 setpoint
%estimate confidence interval on the mean
x_bar_390 = mean(Density_390sp);%sample mean at 390setpoint
sum=0;
for i=1:length(Density_390sp)
    sum=(Density_390sp(i)-x_bar_390)^2+sum;
end
sample_std_390 = sqrt((sum/(n))); %standard deviation of the sample
%% Estimate sample mean at 400 setpoint
%estimate confidence interval on the mean
x_bar_400 = mean(Density_400sp);%sample mean at 400setpoint
sum=0;
for i=1:length(Density_400sp)
    sum=(Density_400sp(i)-x_bar_400)^2+sum;
end
sample_std_400 = sqrt((sum/(n))); %standard deviation of the sample
%% for normal-distribution (since values is greater than 30)
alpha_by_2 = 0.025;
z_alfa_by_2 = 1.96; %value gotten from the standard normal distribution
table
%%
% calculating the random uncertainty of each measurement
P_x_250 = z_alfa_by_2*sample_std_250;
P_x_260 = z_alfa_by_2*sample_std_260;
P_x_270 = z_alfa_by_2*sample_std_270;
P_x_280 = z_alfa_by_2*sample_std_280;
P_x_290 = z_alfa_by_2*sample_std_290;
P_x_300 = z_alfa_by_2*sample_std_300;
P_x_310 = z_alfa_by_2*sample_std_310;
P_x_320 = z_alfa_by_2*sample_std_320;
P_x_330 = z_alfa_by_2*sample_std_330;
P_x_340 = z_alfa_by_2*sample_std_340;
P_x_350 = z_alfa_by_2*sample_std_350;
P_x_360 = z_alfa_by_2*sample_std_360;
P_x_370 = z_alfa_by_2*sample_std_370;
P_x_380 = z_alfa_by_2*sample_std_380;
P_x_390 = z_alfa_by_2*sample_std_390;
P_x_400 = z_alfa_by_2*sample_std_400;
%calculating random uncertainty of the mean value
P_x_bar_250 = P_x_250/(n)^(1/2);
P_x_bar_260 = P_x_260/(n)^(1/2);
      P_x_bar_270 = P_x_270/(n)^(1/2);
```

```
P_x_bar_280 = P_x_280/(n)^(1/2);
P_x_bar_290 = P_x_290/(n)^(1/2);
P_x_bar_300 = P_x_300/(n)^(1/2);
P_x_bar_310 = P_x_310/(n)^(1/2);
P_x_bar_320 = P_x_320/(n)^(1/2);
P_x_bar_330 = P_x_330/(n)^(1/2);
P_x_bar_340 = P_x_340/(n)^(1/2);
P_x_bar_350 = P_x_350/(n)^(1/2);
P_x_bar_360 = P_x_360/(n)^(1/2);
P_x_bar_370 = P_x_370/(n)^(1/2);
P_x_bar_380 = P_x_380/(n)^(1/2);
P_x_bar_390 = P_x_390/(n)^(1/2);
P_x_bar_400 = P_x_400/(n)^(1/2);


%% display
fprintf('Standard deviation at 250sp=%f\n', sample_std_250)
fprintf('Standard deviation at 260sp=%f\n', sample_std_260)
fprintf('Standard deviation at 270sp=%f\n', sample_std_270)
fprintf('Standard deviation at 280sp=%f\n', sample_std_280)
fprintf('Standard deviation at 290sp=%f\n', sample_std_290)
fprintf('Standard deviation at 300sp=%f\n', sample_std_300)
fprintf('Standard deviation at 310sp=%f\n', sample_std_310)
fprintf('Standard deviation at 320sp=%f\n', sample_std_320)
fprintf('Standard deviation at 330sp=%f\n', sample_std_330)
fprintf('Standard deviation at 340sp=%f\n', sample_std_340)
fprintf('Standard deviation at 350sp=%f\n', sample_std_350)
fprintf('Standard deviation at 360sp=%f\n', sample_std_360)
fprintf('Standard deviation at 370sp=%f\n', sample_std_370)
fprintf('Standard deviation at 380sp=%f\n', sample_std_380)
fprintf('Standard deviation at 390sp=%f\n', sample_std_390)
fprintf('Standard deviation at 400sp=%f\n', sample_std_400)
fprintf('Random Uncertainty of each measurement at 250sp=%f\n',
P_x_250)
fprintf('Random Uncertainty of each measurement at 260sp=%f\n',
P_x_260)
fprintf('Random Uncertainty of each measurement at 270sp=%f\n',
P_x_270)
fprintf('Random Uncertainty of each measurement at 280sp=%f\n',
P_x_280)
fprintf('Random Uncertainty of each measurement at 290sp=%f\n',
P_x_290)
fprintf('Random Uncertainty of each measurement at 300sp=%f\n',
P_x_300)
fprintf('Random Uncertainty of each measurement at 310sp=%f\n',
P_x_310)
fprintf('Random Uncertainty of each measurement at 320sp=%f\n',
P_x_320)
fprintf('Random Uncertainty of each measurement at 330sp=%f\n',
P_x_330)
fprintf('Random Uncertainty of each measurement at 340sp=%f\n',
P_x_340)
fprintf('Random Uncertainty of each measurement at 350sp=%f\n',
P_x_350)
fprintf('Random Uncertainty of each measurement at 360sp=%f\n',
P_x_360)
fprintf('Random Uncertainty of each measurement at 370sp=%f\n',
P_x_370)
fprintf('Random Uncertainty of each measurement at 380sp=%f\n',
P_x_380)
```

```
        fprintf('Random Uncertainty of each measurement at 390sp=%f\n',
        P_x_390)
        fprintf('Random Uncertainty of each measurement at 400sp=%f\n',
        P_x_400)
        fprintf('Random Uncertainty of the mean measurement at 250sp=%f\n',
        P_x_bar_250)
        fprintf('Random Uncertainty of the mean measurement at 260sp=%f\n',
        P_x_bar_260)
        fprintf('Random Uncertainty of the mean measurement at
        270spt=%f\n',P_x_bar_270)
        fprintf('Random Uncertainty of the mean measurement at 280sp=%f\n',
        P_x_bar_280)
        fprintf('Random Uncertainty of the mean measurement at 290sp=%f\n',
        P_x_bar_290)
        fprintf('Random Uncertainty of the mean measurement at 300sp=%f\n',
        P_x_bar_300)
        fprintf('Random Uncertainty of the mean measurement at 310sp=%f\n',
        P_x_bar_310)
fprintf('Random Uncertainty of the mean measurement at 320sp=%f\n',
P_x_bar_320)
fprintf('Random Uncertainty of the mean measurement at 330sp=%f\n',
P_x_bar_330)
fprintf('Random Uncertainty of the mean measurement at 340sp=%f\n',
P_x_bar_340)
fprintf('Random Uncertainty of the mean measurement at 350sp=%f\n',
P_x_bar_350)
fprintf('Random Uncertainty of the mean measurement at 360sp=%f\n',
P_x_bar_360)
fprintf('Random Uncertainty of the mean measurement at 370sp=%f\n',
P_x_bar_370)
fprintf('Random Uncertainty of the mean measurement at 380sp=%f\n',
P_x_bar_380)
fprintf('Random Uncertainty of the mean measurement at 390sp=%f\n',
P_x_bar_390)
fprintf('Random Uncertainty of the mean measurement at 400sp=%f\n',
P_x_bar_400)
```

D. Comparison of Coriolis mass flow rate measurement MATLAB codes

```
% Hysteresis Plot of Old and NewCoriolis Massflowrate for fluid1
Measurement
Number_of_samples_rising = linspace(1,816,816);
Number_of_samples_falling = linspace(816,1,816);
Old_coriolis_increase_massflow_fluid1 =
Old_coriolis_increasing_flowrate_fluid1; % massflow rate(250-400kg/min)
Old_coriolis_decrease_massflow_fluid1 =
Old_coriolis_decreasing_flowrate_fluid1; % massflow rate(400-250kg/min)
New_coriolis_increase_fluid1 = New_coriolis_increasing_flowrate_fluid1; %
massflow rate(250-400kg/min)
New_coriolis_decrease_fluid1 = New_coriolis_decreasing_flowrate_fluid1; %
massflow rate(400-250kg/min)
subplot(1,2,1)
plot(Number_of_samples_rising,Old_coriolis_increase_massflow_fluid1)
hold on
plot(Number_of_samples_falling,Old_coriolis_decrease_massflow_fluid1,'r')
hold off
legend('Increasing Massflowrate','Decreasing Mass flowrate')
hold off
title('Hysteresis Plot of Old Coriolis Mass Flow Rate ')
xlabel('Number of Samples')
ylabel('Mass Flow Rate (kg/min)')
```

```
grid on
subplot(1,2,2)
plot(Number_of_samples_rising,New_coriolis_increase_fluid1)
hold on
plot(Number_of_samples_falling,New_coriolis_decrease_fluid1,'r')
hold off
legend('Increasing Massflowrate','Decreasing Mass flowrate')
hold off
title('Hysteresis Plot of New Coriolis Mass Flow Rate ')
xlabel('Number of Samples')
ylabel('Mass Flow Rate (kg/min)')
grid on

% Fluid -1 Mass flow rate Comparison betweeen old(serial:24520087 and New
coriolis(Serial:K6071D02000')
%Time series plot
Time = linspace(0,100,1581);% minutes
flow = linspace(250,400,16);
Old_Coriolis_massflow_fluid1 = Old_coriolis_massflow_fluid1;
New_Coriolis_massflow_fluid1 = New_coriolis_massflow_fluid1;
setpoint = [250 260 270 280 290 300 310 320 330 340 350 360 370 380 390
400];
Old_Coriolis_massflow_fluid1_half = old_Coriolis_250_to_400Sp;%(kg/min)
new__Coriolis_massflow_fluid1_half = new_Coriolis_250_to_400Sp;%(kg/min)
subplot(1,2,1)
scatter(Time,Old_Coriolis_massflow_fluid1)
hold on
scatter (Time,New_Coriolis_massflow_fluid1,'r')
hold off
legend('Old Coriolis Mass Flow Rate', 'New Coriolis Mass Flow Rate')
hold off
title('Old and New Coriolis Mass flow Rate of Fluid-1')
xlabel('Time (minutes)')
ylabel('Mass Flow Rate (kg/min)')
grid on
subplot(1,2,2)
scatter(Old_Coriolis_massflow_fluid1_half,new__Coriolis_massflow_fluid1_hal
f)
hold on
plot(flow,setpoint,'r')
legend('Old and New Coriolis Correlation', 'Set Point')
title('Correlation of Old and New Coriolis')
xlabel('Old Coriolis(kg/min)')
ylabel('New Coriolis(kg/min)')
grid on

% Uncertainty Plot of old and New coriolis flow meter using fluid-1
flow = linspace(250,400,16);
old_coriolis_massmean_fluid1 = [250.38 260.04 269.95 279.89 289.91 300.09
310.03 319.91 330.00 340.02 350.02 360.17 370.21 379.89 390.12 400.10];
new_coriolis_massmean_fluid1 = [254.15 264.23 274.21 284.29 294.48 304.86
315.06 325.42 335.93 346.08 356.45 366.94 377.58 387.97 398.07 409.25];
setpoint = [250 260 270 280 290 300 310 320 330 340 350 360 370 380 390
400];
error_old = [0.14 0.16 0.12 0.14 0.14 0.12 0.13 0.13 0.12 0.12 0.11 0.11
0.11 0.11 0.11 0.11];
error_new = [0.18 0.13 0.12 0.13 0.11 0.16 0.11 0.12 0.13 0.13 0.11 0.12
0.12 0.11 0.11 0.14];
 errorbar(flow,old_coriolis_massmean_fluid1,error_old)
 hold on
 errorbar(flow,new_coriolis_massmean_fluid1,error_new,'r')
```

```
 hold on
 plot(flow,setpoint,'g')
 hold off
 legend('Old Coriolis Mass flow Rate', 'New Coriolis Mass flow
 Rate','Setpoint')
 title('Uncertaity of Old and New Coriolis')
 xlabel('mass flow Rate(kg/min)')
 grid on
 ylabel('Mean Mass Flow Rate (kg/min)')

% Hysteresis Plot of Old and new  Coriolis Massflowrate of fluid-2
Number_of_samples_rising = linspace(1,306,306);
Number_of_samples_falling = linspace(306,1,306);
Old_coriolis_increase_massflow_fluid2 =
Old_coriolis_increasing_flowrate_fluid2; % massflow rate(250-400kg/min)
Old_coriolis_decrease_massflow_fluid2 =
Old_coriolis_decreasing_flowrate_fluid2; % massflow rate(400-250kg/min)
New_coriolis_increase_flud2 = New_coriolis_increasing_flowrate_fluid2; %
massflow rate(250-400kg/min)
New_coriolis_decrease_fluid2 = New_coriolis_decreasing_flowrate_fluid2; %
massflow rate(400-250kg/min)
subplot(1,2,1)
plot(Number_of_samples_rising,Old_coriolis_increase_massflow_fluid2)
hold on
plot(Number_of_samples_falling,Old_coriolis_decrease_massflow_fluid2,'r')
hold off
legend('Increasing Massflowrate','Decreasing Mass flowrate')
hold off
title('Hysteresis Plot of Old Coriolis Mass Flow Rate ')
xlabel('Number of Samples')
ylabel('Mass Flow Rate (kg/min)')
grid on
subplot(1,2,2)
plot(Number_of_samples_rising,New_coriolis_increase_flud2)
hold on
plot(Number_of_samples_falling,New_coriolis_decrease_fluid2,'r')
hold off
legend('Increasing Massflowrate','Decreasing Mass flowrate')
hold off
title('Hysteresis Plot of New Coriolis Mass Flow Rate ')
xlabel('Number of Samples')
ylabel('Mass Flow Rate (kg/min)')
grid on

% Fluid - 2 Mass flow rate Comparison betweeen old(serial:24520087 and New
coriolis(Serial:K6071D02000')
%Time series plot
Time = linspace(0,40,561);% minutes
flow = linspace(250,300,6);
setpoint = [250 260 270 280 290 300];
Old_Coriolis_massflow_fluid2 = Old_coriolis_massflow_fluid2;%(kg/min)
New_Coriolis_massflow_fluid2 = New_coriolis_massflow_fluid2;%(kg/min)
Old_Coriolis_massflow_fluid2_half = old_Coriolis_250_to_400Sp;%(kg/min)
new_Coriolis_massflow_fluid2_half = new_Coriolis_250_to_400Sp;%(kg/min)
subplot(1,2,1)
scatter(Time,Old_Coriolis_massflow_fluid2)
hold on
scatter (Time,New_Coriolis_massflow_fluid2,'r')
hold off
legend('Old Coriolis Mass Flow Rate', 'New Coriolis Mass Flow Rate')
hold off
```

```
title('Old and New Coriolis Mass flow Rate of Water')
xlabel('Time (minutes)')
ylabel('Mass Flow Rate (kg/min)')
grid on
subplot(1,2,2)
scatter(Old_Coriolis_massflow_fluid2_half,new_Coriolis_massflow_fluid2_half
)
hold on
plot(flow,setpoint,'r')
legend('Old and New Coriolis Correlation', 'Set Point')
title('Correlation of Old and New Coriolis')
xlabel('Old Coriolis(kg/min)')
ylabel('New Coriolis(kg/min)')
grid on

% Uncertainty Plot of old and New coriolis flow meter using fluid-2
flow = linspace(250,400,6);
old_coriolis_massmean_fluid2 = [272.84 272.90 273.02 280.45 291.69 300.97];
new_coriolis_massmean_fluid2 = [289.04 289.79 289.85 297.79 311.25 321.69];
setpoint = [250 260 270 280 290 300];
error_new = [0.16 0.15 0.17 0.19 0.17 0.16];
error_old = [0.13 0.13 0.13 0.17 0.16 0.15];
errorbar(flow,old_coriolis_massmean_fluid2,error_old)
hold on
errorbar(flow,new_coriolis_massmean_fluid2,error_new,'r')
hold on
plot(flow,setpoint,'g')
hold off
legend('Old Coriolis Mass flow Rate', 'New Coriolis Mass flow
Rate','Setpoint')
title('Uncertaity of Old and New Coriolis')
xlabel('mass flow Rate(kg/min)')
ylabel('Mean Mass Flow Rate (kg/min)')
grid on

% Hysteresis Plot of Old and NewCoriolis Massflowrate for water Measurement
Number_of_samples_rising = linspace(1,816,816);
Number_of_samples_falling = linspace(816,1,816);
Old_coriolis_increase_massflow = Old_coriolis_increasing_flowrate; %
massflow rate(250-400kg/min)
Old_coriolis_decrease_massflow = Old_coriolis_decreasing_flowrate; %
massflow rate(400-250kg/min)
New_coriolis_increase = New_coriolis_increasing_flowrate; % massflow
rate(250-400kg/min)
New_coriolis_decrease = New_coriolis_decreasing_flowrate; % massflow
rate(400-250kg/min)
subplot(1,2,1)
plot(Number_of_samples_rising,Old_coriolis_increase_massflow)
hold on
plot(Number_of_samples_falling,Old_coriolis_decrease_massflow,'r')
hold off
legend('Increasing Massflowrate','Decreasing Mass flowrate')
hold off
      title('Hysteresis Plot of Old Coriolis Mass Flow Rate ')
      xlabel('Number of Samples')
      ylabel('Mass Flow Rate (kg/min)')
      grid on
      subplot(1,2,2)
      plot(Number_of_samples_rising,New_coriolis_increase)
      hold on
      plot(Number_of_samples_falling,New_coriolis_decrease,'r')
```

```
        hold off
        legend('Increasing Massflowrate','Decreasing Mass flowrate')
        hold off
        title('Hysteresis Plot of New Coriolis Mass Flow Rate ')
        xlabel('Number of Samples')
        ylabel('Mass Flow Rate (kg/min)')
        grid on

        % Hysteresis Error of old and New Coriolis massflow rate for water
        % measurement
        ymin_old_massflow = 247.94;
        ymin_new_massflow = 249.2;
        ymax_old_massflow = 401.64;
        ymax_new_massflow = 402.21;
        ymn_old_massflow = 330.48;
        ymn_new_massflow = 330.89;
        ymp_old_massflow = 320.34;
        ymp_new_massflow = 321.20;
        Hysteresis_error_old_dens = (ymn_old_massflow-
        ymp_old_massflow)/(ymax_old_massflow-ymin_old_massflow);
        Hysteresis_error_new_dens = (ymn_new_massflow-
        ymp_new_massflow)/(ymax_new_massflow-ymin_new_massflow);
        %% display
        fprintf('Hysteresis Error of old coriolis massflow=%f\n',
        Hysteresis_error_old_dens)
        fprintf('Hysteresis Error of New coriolis massflow=%f\n',
        Hysteresis_error_new_dens)

% Water Mass flow rate Comparison betweeen old(serial:24520087 and New
coriolis(Serial:K6071D02000')
        %Time series and correlation plots
        Time = linspace(0,100,1581);% minutes
        flow = linspace(250,400,16);%(kg/min)
        setpoint = [250 260 270 280 290 300 310 320 330 340 350 360 370 380
        390 400];%(kg/min)
        Old_Coriolis_massflow_water = Old_coriolis_massflow_water; %(kg/min)
        New_Coriolis_massflow_water = New_coriolis_massflo_water;%(kg/min)
        Old_Coriolis_massflow_water_half =
        old_Coriolis_250_to_400Sp;%(kg/min)
        New_Coriolis_massflow_water_half =
        new_Coriolis_250_to_400Sp;%(kg/min)
        subplot(1,2,1)
        scatter(Time,Old_Coriolis_massflow_water)
        hold on
        scatter (Time,New_Coriolis_massflow_water,'r')
        hold off
        legend('Old Coriolis Mass Flow Rate', 'New Coriolis Mass Flow Rate')
        hold off
        title('Old and New Coriolis Mass flow Rate of Water')
        xlabel('Time (minutes)')
        ylabel('Mass Flow Rate (kg/min)')
        grid on
        subplot(1,2,2)
        scatter(Old_Coriolis_massflow_water_half,New_Coriolis_massflow_water_
        half)
        hold on
        plot(flow,setpoint,'r')
        legend('Old and New Coriolis Correlation', 'Set Point')
        title('Correlation of Old and New Coriolis')
        xlabel('Old Coriolis(kg/min)')
        ylabel('New Coriolis(kg/min)')
```

```
      grid on

% Uncertainty of old and New Coriolis for water
      flow = linspace(250,400,16);
      old_coriolis_massmean_water = [249.97 260.11 269.87 280.08 290.02
      299.97 309.96 320.03 329.92 340.07 350.04 359.93 370.00 380.03 390.01
      399.94];
      new_coriolis_massmean_water = [250.48 260.36 270.50 280.36 290.49
      300.46 310.46 320.72 330.46 340.47 350.83 360.50 370.38 380.28 390.47
      400.61];
      setpoint = [250 260 270 280 290 300 310 320 330 340 350 360 370 380
      390 400];
      Old_coriolis_error_water = [0.13 0.13 0.14 0.13 0.12 0.12 0.11 0.12
      0.11 0.11 0.11 0.11 0.11 0.11 0.11 0.11];
      new_coriolis_error_water = [0.12 0.11 0.11 0.11 0.12 0.11 0.11 0.11
      0.11 0.11 0.10 0.11 0.10 0.11 0.11 0.11];
      errorbar(flow,old_coriolis_massmean_water,Old_coriolis_error_water)
      hold on
      errorbar(flow,new_coriolis_massmean_water,new_coriolis_error_water,'r
      ')
      hold on
       plot(flow,setpoint,'g')
       hold off
       legend('Old Coriolis Mass flow Rate', 'New Coriolis Mass flow
       Rate','Setpoint')
       title('Uncertaity of Old and New Coriolis')
       xlabel('mass flow Rate(kg/min)')
       grid on
       ylabel('Mean Mass Flow Rate (kg/min)')

% Fluid - 2(higher flow rate) Mass flow rate Comparison betweeen
old(serial:24520087 and New coriolis(Serial:K6071D02000')
%Time series plot
Time = linspace(0,50,663);% minutes
flow = linspace(250,550,7);
setpoint = [250 300 350 400 450 500 550];
Old_Coriolis_massflow_fluid2_higher =
Old_coriolis_massflow_fluid2_higher;%(kg/min)
New_Coriolis_massflow_fluid2_higher =
New_coriolis_massflow_fluid2_higher;%(kg/min)
Old_Coriolis_massflow_fluid2_half_higher_ft =
old_Coriolis_250_to_550Sp;%(kg/min)
new_Coriolis_massflow_fluid2_half_higher_ft =
new_Coriolis_250_to_550Sp;%(kg/min)
subplot(1,2,1)
scatter(Time,Old_Coriolis_massflow_fluid2_higher)
hold on
scatter (Time,New_Coriolis_massflow_fluid2_higher,'r')
hold off
legend('Old Coriolis Mass Flow Rate', 'New Coriolis Mass Flow Rate')
hold off
title('Old and New Coriolis Mass flow Rate of Fluid-2 at higher flow rate')
xlabel('Time (minutes)')
ylabel('Mass Flow Rate (kg/min)')
grid on
      subplot(1,2,2)
      scatter(Old_Coriolis_massflow_fluid2_half_higher_ft,new_Coriolis_mass
      flow_fluid2_half_higher_ft)
      hold on
      plot(flow,setpoint,'r')
      legend('Old and New Coriolis Correlation', 'Set Point')
```

```
      title('Correlation of Old and New Coriolis')
      xlabel('Old Coriolis(kg/min)')
      ylabel('New Coriolis(kg/min)')
      grid on

%% Estimating the random uncertainty with 95% confidence level
%for Mass flow rate of New Coriolis flow meter of Water.
%% given data
confidence_level=0.95; %95%
alfa=1-confidence_level; %level of significance
massflow_250sp = massflow_250sp_new;% Kg/min
massflow_260sp = massflow_260sp_new; %kg/min
massflow_270sp = massflow_270sp_new; %kg/min
massflow_280sp = massflow_280sp_new; %kg/min
massflow_290sp = massflow_290sp_new; %kg/min
massflow_300sp = massflow_300sp_new; %kg/min
massflow_310sp = massflow_310sp_new; %kg/min
massflow_320sp = massflow_320sp_new; %kg/min
massflow_330sp = massflow_330sp_new; %kg/min
massflow_340sp = massflow_340sp_new; %kg/min
massflow_350sp = massflow_350sp_new; %kg/min
massflow_360sp = massflow_360sp_new; %kg/min
massflow_370sp = massflow_370sp_new; %kg/min
massflow_380sp = massflow_380sp_new; %kg/min
massflow_390sp = massflow_390sp_new; %kg/min
massflow_400sp = massflow_400sp_new; %kg/min
n=length(massflow_400sp);

%% Estimate sample mean at 250 setpoint
%estimate confidence interval on the mean
x_bar_250 = mean(massflow_250sp);%sample mean at 250setpoint
sum=0;
for i=1:length(massflow_250sp)
    sum=(massflow_250sp(i)-x_bar_250)^2+sum;
end
sample_std_250 = sqrt((sum/(n))); %standard deviation of the sample
%% Estimate sample mean at 260
%estimate confidence interval on the mean
x_bar_260 = mean(massflow_260sp);%sample mean at 260setpoint
sum=0;
for i=1:length(massflow_260sp)
    sum=(massflow_260sp(i)-x_bar_260)^2+sum;
end
sample_std_260 = sqrt((sum/(n))); %standard deviation of the sample
%% Estimate sample mean at 270 setpoint
%estimate confidence interval on the mean
x_bar_270 = mean(massflow_270sp);%sample mean at 270setpoint
sum=0;
for i=1:length(massflow_270sp)
    sum=(massflow_270sp(i)-x_bar_270)^2+sum;
end
sample_std_270 = sqrt((sum/(n))); %standard deviation of the sample
%% Estimate sample mean at 280 setpoint
%estimate confidence interval on the mean
x_bar_280 = mean(massflow_280sp);%sample mean at 280setpoint
sum=0;
for i=1:length(massflow_280sp)
    sum=(massflow_280sp(i)-x_bar_280)^2+sum;
end
sample_std_280 = sqrt((sum/(n))); %standard deviation of the sample
%% Estimate sample mean at 290 setpoint
```

```
%estimate confidence interval on the mean
x_bar_290 = mean(massflow_290sp);%sample mean at 290setpoint
sum=0;
for i=1:length(massflow_290sp)
    sum=(massflow_290sp(i)-x_bar_290)^2+sum;
end
sample_std_290 = sqrt((sum/(n))); %standard deviation of the sample
%% Estimate sample mean at 300 setpoint
%estimate confidence interval on the mean
x_bar_300 = mean(massflow_300sp);%sample mean at 300setpoint
sum=0;
for i=1:length(massflow_300sp)
    sum=(massflow_300sp(i)-x_bar_300)^2+sum;
end
sample_std_300 = sqrt((sum/(n))); %standard deviation of the sample
%% Estimate sample mean at 310 setpoint
%estimate confidence interval on the mean
x_bar_310 = mean(massflow_310sp);%sample mean at 310setpoint
sum=0;
for i=1:length(massflow_310sp)
    sum=(massflow_310sp(i)-x_bar_310)^2+sum;
end
sample_std_310 = sqrt((sum/(n))); %standard deviation of the sample
%% Estimate sample mean at 320 setpoint
%estimate confidence interval on the mean
x_bar_320 = mean(massflow_320sp);%sample mean at 320setpoint
sum=0;
for i=1:length(massflow_320sp)
    sum=(massflow_320sp(i)-x_bar_320)^2+sum;
end
sample_std_320 = sqrt((sum/(n))); %standard deviation of the sample
%% Estimate sample mean at 330 setpoint
%estimate confidence interval on the mean
x_bar_330 = mean(massflow_330sp);%sample mean at 330setpoint
sum=0;
for i=1:length(massflow_330sp)
    sum=(massflow_330sp(i)-x_bar_330)^2+sum;
end
sample_std_330 = sqrt((sum/(n))); %standard deviation of the sample
%% Estimate sample mean at 340 setpoint
%estimate confidence interval on the mean
x_bar_340 = mean(massflow_340sp);%sample mean at 340setpoint
sum=0;
for i=1:length(massflow_340sp)
    sum=(massflow_340sp(i)-x_bar_340)^2+sum;
end
sample_std_340 = sqrt((sum/(n))); %standard deviation of the sample
%% Estimate sample mean at 350 setpoint
%estimate confidence interval on the mean
x_bar_350 = mean(massflow_350sp);%sample mean at 350setpoint
sum=0;
for i=1:length(massflow_350sp)
    sum=(massflow_350sp(i)-x_bar_350)^2+sum;
end
sample_std_350 = sqrt((sum/(n))); %standard deviation of the sample
%% Estimate sample mean at 360 setpoint
%estimate confidence interval on the mean
x_bar_360 = mean(massflow_360sp);%sample mean at 360setpoint
sum=0;
for i=1:length(massflow_360sp)
    sum=(massflow_360sp(i)-x_bar_360)^2+sum;
```

```
end
sample_std_360 = sqrt((sum/(n))); %standard deviation of the sample
%% Estimate sample mean at 370 setpoint
%estimate confidence interval on the mean
x_bar_370 = mean(massflow_370sp);%sample mean at 370setpoint
sum=0;
for i=1:length(massflow_370sp)
    sum=(massflow_370sp(i)-x_bar_370)^2+sum;
end
sample_std_370 = sqrt((sum/(n))); %standard deviation of the sample
%% Estimate sample mean at 380 setpoint
%estimate confidence interval on the mean
x_bar_380 = mean(massflow_380sp);%sample mean at 380setpoint
sum=0;
for i=1:length(massflow_380sp)
    sum=(massflow_380sp(i)-x_bar_380)^2+sum;
end
sample_std_380 = sqrt((sum/(n))); %standard deviation of the sample
%% Estimate sample mean at 390 setpoint
%estimate confidence interval on the mean
x_bar_390 = mean(massflow_390sp);%sample mean at 390setpoint
sum=0;
for i=1:length(massflow_390sp)
    sum=(massflow_390sp(i)-x_bar_390)^2+sum;
end
sample_std_390 = sqrt((sum/(n))); %standard deviation of the sample
%% Estimate sample mean at 400 setpoint
%estimate confidence interval on the mean
x_bar_400 = mean(massflow_400sp);%sample mean at 400setpoint
sum=0;
for i=1:length(massflow_400sp)
    sum=(massflow_400sp(i)-x_bar_400)^2+sum;
end
sample_std_400 = sqrt((sum/(n))); %standard deviation of the sample
%% for normal-distribution (since values is greater than 30)
alpha_by_2 = 0.025;
z_alfa_by_2 = 1.96; %value gotten from the standard normal distribution
table
%%
% calculating the random uncertainty of each measurement
P_x_250 = z_alfa_by_2*sample_std_250;
P_x_260 = z_alfa_by_2*sample_std_260;
P_x_270 = z_alfa_by_2*sample_std_270;
P_x_280 = z_alfa_by_2*sample_std_280;
P_x_290 = z_alfa_by_2*sample_std_290;
P_x_300 = z_alfa_by_2*sample_std_300;
P_x_310 = z_alfa_by_2*sample_std_310;
P_x_320 = z_alfa_by_2*sample_std_320;
P_x_330 = z_alfa_by_2*sample_std_330;
P_x_340 = z_alfa_by_2*sample_std_340;
P_x_350 = z_alfa_by_2*sample_std_350;
P_x_360 = z_alfa_by_2*sample_std_360;
P_x_370 = z_alfa_by_2*sample_std_370;
P_x_380 = z_alfa_by_2*sample_std_380;
P_x_390 = z_alfa_by_2*sample_std_390;
P_x_400 = z_alfa_by_2*sample_std_400;
%calculating random uncertainty of the mean value
P_x_bar_250 = P_x_250/(n)^(1/2);
P_x_bar_260 = P_x_260/(n)^(1/2);
P_x_bar_270 = P_x_270/(n)^(1/2);
P_x_bar_280 = P_x_280/(n)^(1/2);
```

```
P_x_bar_290 = P_x_290/(n)^(1/2);
P_x_bar_300 = P_x_300/(n)^(1/2);
P_x_bar_310 = P_x_310/(n)^(1/2);
P_x_bar_320 = P_x_320/(n)^(1/2);
P_x_bar_330 = P_x_330/(n)^(1/2);
P_x_bar_340 = P_x_340/(n)^(1/2);
P_x_bar_350 = P_x_350/(n)^(1/2);
P_x_bar_360 = P_x_360/(n)^(1/2);
P_x_bar_370 = P_x_370/(n)^(1/2);
P_x_bar_380 = P_x_380/(n)^(1/2);
P_x_bar_390 = P_x_390/(n)^(1/2);
P_x_bar_400 = P_x_400/(n)^(1/2);

 %% display
fprintf('Standard deviation at 250sp=%f\n', sample_std_250)
fprintf('Standard deviation at 260sp=%f\n', sample_std_260)
fprintf('Standard deviation at 270sp=%f\n', sample_std_270)
fprintf('Standard deviation at 280sp=%f\n', sample_std_280)
fprintf('Standard deviation at 290sp=%f\n', sample_std_290)
fprintf('Standard deviation at 300sp=%f\n', sample_std_300)
fprintf('Standard deviation at 310sp=%f\n', sample_std_310)
fprintf('Standard deviation at 320sp=%f\n', sample_std_320)
fprintf('Standard deviation at 330sp=%f\n', sample_std_330)
fprintf('Standard deviation at 340sp=%f\n', sample_std_340)
fprintf('Standard deviation at 350sp=%f\n', sample_std_350)
fprintf('Standard deviation at 360sp=%f\n', sample_std_360)
fprintf('Standard deviation at 370sp=%f\n', sample_std_370)
fprintf('Standard deviation at 380sp=%f\n', sample_std_380)
fprintf('Standard deviation at 390sp=%f\n', sample_std_390)
fprintf('Standard deviation at 400sp=%f\n', sample_std_400)
fprintf('Random Uncertainty of each measurement at 250sp=%f\n', P_x_250)
fprintf('Random Uncertainty of each measurement at 260sp=%f\n', P_x_260)
fprintf('Random Uncertainty of each measurement at 270sp=%f\n', P_x_270)
fprintf('Random Uncertainty of each measurement at 280sp=%f\n', P_x_280)
fprintf('Random Uncertainty of each measurement at 290sp=%f\n', P_x_290)
fprintf('Random Uncertainty of each measurement at 300sp=%f\n', P_x_300)
fprintf('Random Uncertainty of each measurement at 310sp=%f\n', P_x_310)
fprintf('Random Uncertainty of each measurement at 320sp=%f\n', P_x_320)
fprintf('Random Uncertainty of each measurement at 330sp=%f\n', P_x_330)
fprintf('Random Uncertainty of each measurement at 340sp=%f\n', P_x_340)
fprintf('Random Uncertainty of each measurement at 350sp=%f\n', P_x_350)
fprintf('Random Uncertainty of each measurement at 360sp=%f\n', P_x_360)
fprintf('Random Uncertainty of each measurement at 370sp=%f\n', P_x_370)
fprintf('Random Uncertainty of each measurement at 380sp=%f\n', P_x_380)
fprintf('Random Uncertainty of each measurement at 390sp=%f\n', P_x_390)
fprintf('Random Uncertainty of each measurement at 400sp=%f\n', P_x_400)
fprintf('Random Uncertainty of the mean measurement at 250sp=%f\n',
P_x_bar_250)
fprintf('Random Uncertainty of the mean measurement at 260sp=%f\n',
P_x_bar_260)
fprintf('Random Uncertainty of the mean measurement at
270spt=%f\n',P_x_bar_270)
fprintf('Random Uncertainty of the mean measurement at 280sp=%f\n',
P_x_bar_280)
fprintf('Random Uncertainty of the mean measurement at 290sp=%f\n',
P_x_bar_290)
fprintf('Random Uncertainty of the mean measurement at 300sp=%f\n',
P_x_bar_300)
fprintf('Random Uncertainty of the mean measurement at 310sp=%f\n',
P_x_bar_310)
```

```
fprintf('Random Uncertainty of the mean measurement at 320sp=%f\n',
P_x_bar_320)
fprintf('Random Uncertainty of the mean measurement at 330sp=%f\n',
P_x_bar_330)
fprintf('Random Uncertainty of the mean measurement at 340sp=%f\n',
P_x_bar_340)
fprintf('Random Uncertainty of the mean measurement at 350sp=%f\n',
P_x_bar_350)
fprintf('Random Uncertainty of the mean measurement at 360sp=%f\n',
P_x_bar_360)
fprintf('Random Uncertainty of the mean measurement at 370sp=%f\n',
P_x_bar_370)
fprintf('Random Uncertainty of the mean measurement at 380sp=%f\n',
P_x_bar_380)
fprintf('Random Uncertainty of the mean measurement at 390sp=%f\n',
P_x_bar_390)
fprintf('Random Uncertainty of the mean measurement at 400sp=%f\n',
P_x_bar_400)

%% Estimating the random uncertainty with 95% confidence level
%for Mass flow rate of old Coriolis flow meter of Water.
 %% given data
confidence_level=0.95; %95%
alfa=1-confidence_level; %level of significance
massflow_250sp = massflow_250sp_old;% Kg/min
massflow_260sp = massflow_260sp_old; %kg/min
massflow_270sp = massflow_270sp_old; %kg/min
massflow_280sp = massflow_280sp_old; %kg/min
massflow_290sp = massflow_290sp_old; %kg/min
massflow_300sp = massflow_300sp_old; %kg/min
massflow_310sp = massflow_310sp_old; %kg/min
massflow_320sp = massflow_320sp_old; %kg/min
massflow_330sp = massflow_330sp_old; %kg/min
massflow_340sp = massflow_340sp_old; %kg/min
massflow_350sp = massflow_350sp_old; %kg/min
massflow_360sp = massflow_360sp_old; %kg/min
massflow_370sp = massflow_370sp_old; %kg/min
massflow_380sp = massflow_380sp_old; %kg/min
massflow_390sp = massflow_390sp_old; %kg/min
massflow_400sp = massflow_400sp_old; %kg/min
n=length(massflow_400sp); % all length are the same value i.e. 51

%% Estimate sample mean at 250 setpoint
%estimate confidence interval on the mean
x_bar_250 = mean(massflow_250sp);%sample mean at 250setpoint
sum=0;
for i=1:length(massflow_250sp)
    sum=(massflow_250sp(i)-x_bar_250)^2+sum;
end
sample_std_250 = sqrt((sum/(n))); %standard deviation of the sample
%% Estimate sample mean at 260
%estimate confidence interval on the mean
x_bar_260 = mean(massflow_260sp);%sample mean at 260setpoint
sum=0;
for i=1:length(massflow_260sp)
    sum=(massflow_260sp(i)-x_bar_260)^2+sum;
end
sample_std_260 = sqrt((sum/(n))); %standard deviation of the sample
%% Estimate sample mean at 270 setpoint
%estimate confidence interval on the mean
x_bar_270 = mean(massflow_270sp);%sample mean at 270setpoint
```

```
sum=0;
for i=1:length(massflow_270sp)
    sum=(massflow_270sp(i)-x_bar_270)^2+sum;
end
sample_std_270 = sqrt((sum/(n))); %standard deviation of the sample
%% Estimate sample mean at 280 setpoint
%estimate confidence interval on the mean
x_bar_280 = mean(massflow_280sp);%sample mean at 280setpoint
sum=0;
for i=1:length(massflow_280sp)
    sum=(massflow_280sp(i)-x_bar_280)^2+sum;
end
sample_std_280 = sqrt((sum/(n))); %standard deviation of the sample
%% Estimate sample mean at 290 setpoint
%estimate confidence interval on the mean
x_bar_290 = mean(massflow_290sp);%sample mean at 290setpoint
sum=0;
for i=1:length(massflow_290sp)
    sum=(massflow_290sp(i)-x_bar_290)^2+sum;
end
sample_std_290 = sqrt((sum/(n))); %standard deviation of the sample
%% Estimate sample mean at 300 setpoint
%estimate confidence interval on the mean
x_bar_300 = mean(massflow_300sp);%sample mean at 300setpoint
sum=0;
for i=1:length(massflow_300sp)
    sum=(massflow_300sp(i)-x_bar_300)^2+sum;
end
sample_std_300 = sqrt((sum/(n))); %standard deviation of the sample
%% Estimate sample mean at 310 setpoint
%estimate confidence interval on the mean
x_bar_310 = mean(massflow_310sp);%sample mean at 310setpoint
sum=0;
for i=1:length(massflow_310sp)
    sum=(massflow_310sp(i)-x_bar_310)^2+sum;
end
sample_std_310 = sqrt((sum/(n))); %standard deviation of the sample
%% Estimate sample mean at 320 setpoint
%estimate confidence interval on the mean
x_bar_320 = mean(massflow_320sp);%sample mean at 320setpoint
sum=0;
for i=1:length(massflow_320sp)
    sum=(massflow_320sp(i)-x_bar_320)^2+sum;
end
sample_std_320 = sqrt((sum/(n))); %standard deviation of the sample
%% Estimate sample mean at 330 setpoint
%estimate confidence interval on the mean
x_bar_330 = mean(massflow_330sp);%sample mean at 330setpoint
sum=0;
for i=1:length(massflow_330sp)
    sum=(massflow_330sp(i)-x_bar_330)^2+sum;
end
sample_std_330 = sqrt((sum/(n))); %standard deviation of the sample
%% Estimate sample mean at 340 setpoint
%estimate confidence interval on the mean
x_bar_340 = mean(massflow_340sp);%sample mean at 340setpoint
sum=0;
for i=1:length(massflow_340sp)
    sum=(massflow_340sp(i)-x_bar_340)^2+sum;
end
sample_std_340 = sqrt((sum/(n))); %standard deviation of the sample
```

```
%% Estimate sample mean at 350 setpoint
%estimate confidence interval on the mean
x_bar_350 = mean(massflow_350sp);%sample mean at 350setpoint
sum=0;
for i=1:length(massflow_350sp)
    sum=(massflow_350sp(i)-x_bar_350)^2+sum;
end
sample_std_350 = sqrt((sum/(n))); %standard deviation of the sample
%% Estimate sample mean at 360 setpoint
%estimate confidence interval on the mean
x_bar_360 = mean(massflow_360sp);%sample mean at 360setpoint
sum=0;
for i=1:length(massflow_360sp)
    sum=(massflow_360sp(i)-x_bar_360)^2+sum;
end
sample_std_360 = sqrt((sum/(n))); %standard deviation of the sample
%% Estimate sample mean at 370 setpoint
%estimate confidence interval on the mean
x_bar_370 = mean(massflow_370sp);%sample mean at 370setpoint
sum=0;
for i=1:length(massflow_370sp)
    sum=(massflow_370sp(i)-x_bar_370)^2+sum;
end
sample_std_370 = sqrt((sum/(n))); %standard deviation of the sample
%% Estimate sample mean at 380 setpoint
%estimate confidence interval on the mean
x_bar_380 = mean(massflow_380sp);%sample mean at 380setpoint
sum=0;
for i=1:length(massflow_380sp)
    sum=(massflow_380sp(i)-x_bar_380)^2+sum;
end
sample_std_380 = sqrt((sum/(n))); %standard deviation of the sample
%% Estimate sample mean at 390 setpoint
%estimate confidence interval on the mean
x_bar_390 = mean(massflow_390sp);%sample mean at 390setpoint
sum=0;
for i=1:length(massflow_390sp)
    sum=(massflow_390sp(i)-x_bar_390)^2+sum;
end
sample_std_390 = sqrt((sum/(n))); %standard deviation of the sample
%% Estimate sample mean at 400 setpoint
%estimate confidence interval on the mean
x_bar_400 = mean(massflow_400sp);%sample mean at 400setpoint
sum=0;
for i=1:length(massflow_400sp)
    sum=(massflow_400sp(i)-x_bar_400)^2+sum;
end
sample_std_400 = sqrt((sum/(n))); %standard deviation of the sample
%% for normal-distribution (since values is greater than 30)
alpha_by_2 = 0.025;
z_alfa_by_2 = 1.96; %value gotten from the standard normal distribution
table
%%
% calculating the random uncertainty of each measurement
P_x_250 = z_alfa_by_2*sample_std_250;
P_x_260 = z_alfa_by_2*sample_std_260;
P_x_270 = z_alfa_by_2*sample_std_270;
P_x_280 = z_alfa_by_2*sample_std_280;
P_x_290 = z_alfa_by_2*sample_std_290;
P_x_300 = z_alfa_by_2*sample_std_300;
P_x_310 = z_alfa_by_2*sample_std_310;
```

```
P_x_320 = z_alfa_by_2*sample_std_320;
P_x_330 = z_alfa_by_2*sample_std_330;
P_x_340 = z_alfa_by_2*sample_std_340;
P_x_350 = z_alfa_by_2*sample_std_350;
P_x_360 = z_alfa_by_2*sample_std_360;
P_x_370 = z_alfa_by_2*sample_std_370;
P_x_380 = z_alfa_by_2*sample_std_380;
P_x_390 = z_alfa_by_2*sample_std_390;
P_x_400 = z_alfa_by_2*sample_std_400;
%calculating random uncertainty of the mean value
P_x_bar_250 = P_x_250/(n)^(1/2);
P_x_bar_260 = P_x_260/(n)^(1/2);
P_x_bar_270 = P_x_270/(n)^(1/2);
P_x_bar_280 = P_x_280/(n)^(1/2);
P_x_bar_290 = P_x_290/(n)^(1/2);
P_x_bar_300 = P_x_300/(n)^(1/2);
P_x_bar_310 = P_x_310/(n)^(1/2);
P_x_bar_320 = P_x_320/(n)^(1/2);
P_x_bar_330 = P_x_330/(n)^(1/2);
P_x_bar_340 = P_x_340/(n)^(1/2);
P_x_bar_350 = P_x_350/(n)^(1/2);
P_x_bar_360 = P_x_360/(n)^(1/2);
P_x_bar_370 = P_x_370/(n)^(1/2);
P_x_bar_380 = P_x_380/(n)^(1/2);
P_x_bar_390 = P_x_390/(n)^(1/2);
P_x_bar_400 = P_x_400/(n)^(1/2);

%% display
fprintf('Standard deviation at 250sp=%f\n', sample_std_250)
fprintf('Standard deviation at 260sp=%f\n', sample_std_260)
fprintf('Standard deviation at 270sp=%f\n', sample_std_270)
fprintf('Standard deviation at 280sp=%f\n', sample_std_280)
fprintf('Standard deviation at 290sp=%f\n', sample_std_290)
fprintf('Standard deviation at 300sp=%f\n', sample_std_300)
fprintf('Standard deviation at 310sp=%f\n', sample_std_310)
fprintf('Standard deviation at 320sp=%f\n', sample_std_320)
fprintf('Standard deviation at 330sp=%f\n', sample_std_330)
fprintf('Standard deviation at 340sp=%f\n', sample_std_340)
fprintf('Standard deviation at 350sp=%f\n', sample_std_350)
fprintf('Standard deviation at 360sp=%f\n', sample_std_360)
fprintf('Standard deviation at 370sp=%f\n', sample_std_370)
fprintf('Standard deviation at 380sp=%f\n', sample_std_380)
fprintf('Standard deviation at 390sp=%f\n', sample_std_390)
fprintf('Standard deviation at 400sp=%f\n', sample_std_400)
fprintf('Random Uncertainty of each measurement at 250sp=%f\n', P_x_250)
fprintf('Random Uncertainty of each measurement at 260sp=%f\n', P_x_260)
fprintf('Random Uncertainty of each measurement at 270sp=%f\n', P_x_270)
fprintf('Random Uncertainty of each measurement at 280sp=%f\n', P_x_280)
fprintf('Random Uncertainty of each measurement at 290sp=%f\n', P_x_290)
fprintf('Random Uncertainty of each measurement at 300sp=%f\n', P_x_300)
fprintf('Random Uncertainty of each measurement at 310sp=%f\n', P_x_310)
fprintf('Random Uncertainty of each measurement at 320sp=%f\n', P_x_320)
fprintf('Random Uncertainty of each measurement at 330sp=%f\n', P_x_330)
fprintf('Random Uncertainty of each measurement at 340sp=%f\n', P_x_340)
fprintf('Random Uncertainty of each measurement at 350sp=%f\n', P_x_350)
fprintf('Random Uncertainty of each measurement at 360sp=%f\n', P_x_360)
fprintf('Random Uncertainty of each measurement at 370sp=%f\n', P_x_370)
fprintf('Random Uncertainty of each measurement at 380sp=%f\n', P_x_380)
fprintf('Random Uncertainty of each measurement at 390sp=%f\n', P_x_390)
fprintf('Random Uncertainty of each measurement at 400sp=%f\n', P_x_400)
```

```
fprintf('Random Uncertainty of the mean measurement at 250sp=%f\n',
P_x_bar_250)
fprintf('Random Uncertainty of the mean measurement at 260sp=%f\n',
P_x_bar_260)
fprintf('Random Uncertainty of the mean measurement at
270spt=%f\n',P_x_bar_270)
fprintf('Random Uncertainty of the mean measurement at 280sp=%f\n',
P_x_bar_280)
fprintf('Random Uncertainty of the mean measurement at 290sp=%f\n',
P_x_bar_290)
fprintf('Random Uncertainty of the mean measurement at 300sp=%f\n',
P_x_bar_300)
fprintf('Random Uncertainty of the mean measurement at 310sp=%f\n',
P_x_bar_310)
fprintf('Random Uncertainty of the mean measurement at 320sp=%f\n',
P_x_bar_320)
fprintf('Random Uncertainty of the mean measurement at 330sp=%f\n',
P_x_bar_330)
fprintf('Random Uncertainty of the mean measurement at 340sp=%f\n',
P_x_bar_340)
fprintf('Random Uncertainty of the mean measurement at 350sp=%f\n',
P_x_bar_350)
fprintf('Random Uncertainty of the mean measurement at 360sp=%f\n',
P_x_bar_360)
fprintf('Random Uncertainty of the mean measurement at 370sp=%f\n',
P_x_bar_370)
fprintf('Random Uncertainty of the mean measurement at 380sp=%f\n',
P_x_bar_380)
fprintf('Random Uncertainty of the mean measurement at 390sp=%f\n',
P_x_bar_390)
fprintf('Random Uncertainty of the mean measurement at 400sp=%f\n',
P_x_bar_400)
```

E. Mass flow rate estimation model MATLAB code

```
function [y1] = myNeural_first_int(x1)
%MYNEURALNETWORKFUNCTION neural network simulation function.
%
% Generated by Neural Network Toolbox function genFunction, 14-May-2016
10:01:50.
%
% [y1] = myNeuralNetworkFunction(x1) takes these arguments:
%   x = 5xQ matrix, input #1
% and returns:
%   y = 1xQ matrix, output #1
% where Q is the number of samples.

%#ok<*RPMT0>

  % ===== NEURAL NETWORK CONSTANTS =====
  x1=x1';
  % Input 1
  x1_step1_xoffset = [29.327184;55.157916;53.355545;3.686734;1000.126655];
  x1_step1_gain =
[0.0513751997885191;0.0482857776366546;0.0478599300656344;0.212214470734988
;0.00549860293558589];
  x1_step1_ymin = -1;

  % Layer 1
```

```
  b1 = [2.0539655111104467;0.58163914530106242;2.021703776030126;-
2.0272731765336496;2.2644268329549839;-
0.6271081763583245;0.6274594676429357;1.1492635982713812;1.0703593527215447
;-0.53390316835396945;1.3389198418802639;-
0.53645473161059953;2.6381118000358881;1.0818582450942806;-
1.1219570889212056];
  IW1_1 = [1.5222433298796512 -3.2077818621468084 0.62103833957048071
0.2414207760172051 -0.85450478342711167;-0.18200224411269741
0.14712912201028336 1.8589632546580559 -0.50490141292545287
0.3071030814570786;-1.92170650063058 1.1148797830598454 1.6277038159280957
-3.8056819591789752 -0.84231912087551142;0.69994140304471064 -
0.29585459328443786 -1.1817637042452585 -1.4375710022077544
0.25330034324438866;-2.1125221929751747 0.57530595616500002
0.4819628005235177 -0.96668677955103766
3.0055102206151978;3.5472327412931657 -2.4741616214571081 -
0.6649764087753175 -1.4187634583262487 -
0.34709412854941646;0.48123794845372148 2.9806759842932355 -
2.5420619132807714 -0.16100690762165132 -0.10570225957611323;-
1.8170825626389864 -0.78729623891045675 -0.242290250187287
0.61332279347123742 0.14308667638598382;-0.81383226147075871
1.4740639695647555 0.094426323380942812 -1.4505324620048734
0.77809089391818653;-0.7727511358827297 -1.787206122517087 -
1.430586094333548 0.4136180742459501 -
1.4651941878617141;0.065803964540497722 1.8900235606187483
1.3430784373500542 0.84309955372356671 1.828200725824622;-
0.37609494211269884 2.3363526720138608 0.40150647857892041
0.40476016616399307 0.4004286658735155;0.57601581509917055
1.8817249155300164 0.50466232801903066 0.63663850588954618 -
0.02703198327790806;0.87873291019785371 1.4456639810915899
2.0167340619235579 -0.37834056459543908
0.53555377366727686;1.0521208582981727 -1.3191721765499391
0.17695633698683971 1.5133341800459013 -1.608857508719955];

  % Layer 2
  b2 = 0.96741794351907906;
  LW2_1 = [-0.88336689376747868 -0.87418505155402515 -0.17597115085470888
0.12194589608481315 0.35299641421926475 -0.1211241371050276 -
0.45891361353412458 -0.48168469373019696 1.4110281582124198 -
0.4048729653944878 -0.2438667324633253 0.33820390521399601
0.0053638655928441286 0.48620048513148906 0.93414748794606806];

  % Output 1
  y1_step1_ymin = -1;
  y1_step1_gain = 0.0130066726571932;
  y1_step1_xoffset = 247.883245;

  % ===== SIMULATION ========

  % Dimensions
  Q = size(x1,2); % samples

  % Input 1
  xp1 = mapminmax_apply(x1,x1_step1_gain,x1_step1_xoffset,x1_step1_ymin);

  % Layer 1
  a1 = tansig_apply(repmat(b1,1,Q) + IW1_1*xp1);

  % Layer 2
  a2 = repmat(b2,1,Q) + LW2_1*a1;
```

```
  % Output 1
  y1 = mapminmax_reverse(a2,y1_step1_gain,y1_step1_xoffset,y1_step1_ymin);
end

% ===== MODULE FUNCTIONS ========

% Map Minimum and Maximum Input Processing Function
function y =
mapminmax_apply(x,settings_gain,settings_xoffset,settings_ymin)
  y = bsxfun(@minus,x,settings_xoffset);
  y = bsxfun(@times,y,settings_gain);
  y = bsxfun(@plus,y,settings_ymin);
end

% Sigmoid Symmetric Transfer Function
function a = tansig_apply(n)
  a = 2 ./ (1 + exp(-2*n)) - 1;
end

% Map Minimum and Maximum Output Reverse-Processing Function
function x =
mapminmax_reverse(y,settings_gain,settings_xoffset,settings_ymin)
  x = bsxfun(@minus,y,settings_ymin);
  x = bsxfun(@rdivide,x,settings_gain);
  x = bsxfun(@plus,x,settings_xoffset);
end
```